Mechanistic Studies of Desaturase-Mediated Oxidations

By

Amy E. Tremblay, B.Sc.

A thesis submitted to the Department of Chemistry
in partial fulfillment of the requirements for the degree of
Master of Science

to

The Faculty of Graduate Studies
Department of Chemistry
Carleton University
Ottawa, Canada
March 2009

The undersigned hereby recommend to
The Faculty of Graduate Studies and Research
Department of Chemistry
acceptance of the thesis

Mechanistic Studies of Destaurase-Mediated Oxidations

Submitted by

Amy E. Tremblay

In partial fulfillment of the requirements for the degree of

Master of Science

Dr. Robert C. Burk
Chair, Department of Chemistry

Dr. Peter H. Buist
Thesis Supervisor

Abstract

The study of the mechanism of fatty acid desaturases often requires the use of synthetic probes and/or standards. In this work, a general procedure for preparing chiral fluorine-tagged dialkyl sulfoxides was developed using DAG methodology. 18-fluoro-(10*S*)-sulfoxy-1-octadecanol, 18-fluoro-(10*R*)-sulfoxy-1-octadecanol, 15-fluoro-(11*S*)-sulfoxy-pentadecane, and 15-fluoro-(11*R*)-sulfoxypentadecane were prepared. These standards were used in the determination of the stereochemistry of enzymatically produced sulfoxides arising from the introduction of fluorine-tagged thia fatty acid analogues to a soluble and a membrane-bound Δ^9 desaturase.

In this study, it has been shown that the Pirkle binding model is successful for predicting the direction of induced non-equivalence of fluorine-tagged dialkyl sulfoxide enantiomers by ^{1}H NMR using the chiral solvating agents AMA, MPAA and TFAE. However, the observed non-equivalence of ^{19}F NMR signals of these sulfoxides under similar conditions is dependent on the nature of the chiral reagent used.

The identification of the products of a triple mutant, T117R/G188L/D280K of the castor Δ^9 desaturase was also undertaken using synthetic standards in combination with GC-MS. (10*Z*)- and (10*E*)-9-hydroxy-10-octadecenoate and (9*Z*)- and (9*E*)-11-hydroxy-9-octadecenoate were synthesized by known methods. The dienoic fatty acid esters, methyl 9*Z*,11*E*-octadecadienoate with a minor component of methyl 9*E*,11*E*-octadecadienoate were prepared in a 9:1 ratio and a mixture of 9*Z*,11*Z*-octadecadienoate and methyl 9*E*,11*Z*-octadecadienoate were also prepared.

Acknowledgements

"Success is the ability to go from one failure to another with no loss of enthusiasm."
- Sir Winston Churchill

First and foremost, thank you to Dr. Peter H. Buist. I know that I would never have been able to achieve all that I have without your guidance and encouragement. Thank you for your support, your understanding and the opportunity to do some interesting research.

Appreciation goes out to all those who assisted in these projects and were generous with their time and advice: Jeff Manthorpe (Carleton Univeristy) for many consultations, Keith Bourque (Carleton University) for help with NMR, Tony O'Neil (Carleton University) for IR, polarimetry and UV assistance, Elena Munteanu (Carleton University) for discussions on Wittig salts, José Abad (IIQAB) for the AMA procedure, Hooman Shadnia (Carleton University) for graphics and Clem Kazakoff (University of Ottawa) for GC/MS analyses. The success of these projects would also not have been possible without our collaborators, John Shanklin and Ed Whittle (Brookhaven National Laboratories) and Brian Dawson and Derek Hodgson (Health Canada). Financial support from NSERC, Merck and Carleton University has also been appreciated.

Many thanks to all of the past and present members of Delta Force who have made coming into the lab more enjoyable during the past few years. In particular I am grateful to Palash Bhar, with whom I have most recently had the pleasure of sharing the Buist lab.

Thank you to my family and friends for all their love, support and acceptance of my busy schedule throughout my Carleton years. Finally, I'd like to give thanks to Hani who has been patient and caring and who has helped me keep going.

Table of Contents

List of Figures

List of Tables

List of abbreviations

(*R*)-AMA	(*R*)-(9-anthryl)methoxy acetic acid
(*R*)-MPAA	(*R*)-methyoxyphenylacetic acid
(*R*)-TFAE	(*R*)-(−)-1-(9-Anthryl)-2,2,2-trifluoroethanol
(*S*)-AMA	(*S*)-(9-anthryl)methoxy acetic acid
(*S*)-MPAA	(*S*)-methyoxyphenylacetic acid
(S)-TFAE	(*S*)-(+)-1-(9-Anthryl)-2,2,2-trifluoroethanol
15F-(11*R*)SO	15-fluoro-(11*R*)-sulfoxypentadecane
15F-(11*S*)SO	15-fluoro-(11*S*)-sulfoxypentadecane
18F-(10*R*)SO-OH	18-fluoro-(10*R*)-sulfoxy-1-octadecanol
18F-(10*S*)SO-OH	18-fluoro-(10*S*)-sulfoxy-1-octadecanol
4F-(*R*)-O-DAG	1,2:5,6-di-O-isopropylidene-α-D-glucofuranosyl (*R*)-4-fluorobutanesulfinate
4F-(*S*)-O-DAG	1,2:5,6-di-O-isopropylidene-α-D-glucofuranosyl (*S*)-4-fluorobutanesulfinate
8F-(*R*)-O-DAG	1,2:5,6-di-O-isopropylidene-α-D-glucofuranosyl (*R*)-8-fluorooctanesulfinate
8F-(*S*)-O-DAG	1,2:5,6-di-O-isopropylidene-α-D-glucofuranosyl (*S*)-8-fluorooctanesulfinate
ACP	Acyl carrier protein
BF_3	Borontrifluoride diethyl etherate
CoA	Coenzyme A
CS2	Clavaminate synthase 2
CSA	Chiral solvating agent
DAG	Diacetone-D-glucose
DAST	Diethylaminosulfur trifluoride

DGPC	Deoxyguanidoproclavaminic acid
DIBAL-H	Diisobutylaluminum hydride
DMF	Dimethylformamide
dr	Diastereomeric ratio
ee	Enantiomeric excess
Et_2O	Diethyl ether
EtOAc	Ethyl acetate
EtOH	Ethanol
Fad2	Δ^{12} Desaturase /Fatty acid desaturase 2
GC	Gas chromatography
GC/MS	Gas chromatography/mass spectrometry
Hex	Hexane
KHMDS	Potassium bis(trimethylsilyl)amide
KIE	Kinetic isotope effect
m-CPBA	*meta*-chloroperbenzoic acid
MMO	Methane monooxygenase
MS	Mass spectrometry
NADH	Nicotinamide adenine dinucleotide
n-BuLi	n-Butyllithium
NMR	Nuclear magnetic resonance
PCC	Pyridinium chlorochromate
PL	Phospholipid
SCD	Stearoyl CoA Δ^9 desaturase
TBS	*tert*-Butyl dimethylsilyl
THF	Tetrahydrofuran

TMS	Trimethylsilyl

Chapter 1: Introduction

1.1 Fatty acids

Fatty acids are long-chain carboxylic acids. The chain length of fatty acids can vary; however in biological systems they typically range between 14 and 20 carbons in length, with the number of carbons usually being a multiple of 2.[1] The most common fatty acids found in cellular membranes contain 16 or 18 carbons. Apart from the carboxyl group, fatty acids can feature a variety of other functional groups including C-C double bonds and hydroxyl, alkynyl and epoxy groups (Figure 1.1).[1]

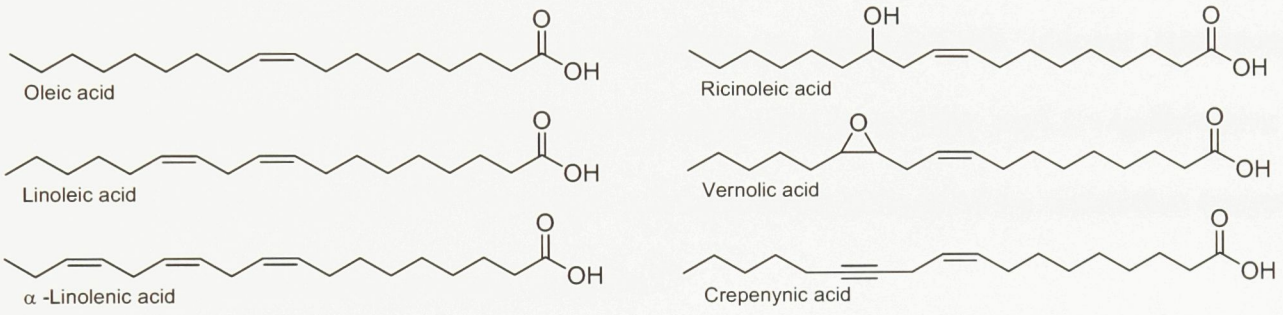

Figure 1.1 Examples of some naturally occurring fatty acids.

More than 300 different fatty acids have been found in seed oils to date, but it is estimated that the plant kingdom contains thousands of structurally distinct fatty acids.[2] Much of the diversity of these fatty acid structures arises from the action of various desaturase or desaturase-like enzymes.[3] These catalysts carry out unique dehydrogenation or related reactions to produce unsaturated fatty acids bearing one or more C-C double bonds at various positions along the hydrocarbon chain.[1]

The relative ratio of cellular saturated and unsaturated lipids is important for the optimizing the biophysical properties of biological membranes.[3] Unsaturated fatty acids are associated with cold acclimation of microorganisms, plants and animals due to the decreased

packing efficiency of lipids resulting from *Z*-desaturation.[3] Fatty acid desaturation is also involved in plant defence and insect communication pathways. Recently, stearoyl CoA (Co-enzyme A) Δ^9 desaturase (SCD) has been implicated in mammalian metabolic diseases such as obesity and diabetes; this finding has increased interest in fatty acid research.[3]

1.2 Fatty acid desaturases

As alluded to in the previous section, unsaturated fatty acids in aerobic organisms are formed via the desaturation of the corresponding saturated fatty acyl substrate. This process was first shown to occur in the yeast *Saccharomyces cerevisiae*, where it was demonstrated that molecular oxygen and a source of two electrons (nicotinamide adenine dinucleotide (NADH)) is required for the desaturation of stearic acid as its fatty acyl-CoA derivative to yield oleyl CoA (Figure 1.2).[4] The regio- and stereocontrol featured by desaturase enzymes cannot be duplicated using synthetic reagents.[3]

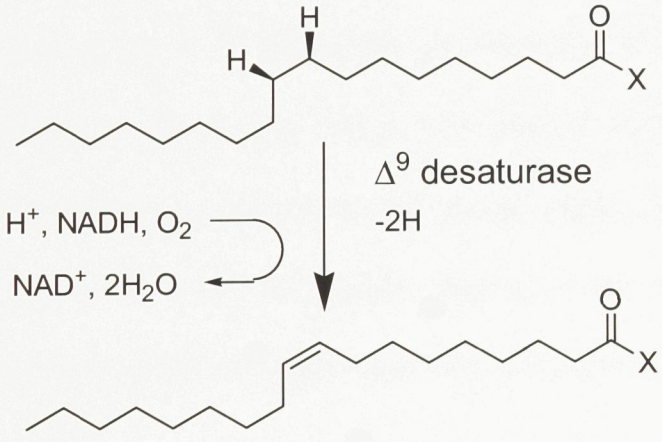

Figure 1.2 Prototypical scheme for the desaturase-mediated formation of unsaturated fatty acids.

Desaturases are generally named according to the location of double bond insertion relative to the carboxyl group. A desaturase that inserts a double bond between the 9th and 10th carbons (the most common case observed), is referred to as a Δ^9 desaturase. Conversely,

some desaturases are regioselective with reference to the methyl terminus of the fatty acid. These desaturases are referred to as ω-n desaturases; for example, an ω-3 desaturase acting on a fatty acid chain would introduce a double bond three carbons in from the methyl end, i.e. between the 15^{th} and 16^{th} positions of an 18C chain.

There exists a large family of desaturase enzymes and their respective structures, mechanisms and regulation are of interest to a wide variety of disciplines due to the broad importance of unsaturated fatty acids in biological species. There are two categories of desaturase proteins: soluble plant desaturases that use fatty acyl carrier protein (ACP) thioesters as substrate and integral membrane-bound desaturases that act on fatty acyl CoA and phospholipid (PL) derivatives.[3]

The study of soluble plant desaturases has achieved significant success because it has been possible to obtain purified stearoyl-ACP Δ^9 desaturase from multiple sources, allowing for sufficient material to be produced for characterization in some cases.[5, 6] A crystal structure of the castor stearoyl-ACP Δ^9 desaturase was obtained showing the presence of a non-heme, carboxylate-bridged diiron core and a hydrophobic proposed substrate binding pocket.[5] This pocket is boomerang-shaped and can accommodate the ACP-bound substrate in a gauche conformation at the C9-C10 position, placing it near the diiron core (Figure 1.3).[5] This arrangement accounts for the regioselectivity exhibited by the Δ^9 desaturase.

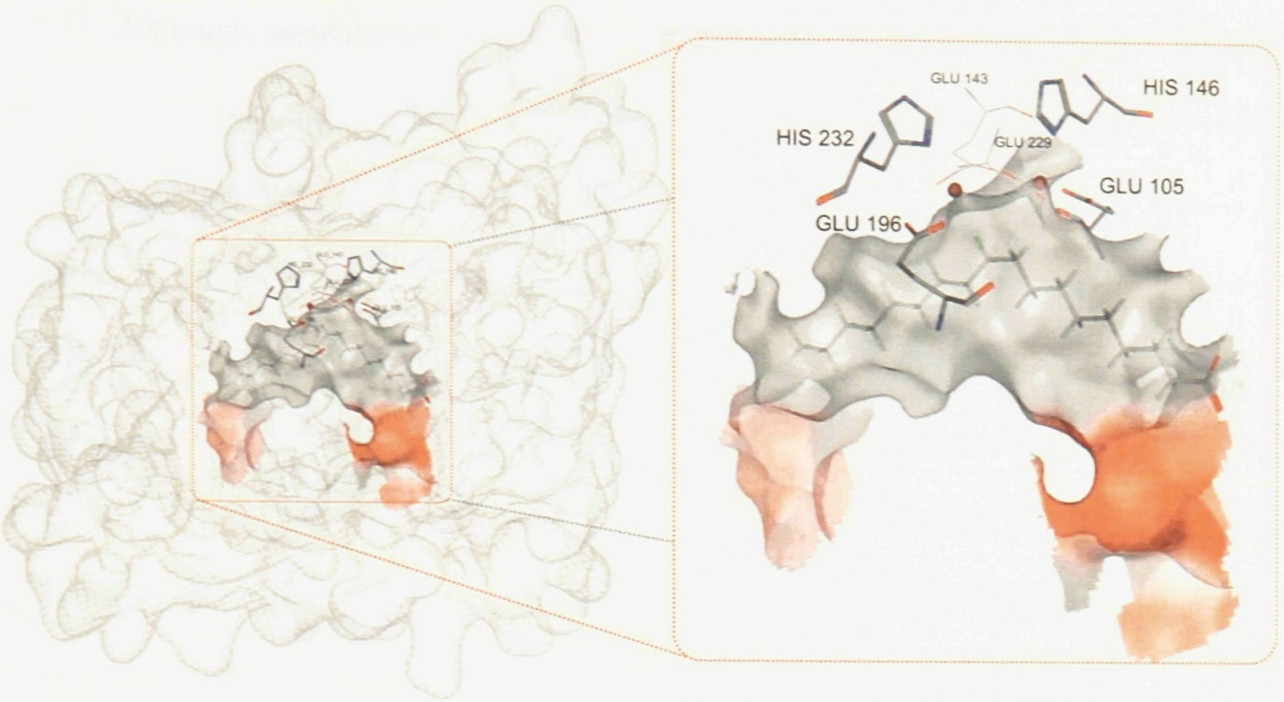

Figure 1.3 Computer model of the soluble castor Δ^9 desaturase (left) and C18 fatty acid modeled in the hydrophobic binding pocket (right); Image adapted from Lindqvist *et al.* [5]

Other soluble desaturases with different region- and chain length selectivities have amino acid sequences that are similar to that of the stearoyl-ACP Δ^9 desaturase.[7] A crystal structure of the soluble *Hedera helix* Δ^4 desaturase was recently obtained and a comparison of the amino acid sequence of this enzyme with the castor stearoyl-ACP Δ^9 desaturase showed 74% homology.[6]

For these desaturases, it is the residues lining the hydrophobic cavity that are responsible for the differing selectivities observed in this family of enzymes. It has been shown in site-specific mutagenesis experiments that substituting as few as two or five of the amino acids in this cavity have permitted the rational design of new enzymes with specificities for different chain lengths and different regiospecificities of double-bond insertion.[7]

Although membrane-bound desaturases have proven to be difficult to purify, some success was achieved in this area by the Strittmatter group who purified an integral membrane-bound stearoyl CoA Δ^9 desaturase from rat liver microsomes, along with its respective electron transport chain, consisting of NADH reductase and cytochrome b5 components.[3] Subsequent work by Shanklin and Fox showed that all membrane-bound desaturases feature eight essential histidines putatively coordinated to a diiron center.[8] Figure 1.4 shows the proposed topology of the membrane-bound Δ^{12} desaturase (Fad2) desaturase (the diiron site is represented as two light gray spheres in the upper centre of the figure).[9] While much information has been obtained through purification, structure-function studies of similar enzymes and site-directed mutagenesis experiments, a crystal structure has not been obtained for a membrane-bound desaturase. Consequently mechanistic investigation of this family of desaturases has been limited.[7]

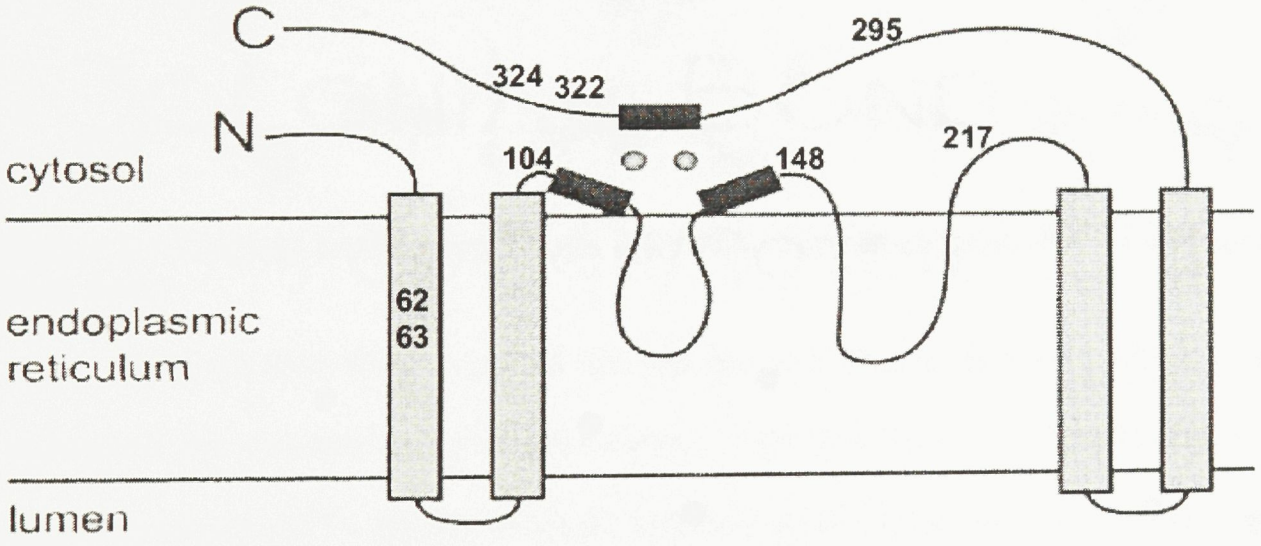

Figure 1.4 Proposed topology of the Fad2 membrane bound desaturase: Image adapted from Meyer *et al.*

The role and production of mono- and polyunsaturated fatty acids in biological systems are of interest to a wide variety of disciplines. Information obtained from studies of these enzymes can be useful to the field of enzyme engineering with the goal of modifying

the efficiency of enzymes or developing enzymes with different specificities to produce novel products. Success in this area could be applied to the area of neutraceutical production and the development of industrial feedstocks.[3] With the association of SCD with metabolic disorders, results obtained from studying desaturases can also be applied to the realm of pharmaceutical and drug design in an effort to develop specific enzyme inhibitors.

1.3 Mechanistic investigations of desaturases

The currently accepted model for the desaturation of fatty acid derivatives by both soluble and membrane-bound proteins is shown in Figure 1.5. Desaturation is initiated *via* abstraction of a hydrogen atom by a high-valent diiron-oxo species to form a carbon-centered radical/FeOH pair. This radical intermediate undergoes a rapid second hydrogen abstraction to give the unsaturated product and iron-bound water.[3]

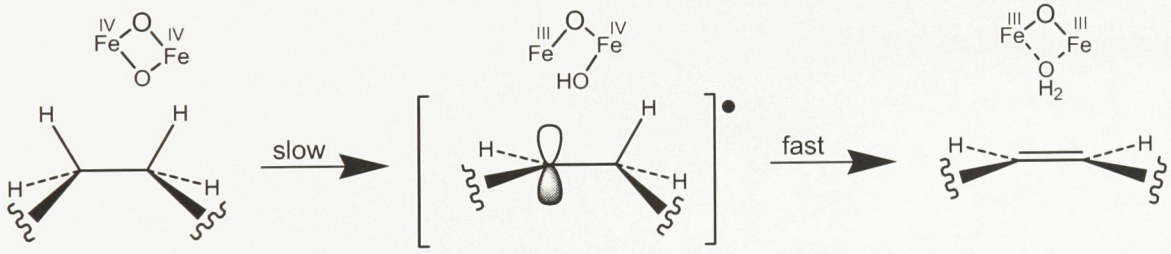

Figure 1.5 General mechanism for the desaturase-mediated formation of unsaturated fatty acids.

There are three features of this reaction that are being studied in an effort to better understand the structure-function relationships. The first aspect of desaturation is the cryptoregiochemistry[3] - the site of initial hydrogen atom abstraction. The second property that is worth examining is the enantioselectivity of desaturation - the determination of which hydrogen atom is removed at each prochiral centre. These two types of investigations give an indication of the position of the substrate with respect to the diiron site. The third important

problem to be solved involves understanding how desaturases prevent a competing hydroxyl transfer to the putative radical intermediate (chemoselectivity).

Information obtained from mechanistic investigations of desaturase enzymes is used to validate the structure of proposed substrate-enzyme complexes or to provide some structural information in the absence of crystallographic data.[10] Improved understanding of the mechanism of oxidation of desaturases and their structures can be exploited in the development of novel desaturase enzymes and in the intelligent design of enzyme inhibitors. If novel enzymes could be developed that offer unique regiospecificity, or modulated activity, they introduce the possibility of integrating them into plants in an effort to yield crops that produce a healthier fat content, or precursors to industrial materials such as polymers and resins.[11] Investigating the cryptoregiochemistry and enantioselectivity of desaturation is traditionally performed using labelled substrates while site-directed mutagenesis provides a tool to probe the chemoselectivity of the reaction. Both *in vivo* and *in vitro* experimental designs have been used in this type of work.

1.3.1 Cryptoregiochemistry

The cryptoregiochemistry (initial site of oxidation) of the dehydrogenation reaction has been most commonly determined using kinetic isotope effect (KIE) methodology.[12] The underlying theory is based on the fact that a carbon-deuterium bond has a higher energy barrier to cleavage than a corresponding carbon-hydrogen bond. The energy difference results in a significantly slower overall reaction rate if the breaking of a C-D bond in comparison to a C-H bond is kinetically important and not masked by other enzymatic events.

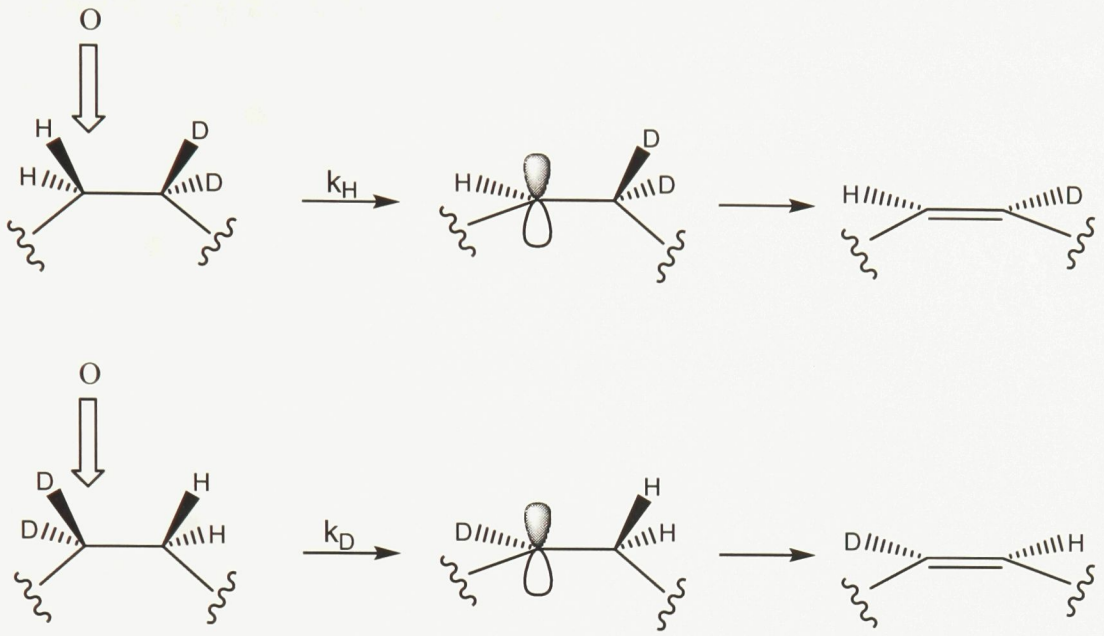

Figure 1.6 Schematic diagram of KIE effects on the 1st (rate limiting) step of desaturation.

If a 1:1 ratio of regioselectively dideuterated and non-labelled substrate is incubated with a desaturase, the KIE can be measured by quenching the reaction prior to completion and measuring the relative amount of mono-deuterated to non-labelled product. A primary deuterium KIE is only observed for the rate determining step of the reaction and is used to determine the initial site of oxidative attack since the first hydrogen abstraction is slower and thus more sensitive to isotopic substitution than the second C-H bond cleavage.[12]

Interestingly, in the case of soluble plant desaturases, the initial hydrogen abstraction is not kinetically important relative to substrate binding or product release.[13] Therefore the replacement of a hydrogen atom with deuterium at the oxidizable positions does not measurably affect the rate of reaction and so an alternative method that had been developed for membrane-bound fatty acids has been used by Buist *et al.*[3] A sulfur atom substituted in the place of a substrate methylene group can act as an oxygen trap resulting in the formation of sulfoxy-fatty acid (Figure 1.7).[3] It has been shown that when a mixture of substrates with

a sulfur atom in either position of the reaction site is introduced to a desaturase enzyme, the relative sulfoxide production for each positional isomer can be used to determine the cryptoregiochemistry of the reaction.[14] The analysis of this reaction may be performed with mass spectrometry (MS), or nuclear magnetic resonance (NMR) spectroscopy.

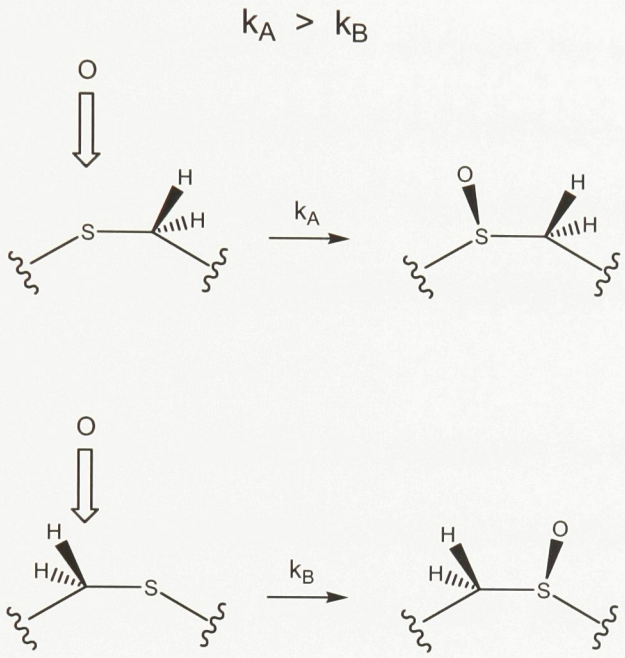

Figure 1.7 Schematic diagram of desaturase-mediated sulfoxide formation.

It is unobvious, based on protein structural data, which hydrogen atom is abstracted first in the desaturation process. To date, the trend appears to be that the membrane-bound desaturases initiate the reaction at the carbon nearest the carboxyl (C1) moiety. Due to the difficulty mentioned above in ascertaining the cryptoregiochemistry of soluble desaturases using traditional methods, there is limited data available for this class of enzymes, however using the thia method, there is some indication that at least one soluble desaturase behaves contrary to the membrane-bound desaturases and the initial site of oxidation is at the carbon nearer the terminal methyl group.[3, 15]

1.3.2 Enantioselectivity

The enantioselectivity of the hydrogen abstraction in the desaturation of fatty acids has been typically studied using stereospecifically deuterated- or tritiated-substrates.[3] The product of the desaturation from deuterated substrates is conveniently analyzed using gas-chromatography/mass spectrometry (GC/MS) to determine the fate of an isotopic label (Figure 1.8). For all desaturases studied to date, it has been shown that both hydrogens are removed with pro-*R* (or equivalent) selectivity.[3] The hydrogen removal occurs in a *syn*-fashion from a quasi-eclipsed substrate conformation resulting in the formation of *Z*-double bonds, as shown in Figure 1.2.

Stereospecifically labelled substrates can sometimes be produced from naturally occurring chiral alcohols of known configuration. *De novo* synthetic methods have also been developed including a general method employing chiral epoxides as precursors to the labelled substrates.[16]

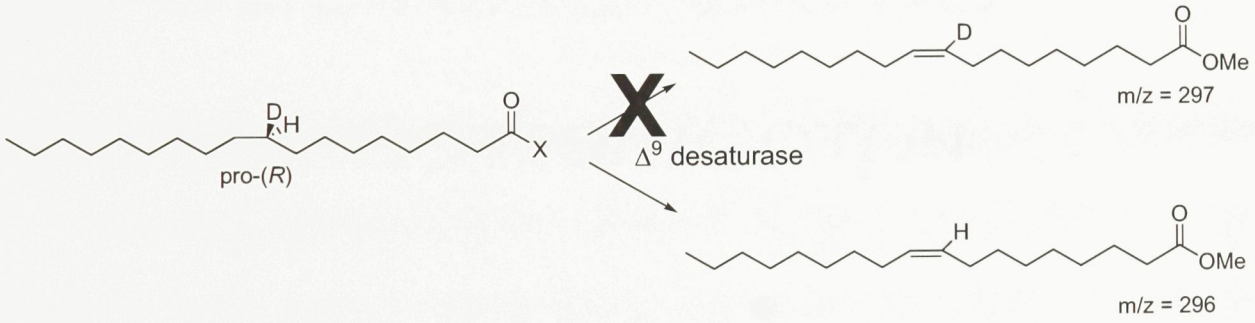

Figure 1.8 Determining enantioselectivity using isotopically-labelled substrates.

A more recent method for tracking desaturase stereochemistry developed by Buist *et al.* obviates the need for the synthesis of chiral substrates. This method employs the same thia-fatty acid substrates described above that are used in cryptoregiochemical studies (Section 1.3.1).[14] The oxo-transfer reaction that occurs upon incubation of selected thia-fatty acid analogues with a desaturase results in the production of sulfoxides in high enantiomeric

excess (Figure 1.9). To date, the absolute configuration of the sulfoxide produced has matched the enantioselectivity of hydrogen removal determined via isotopically-labelled substrate experiments.[14] The stereochemistry of sulfoxides can be elucidated by examining the effect of a chiral solvating agent (CSA) on the NMR chemical shift of suitable reporter groups on the analyte (Figure 1.10).

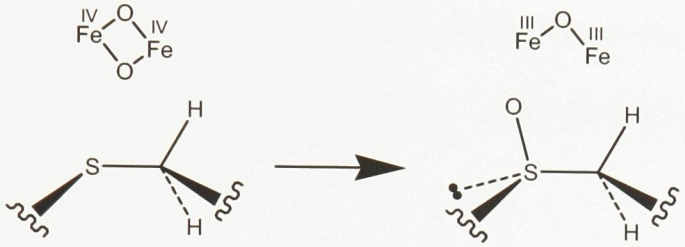

Figure 1.9 Oxidation of thia-fatty acid analogue by a desaturase.

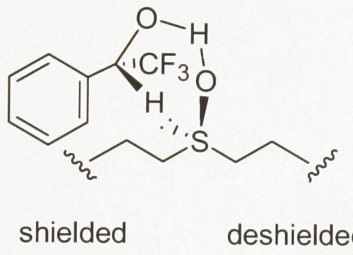

Figure 1.10 Effect of CSA / sulfoxide complexation on the NMR shifts of neighbouring atoms.

1.3.2.1 Chiral solvating agents applied to the NMR analysis of sulfoxides

The Pirkle bonding model of a chiral solvating agent with a sulfoxide is shown in Figure 1.10. This collision complex features a hydrogen bond between the acidic alcohol proton and the oxygen of the sulfoxide.[17] In addition, a stabilizing interaction between the lone pair of the sulfoxide and the methine of the CSA has been proposed to account for the specific shielding effects.[17]

The presence of an aromatic group on the CSA induces a shift non-equivalence in selected signals in the NMR spectrum of the complexed sulfoxide.[17] The magnitude of this

non-equivalence has been shown to increase with the use of larger aromatic systems (i.e. anthryl in place of benzyl).[18]

To apply the Pirkle technique to the stereochemical analysis of chiral sulfoxy-fatty acid analogues, the CSA, (*S*)-methoxyphenylacetic acid ((*S*)-MPAA), was validated using an enantiomerically enriched dibutyl sulfoxide, (*R*)-dibutyl-d_9 sulfoxide, a molecule that is chiral by virtue of isotopic substitution.[14] In this study, it was shown that both the ^{1}H and ^{13}C NMR chemical shift induced non-equivalences could be predicted using a Pirkle-type binding model.[14]

1.3.3 Chemoselectivity

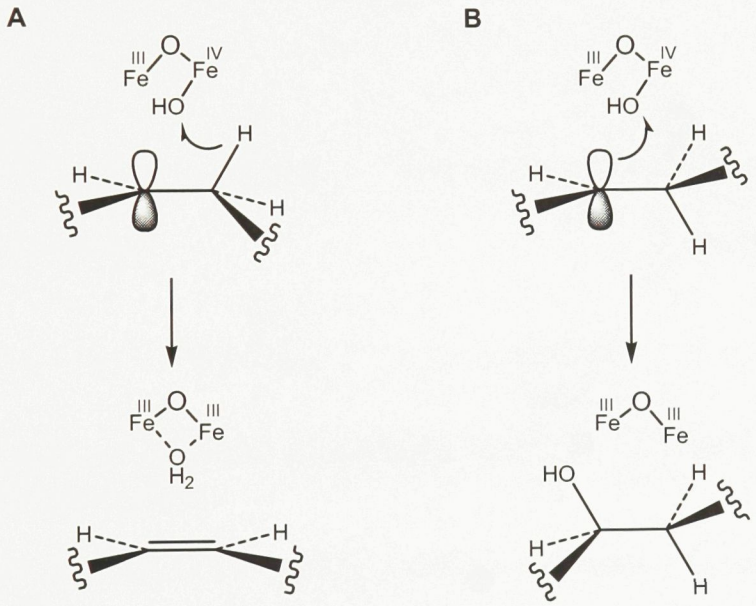

Figure 1.11 Dehydrogenation (A) and hydroxylation (B) pathway of desaturase-catalyzed oxidation.

The consensus mechanism of enzyme-catalyzed desaturation involves the initial abstraction of a hydrogen atom by a high-valent diiron-dioxo species to form an iron-bound hydroxyl / carbon-centered radical pair. A second hydrogen atom abstraction results in iron-bound water and the unsaturated product (Figure 1.11 **A**).[3] Interestingly, in the case of membrane-bound desaturases, a competing hydroxyl rebound pathway, following the initial

hydrogen abstraction, results in the formation of a secondary alcohol by-product (Figure 1.11 **B**).[3] This reaction pathway can be rationalized by noting the similarity of the diiron centre of desaturases to that of methane monooxygenase (MMO), an enzyme that catalyzes the production of methanol from methane.[7] It is also noteworthy to consider the case of hepatic cytochrome p450. This hydroxylase features a mono-iron core, but in some cases has also been shown to result in the dehydrogenation of substrates.[3] Based on similarities between these families of enzymes, three theories have been proposed to account for the relative preference between desaturation and hydroxylation in similar enzymes. These theories consider either electronic, steric or thermodynamic effects; however the factor(s) contributing to the remarkable chemoselectivity of desaturases remains an unresolved issue.[3]

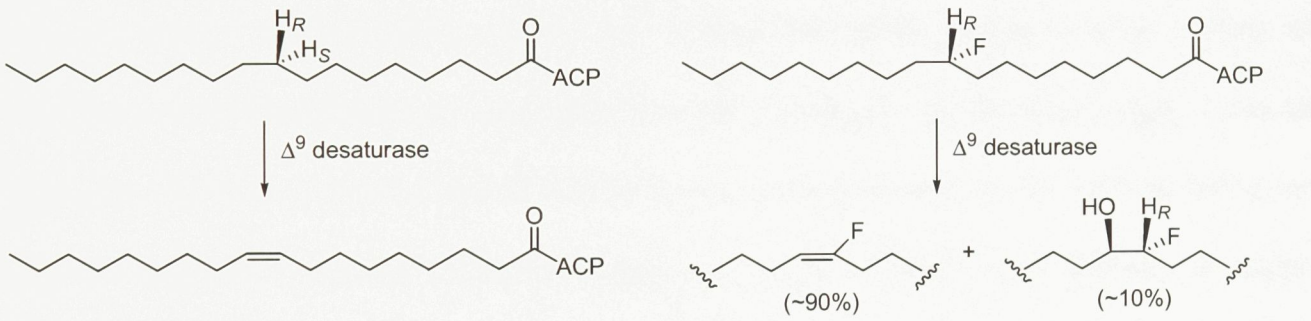

Figure 1.12 The soluble Δ^9 desaturase-mediated oxidation of stearate (left) and a (9*S*)-fluorine-tagged analogue (right).

A consideration of electronic effects involves the redox potential of the short-lived enzyme-bound intermediate (Figure 1.5, centre). Both desaturation and hydroxylation are thought to be initiated by the abstraction of a hydrogen atom. It is possible that a carbon-centered radical will quickly undergo hydroxyl rebound to yield a hydroxylated product.[3] If, however, the radical intermediate can be oxidized to a carbocation by the diiron oxidant, deprotonation will be favoured and olefinic product formed.[3] Evidence for this theory is derived from experiments using fluorinated substrates and soluble stearoyl ACP desaturase

(Figure 1.12). The presence of a fluorine atom at the 9th position (with the 10th position being the site of initial oxidation) resulted in the formation of some 10-hydroxylated product.[19] In this case, it is suggested that the strongly electron-withdrawing nature of the fluorine atom would hinder the formation of a carbocation via a β-inductive effect and hydroxylation is observed.[19]

The example cited above can also be used to support a steric switch controlling the fate of dehydrogenation versus hydroxylation if the fluorine atom perturbs the positioning of the substrate in the active site. The steric argument holds that there must be a *syn*-periplanar alignment of the C-H bond orbital β to the carbon-centred radical that is produced after the abstraction of the first hydrogen atom; in addition, the iron-hydroxy species must be in the correct position to abstract the second hydrogen atom to result in dehydrogenation.[3] Given that the known hydroxylators, MMO and cytochrome p450, accept a wide variety of substrates while desaturases are very specific to fatty acids of a given chain length, it can be reasoned that there is much more flexibility in the binding cavities of the hydroxylators and thus the alignment required for dehydrogenation would be much more unlikely to occur: hydroxylation is the default reaction pathway.[3] Conversely, the binding pocket of the desaturases which are usually specific to a single substrate can be assumed to be more constrained, severely limiting the mobility of the substrate and thus optimizing the alignment of the requisite atoms and orbitals. Further evidence for this idea were obtained by the results of site-directed mutagenesis experiments on a membrane-bound bifunctional 12-hydroxylase/12-desaturase. Modification of selected hydrophobic residues lining the substrate cavity resulted in an increase in the ratio of hydroxylated- relative to dehydrogenated product.[3]

Thermodynamic arguments consider the ligand environment of the iron centre and the formation of the iron-bound water complex. Clavaminate synthase 2 catalyzes hydroxylation followed by oxidative ring closure and desaturation to yield clavulanic acid from deoxyguanidoproclavaminic acid (DGPC) (Figure 1.13).[20] The switch between hydroxylation and desaturation is essentially determined by the relative stability of the iron-bound water complex, which is in turn subtly affected by how the different substrates bind in the active site cavity. A more stable iron-water complex will favour dehydrogenation over hydroxylation (Figure 1.11).[20]

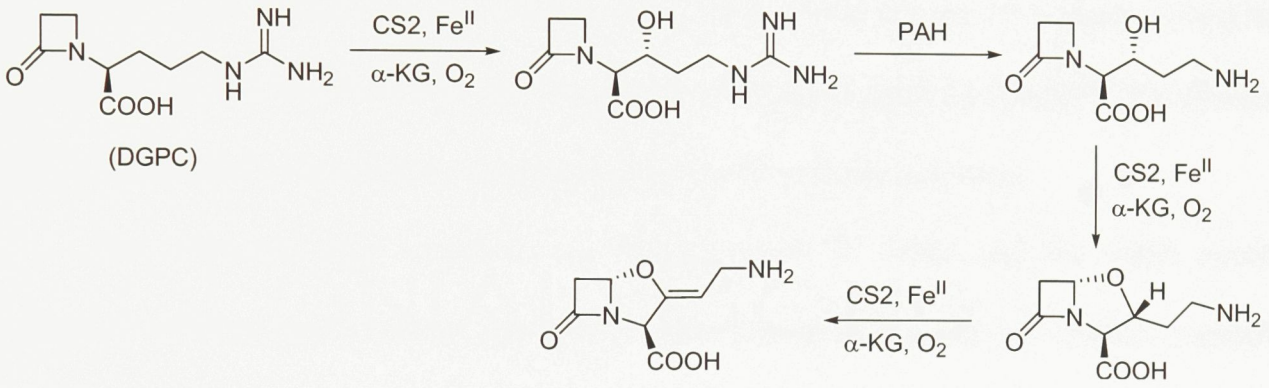

Figure 1.13 Biosynthetic pathway of clavulanic acid.[20]

All three of these effects likely contribute to the chemoselectivity to some degree, but their relative importance remains unknown. Further advances in this area of study may be obtained through site-directed mutagenesis experiments of structurally defined desaturases such as the soluble castor Δ^9 desaturase. Also, further information on active site architecture of this enzyme can be obtained by determining the cryptoregiochemistry and enantioselectivity of desaturase-mediated oxidation of substrate analogues. Some recent results in this area of research that have been obtained in collaboration with the Shanklin group at Brookhaven National Labs and the Biologics groups at Health Canada are featured in the Results and Discussion sections of this thesis.

Chapter 2: Results and Discussion

2.1 Determination of the enantioselectivity of soluble Δ^9 desaturase-mediated sulfoxidation using fluorine-tagged substrates

2.1.1 Introduction

2.1.1.1 Use of ^{1}H-decoupled ^{19}F NMR in the study of desaturase-mediated oxidation

Mechanistic investigations of desaturases can be simplified with the incorporation of a fluorine tag in the substrate in combination with the use of ^{1}H-decoupled ^{19}F NMR spectroscopy. The introduction of a fluorine atom remote from the site of oxidative attack has been shown to not interfere with the desaturase-mediated dehydrogenation;[21] the fluorine atom is considered to function as a hydrogen isostere in optimal situations.

The inherently high sensitivity of ^{1}H-decoupled ^{19}F NMR and the 100% natural abundance of fluorine-19 allows detection of the nanomole amounts of product typically obtained in enzymatic reactions.[21] Another significant advantage is the elimination of the need to significantly purify the product owing to the absence of fluoroorganics in most biological systems. Analysis can be performed on crude material without interference from the sample matrix.[21]

The NMR resonance of a fluorine atom is very sensitive to changes in the oxidation state of a sulfur atom as far as 10 bonds away.[21] This can be taken advantage of for determinations of cryptoregiochemistry. The ability to distinguish between a sulfido and a sulfoxy moiety in the fatty acid chain leads to the ability to measure the relative amounts of sulfoxides produced from a mixture of positional thia-isomers. This approach can be used for the study of both soluble and membrane-bound desaturases and to date, assignment of cryptoregiochemistry via the thia and KIE test give similar results.[3]

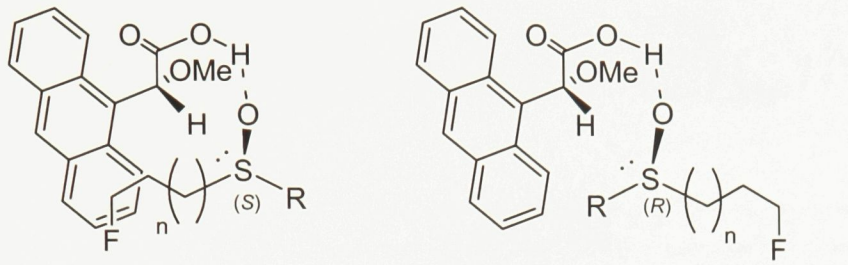

Figure 2.1 Pirkle-type binding model of (*R*)-AMA with an (*S*)- (right) and (*R*)- (left) configured fluorine-tagged dialkyl sulfoxide.

The stereochemistry of the desaturase-catalyzed oxidation of a fluorine-tagged thia fatty acid analogues can also be determined using chiral solvating agents in combination with ^{1}H decoupled ^{19}F NMR spectroscopy.[22] The induced non-equivalence of the remote fluorine reporter group can be predicted based on the shielding effects anticipated in the collision complex of a CSA with the chiral sulfoxide using a Pirkle-type binding model (Figure 2.1).[17, 23] Spiking experiments with racemic sulfoxide mixtures are then used to provide a reference signal to allow the assignment of the stereochemistry of the product.

2.1.1.2 Efforts to determine the enantioselectivity of soluble Δ^9 desaturase-mediated sulfoxidation

The stereochemistry of desaturase-mediated sulfoxidation of 9- or 10- thiasubstrates by the membrane-bound yeast Δ^9 desaturase agrees with the known stereochemistry of hydrogen removal (*pro-R*) for the parent substrate.[3] The corresponding dehydrogenation reaction catalyzed by castor stearoyl-ACP Δ^9 desaturase also occurs with pro-*R* selectivity.[3] This enzyme produces a 10-sulfoxide product from a 10-thiasubstrate (Figure 2.2).[15]

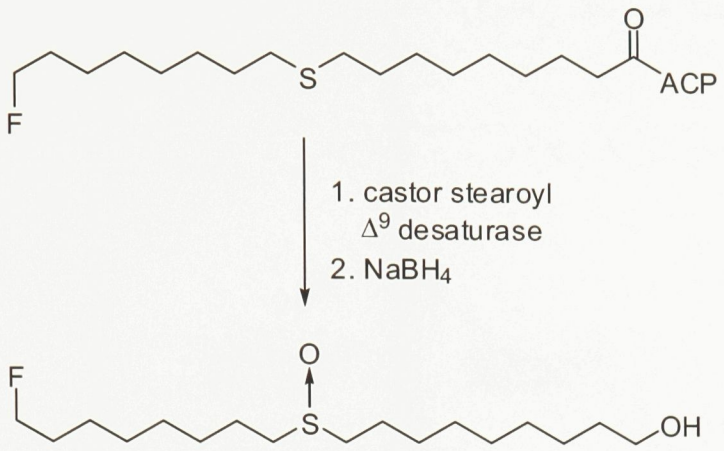

Figure 2.2 Sulfoxide product obtained from incubating 18-fluoro-10-thiastearate as the acyl-ACP with castor stearoyl Δ^9 desaturase.

To study the stereochemistry of 10-sulfoxidation, an ω-fluoro, C10 thia fatty acid analogue was employed and the corresponding 10-sulfoxide product was isolated as the C1-alcohol after reductive workup (Figure 2.2). The stereochemistry of this product was studied using ^{19}F NMR in combination with the CSA, (*R*)-(9-anthryl)methoxy acetic acid ((*R*)-AMA).[24] In the presence of the solvating agent, the enzymatic product exhibited one peak in the ^{19}F NMR spectrum (data not shown). Spiking the product with a racemic mixture of synthetic 18-fluoro-10-sulfoxy-1-octadecanol (obtained through the *m*-CPBA (*meta*-chloroperbenzoic acid) oxidation of the corresponding sulfide) resulted in an enhancement of the product signal (major peak), while the other enantiomer serves as a reference (minor peak) (Figure 2.3). The large peak to the left of the spectrum results from unreacted starting material, 18-fluoro-10-thia-1-octadecanol.

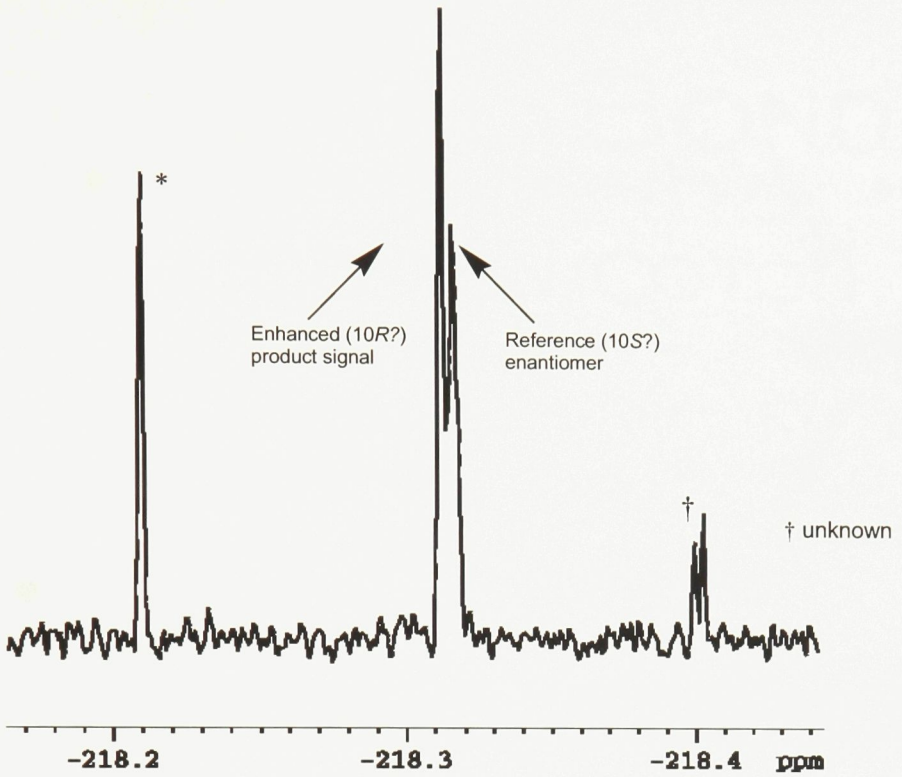

Figure 2.3 Effect of (*R*)-AMA on the ^{1}H-decoupled ^{19}F NMR spectrum of a mixture of enzyme product and racemic 18-fluoro-10-sulfoxy-1-octadecanol. (* Starting material)

This result, when interpreted using a Pirkle-type model[17] suggests that the sulfoxidation occurred with very high pro-(*R*) selectivity (which would be considered equivalent to pro-(*S*) in the absence of the fluorine label). This conclusion was arrived at based on the following consideration: the binding model below shows that the fluorine signal in the (*S*)-enantiomer would be expected to be shielded with respect to the (*R*)-enantiomer (Figure 2.4) in the NMR spectrum.

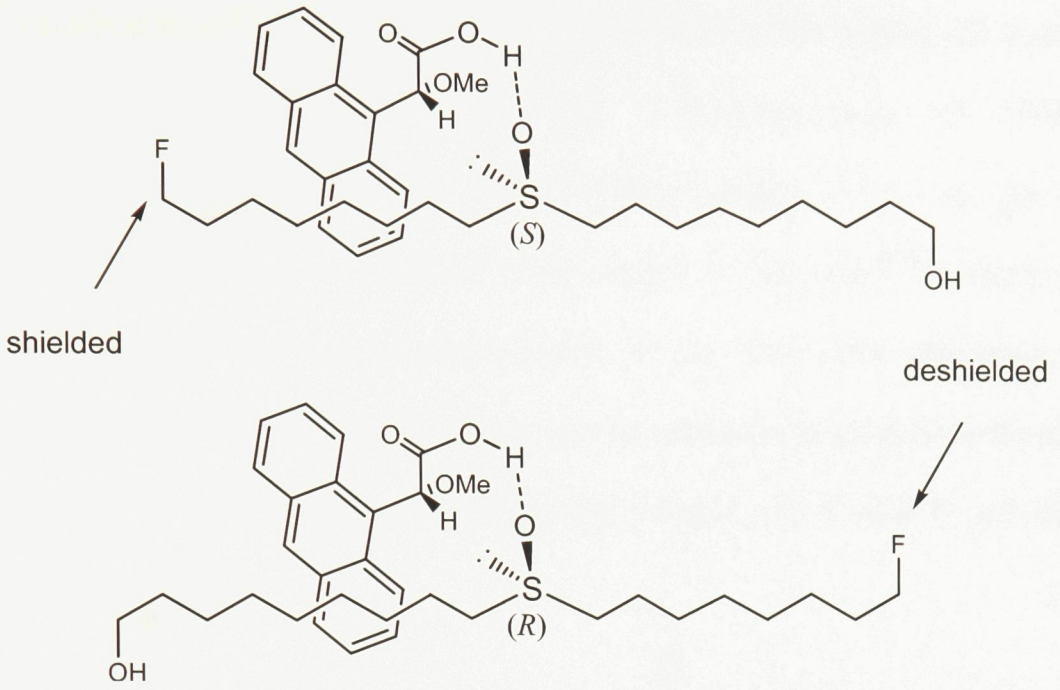

Figure 2.4 The collision complex of (10*S*)- (above) and (10*R*)-18-fluoro-10-sulfoxy-1-octadecanol (below) interacting with the NMR shift agent, (*R*)-AMA, based on a Pirkle-type binding model.

This analysis implied that the stereochemistry of oxo transfer to sulphur by castor stearoyl ACP Δ^9 desaturase did not match that of hydrogen removal for the parent substrate (cf. Figure 1.3).[19] This interpretation would echo a recent example of a cytochrome p450-mediated sulfoxidation of a long chain thia fatty acid which has been shown to occur with the opposite stereochemistry relative to hydroxylation at a methylene group in the same position.[25] However, an alternative explanation for our results would be that the Pirkle binding model shown in Figure 2.4 is not valid for this pair of enantiomers.

2.1.2 Project goals

The aim of this part of the thesis was to test the validity of the Pirkle binding model in the stereochemical analysis of fluorinated sulfoxy fatty acid analogues using ^{19}F NMR. To achieve this, enantiomerically enriched synthetic sulfoxy fatty acid analogue standards were required. The target compounds included the (10*S*)- and (10*R*)-enantiomers of 18-fluoro-10-

sulfoxy-1-octadecanol (**18F-(10*S*)SO-OH** and **18F-(10*S*)SO-OH**) (Figure 2.5 A and B). In addition, the synthesis of the (11*S*)- and (11*R*)-enantiomers of 15-fluoro-11-sulfoxypentadecane (**15F-(11*S*)SO** and **15F-(11*R*)SO**) (Figure 2.5 C and D) was also planned to test the validity of the published results of K.Y.Y. Lao *et al.*[22] in which the use of ^{19}F NMR as a probe for the stereochemistry of the fatty acid desaturase-mediated sulfoxidation reactions was introduced. Finally, it was necessary to synthesize the chiral shift agents (*R*)- and (*S*)-(9-anthryl)methoxyacetic acid (Figure 2.5 E and F) for use in the stereochemical analysis.

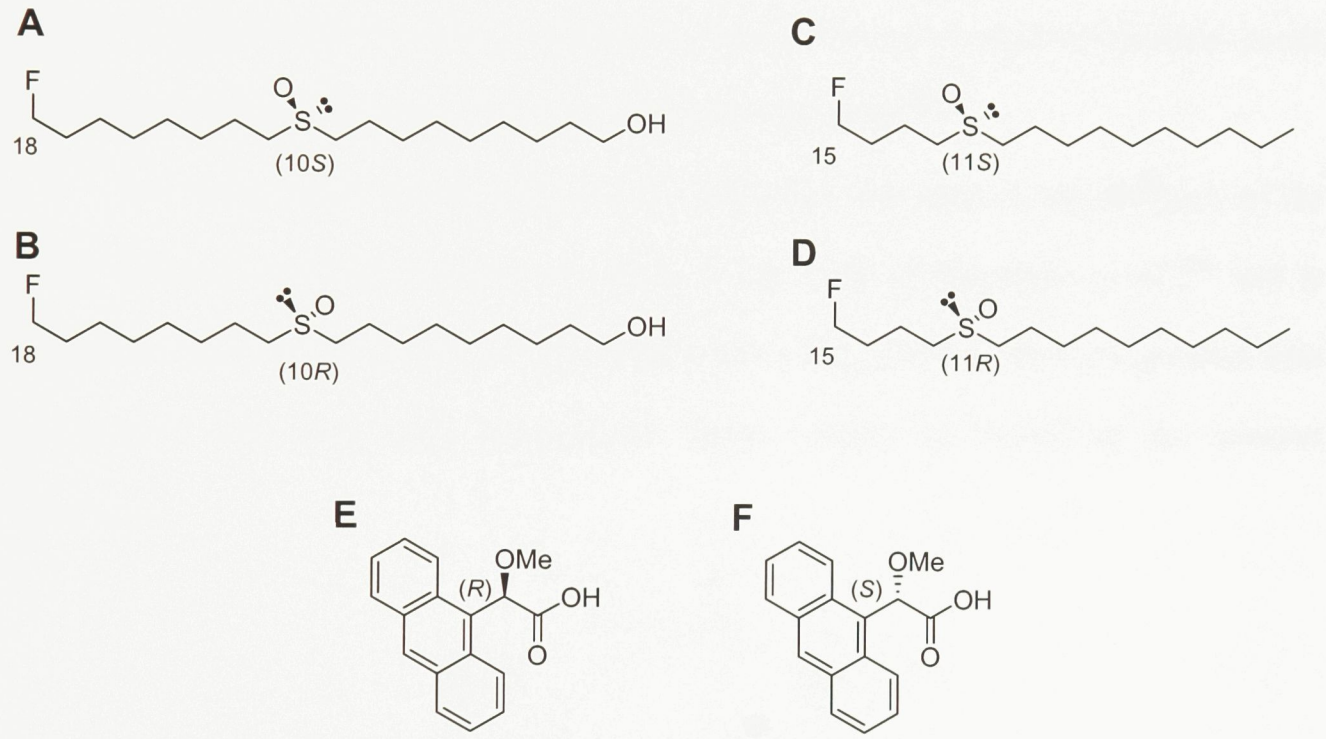

Figure 2.5 Target compounds: A. 18F-(10*S*)SO-OH; B. 18F-(10*R*)SO-OH; C. 15F-(11*S*)SO; D. 15F-(11*R*)SO; E. (*R*)-AMA; F. (*S*)-AMA.

2.1.3 Synthesis of fluorine-tagged chiral sulfoxide standards

Two principal methodologies exist for the chemical synthesis of chiral sulfoxides i) the asymmetric oxidation of a prochiral sulfide and ii) the nucleophilic attack on a sulfinate ester of established chirality to yield the sulfoxide by displacing an alcohol.[26] Since our

synthetic targets were quasi-symmetrical dialkyl sulfoxide, asymmetric oxidation was not considered.[27]

Asymmetric sulfoxide syntheses involving the nucleophilic attack on a sulfinate ester differ chiefly in the type of chiral alcohol group used to form the sulfinate ester.[28] The Andersen synthesis is the prototypical method, which involves the formation of a diastereomerically enriched menthyl sulfinate ester as a synthetic intermediate.[29] This methodology was used in a previous research project; however the yields and the enantiomeric excess obtained were low.[30] Furthermore, the presence of the fluorine tag, which is required for the target compounds, resulted in an unexpected obstacle in the formation of the product which was not overcome at that time.[30]

For this project, diacetone-D-glucose (DAGOH) was used in the synthesis of the chiral sulfinate ester intermediates according to the work of Fernandez *et al.*,[26] and is referred to herein as DAG methodology (Figure 2.6). This method is shown to produce both enantiomers with very high enantiomeric excess simply by modifying the reaction conditions.

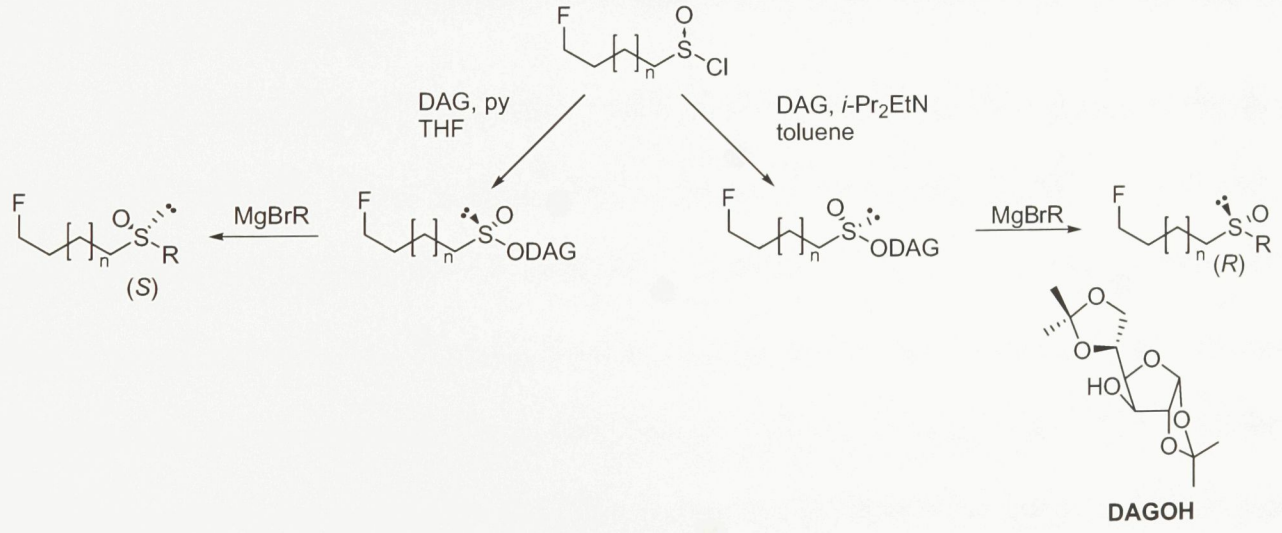

Figure 2.6 General route for the synthesis of both enantiomers of fluorine-tagged chiral dialkyl sulfoxides.

The formation of the DAG sulfinate ester is thought to occur through the addition of the alcohol moiety of DAGOH to the sulfur centre of a sulfinyl chloride via an H-bonded trigonal bipyramidal transition state (Figure 2.7).[31] A tertiary amine base is thought to participate through the formation of an N-H bond with the hydrogen atom being transferred (Figure 2.7). The sulfinyl chloride is proposed to undergo pyramidal inversion in the presence of the tertiary base allowing for high reaction yields of diastereomerically enriched product from this racemic starting material.[32] The product is usually formed with high diastereometric excess; the stereochemistry of the product mixture depending on the nature of the tertiary amine that is used. At higher reaction temperatures, an equimolar mixture of diastereomers is produced but these can be isolated through chromatographic separation.[26]

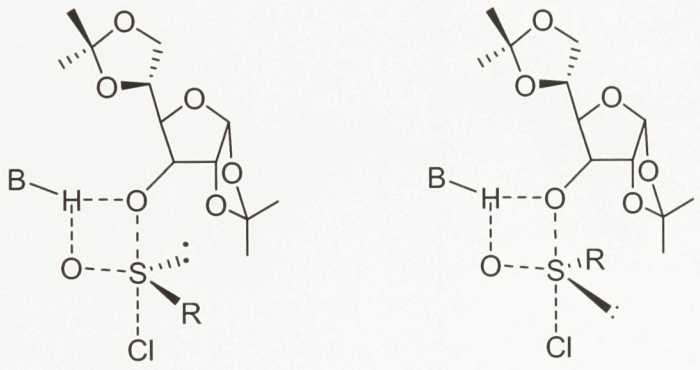

Figure 2.7 Transition states for the formation of the DAG sulfinate esters showing the interaction of the base, B.

When a less sterically active base, such as pyridine is used, the reaction proceeds to give the (*R*) sulfinate; when a bulkier base, such as diisopropylethyl amine or collidine is used, the pathway yielding the (*S*) sulfinate is preferred.[31] Steric interactions have been studied computationally for transition states of each of the four cases and the proposed rationalization for the observed diastereoselectivity is shown in Figure 2.8.[31] The upper half of the figure shows the most stable transitions states for the formation of the *R*- (left) and the *S*- (right) diastereomers when pyridine is used. The base is coplanar with the H-O-S-O plane.

The transition state leading to the *R*- diastereomers is 1.0 kcal mol^{-1} more stable that that of the *S* pathway with the major steric repulsion resulting from the interaction of the alkyl group of the sulfinyl chloride with the bicyclic region of the DAG group.[31]

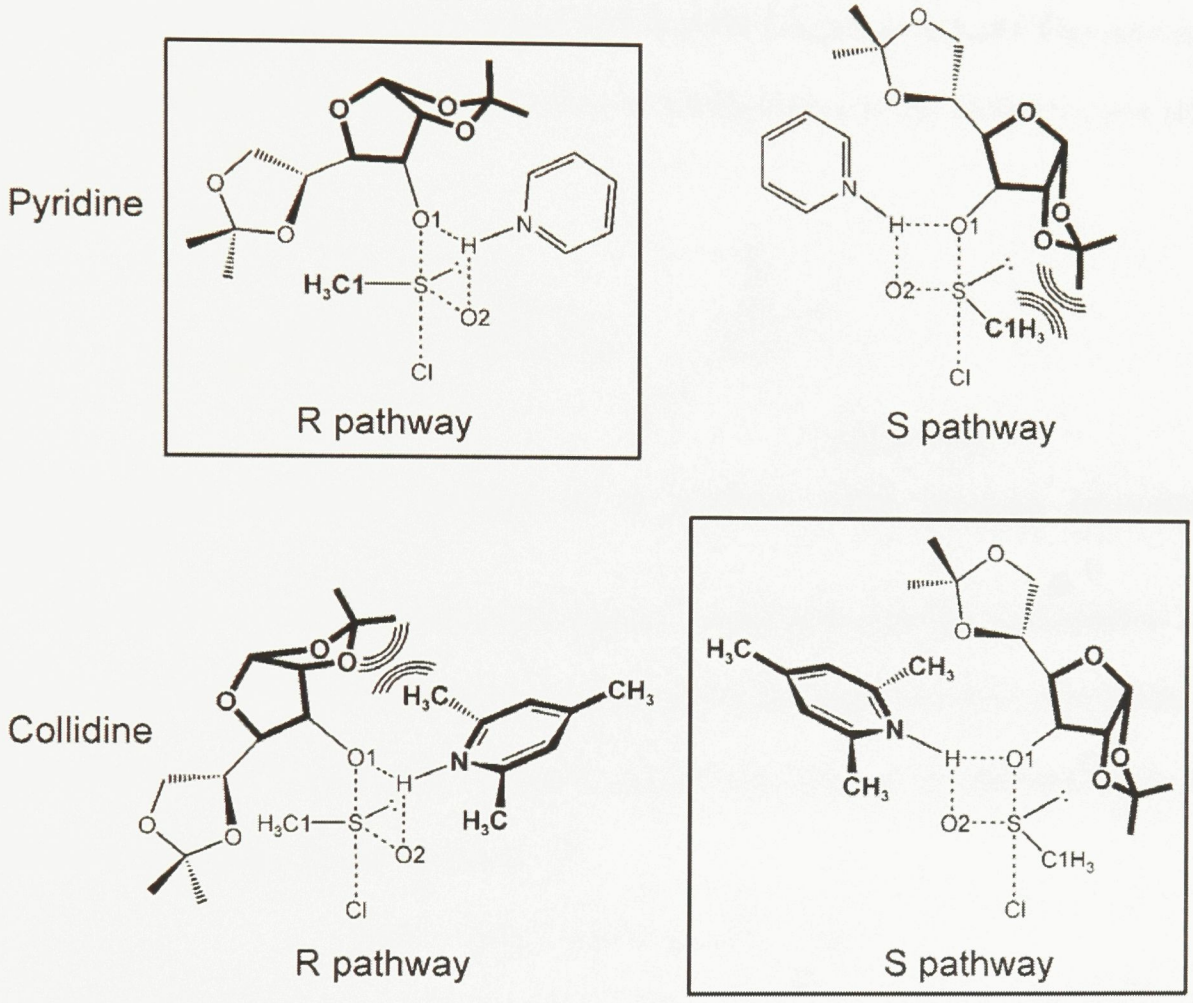

Figure 2.8 Predicted steric interactions leading to the diastereoselectivity in DAG sulfinate ester formation. Use of pyridine (above) results in the formation of the *R* diastereomers; Use of collidine (below) yields the *S* diastereomer. Image adapted from Balcells *et al.*[31]

The most stable transitions states using the bulkier collidine base are shown in the lower half of Figure 2.8. In this case, the most stable geometries show the base to be aligned perpendicularly to the H-O-S-O plane. This results in the steric repulsions between an ortho methyl group of the base and the bicyclic group of the DAG being the more critical interactions in determining the pathway of the reaction.[31] The transition state leading to the

formation of the *S*-DAG sulfinate ester is favored by 2.2 kcal mol^{-1} over that leading to the *R*-DAG sulfinate ester.[31]

To obtain the desired chiral, dialkyl sulfoxide product, the diastereomerically enriched DAG sulfinate esters were treated with suitable Grignard reagents. This substitution reaction is known to occur with an inversion of configuration at the sulfinyl centre (Figure 2.9).[33]

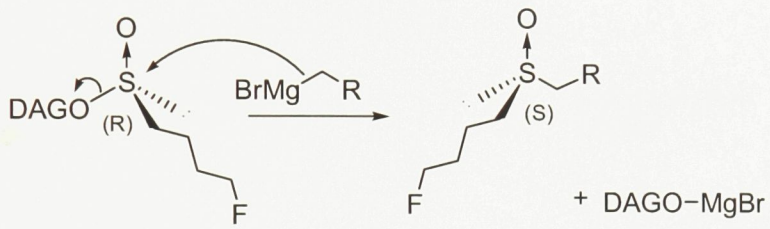

Figure 2.9 The Grignard reaction of a sulfinate ester showing inversion of configuration.

Overall, the synthetic routes were chosen to minimize possible racemization of the sulfoxy centre. Sulfoxides are known to racemize in the presence of acid or base. In the case of hydrochloric acid, this is due to a dynamic equilibrium between the sulfoxide and a sulfur dichloride intermediate, as shown below. [34]

$$R_2SO + 2HCl \rightleftharpoons R_2SCl_2 + H_2O$$

In addition, the use of oxidative reagents can result in the over-oxidation of the sulfoxide moiety to produce the sulfone analogue. For this reason, once the sulfoxide is produced, any subsequent reactions must avoid the use of strong acids, bases and oxidants and be done in a timely manner.

2.1.3.1 Synthesis of (10*R*)- and (10*S*)-18-fluoro-10-sulfoxy-1-octadecanol

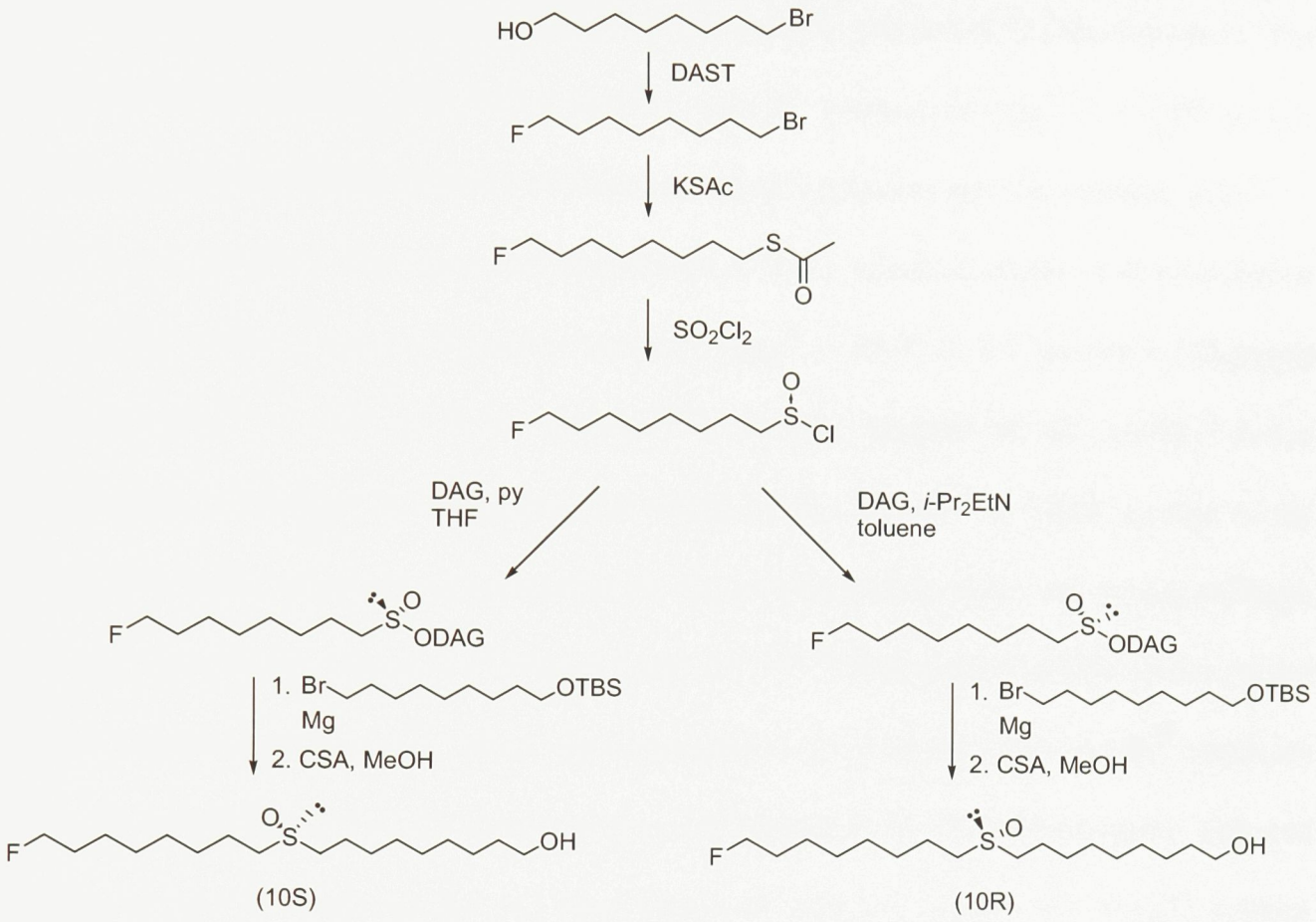

Figure 2.10 Scheme for the synthesis of (10*R*)- and (10*S*)-18-fluoro-10-sulfoxy-1-octadecanol.

The synthesis of **18F-(10*S*)-SO-OH** and **18F-(10*R*)-SO-OH** was achieved with overall yields of 31% and 13% respectively starting with commercially available 8-bromo-1-octanol. The fluorine tag was introduced via diethylaminosulfur trifluoride (DAST) fluorination[35] of the alcohol moiety of the starting material (95% yield). The sulfinyl chloride functional group was introduced in two steps, first a nucleophilic displacement of the bromide by thiolacetate[36] (97%) followed by sulfuryl chloride oxidation.[37, 38]

The (*R*)- and (*S*)-diastereomers of 1,2:5,6-di-*O*-isopropylidene-α-D-glucofuranosyl-8-fluorooctanesulfinates (**8F-(*R*)-O-DAG** and **8F-(*S*)-O-DAG**) were formed from the sulfinyl chloride in yields of 62 and 30% (purification by flash chromatography (40% EtOAc/hex)),

using diisopropylethyl amine and pyridine, respectively, as bases. The absolute configuration of the sulphur centres were assigned based on the specific rotation of the diastereomers. The **8F-(*R*)-O-DAG** sulfinate ester had a positive specific rotation of $[\alpha]_D^{21}$ = +1.39° (*c* 1.1, acetone), while the **8F-(*S*)-O-DAG** sulfinate ester had a negative specific rotation, $[\alpha]_D^{21}$ = -36.2° (*c* 1.2, acetone). The signs and magnitudes of these values correlate well with similar alkyl DAG sulfinate esters ((*R*)-propyl sulfinate: $[\alpha]_D^{25}$ = +6.4° (*c* 1.1, acetone), (*S*)-propyl sulfinate: $[\alpha]_D^{25}$ = -33° (*c* 0.54, acetone)[26]). Further support of the configurational assignments is obtained by comparing the trends in the ^{1}H and ^{13}C NMR spectra of the fluorinated DAG sulfinates with the data for the corresponding butyl and propyl sulfinate esters as found in the literature (Tables 2.1 and 2.2).[26, 39] Particularly helpful in this regard are the comparisons of the ^{13}C NMR shifts assigned to C1-4 on the DAG moiety, which are all more deshielded in the (*R*) diastereomers with respect to the (*S*) diastereomers. Selected signals in the ^{1}H NMR spectra are also diagnostic with the signals for the H2 protons appearing deshielded and the H3 shielded for the (*R*) and (*S*) respectively.

Table 2.1 ^{13}C NMR data for the 8-fluorooctyl- and 4-fluorobutyl DAG sulfinate esters* (Section 2.1.3.2) as well as the literature values for the butyl[39] and propyl[26] sulfinate esters with diagnostic peaks in bold.

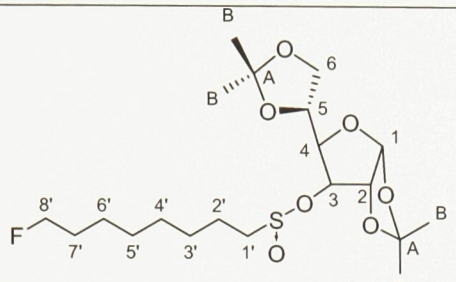

	8F-O-DAG		4F-O-DAG*		Butyl-O-DAG		Propyl-O-DAG	
Assignment	(*R*)	(*S*)	(*R*)	(*S*)	(*R*)	(*S*)	(*R*)	(*S*)
1	**105.35**	**104.97**	**105.31**	**104.96**	**106.00**	**105.64**	**105.47**	**105.05**
2	**83.84**	**83.61**	**83.79**	**83.57**	**84.48**	**84.28**	**84.09**	**83.78**
3	**80.93**	**79.21**	**80.88**	**79.28**	**81.61**	**79.81**	**81.18**	**79.19**
4	**83.05**	**80.38**	**83.14**	**80.35**	**83.70**	**81.05**	**83.00**	**80.57**
5	72.14	72.40	72.10	72.30	72.76	73.07	72.33	72.51
6	67.70	66.71	67.66	67.78	68.37	67.36	67.85	66.82
A	112.40	112.46	112.37	112.47	113.03	113.09	112.46	112.38
A	109.42	109.24	109.43	109.29	110.06	109.86	109.49	109.17
B	26.86	26.74	26.83	26.76	27.50	27.40	26.80	26.70
B	26.74	26.71	26.70	26.69	27.39	27.38	26.80	26.70
B	26.19	26.27	26.15	26.25	26.84	26.94	26.27	26.29
B	25.29	25.19	25.15	25.16	25.91	25.84	25.30	25.20
1'	57.86	57.37	57.15	56.67	58.37	57.80	60.04	59.48
2'	21.03	21.26	17.38	17.66	22.62	22.64	14.84	15.02
3'	29.09[a]	29.06[b]	29.39	29.42	23.75	23.94	13.33	13.27
4'	28.93[a]	28.93[b]	83.12	83.19	14.35	14.34		
5'	28.66[a]	28.64[b]						
6'	25.10	25.10						
7'	30.33	30.32						
8'	84.07	84.08						

* a-a-a and b-b-b are interchangeable; * The synthesis of this compound is described in section 2.1.3.2.

Table 2.2 Diagnostic ^{1}H NMR data for the 8-fluorooctyl- and 4-fluorobutyl* DAG sulfinate esters (Section 2.1.3.2) as well as the literature values for the butyl[39] and propyl[26] sulfinate esters.

	1 – (*d*)		2 – (*d*)		3 – (*d*)	
	δ (ppm)	*J* (Hz)	δ (ppm)	*J* (Hz)	δ (ppm)	*J* (Hz)
8F-(*R*)-O-DAG	5.91	3.5	4.78	3.5	4.71	1.2
8F-(*S*)-O-DAG	5.91	3.7	4.60	3.7	4.74	2.5
4F-(*R*)-O-DAG*	5.89	3.5	4.76	3.5	4.71	*br s*
4F-(*S*)-O-DAG*	5.91	3.7	4.61	3.7	4.75	2.5
Butyl-(*R*)-O-DAG	5.90	3.6	4.72	3.6	4.79	*br s*
Butyl-(*S*)-O-DAG	5.91	3.6	4.60	3.6	4.74	2.6
Propyl-(*R*)-O-DAG	5.91	3.5	4.67-4.83	*m*	4.67-4.83	*m*
Propyl-(*S*)-O-DAG	5.88	3.6	4.85	3.6	4.72	2.1

* The synthesis of this compound is described in Section 2.1.3.2.

Diastereomeric ratios were determined via ^{1}H-decoupled ^{19}F NMR spectroscopy, since each diastereomer featured slightly different chemical shifts. The **8F-(*R*)-O-DAG** sulfinate ester was determined to have a diastereometric ratio of *R* to *S* ($dr_{R/S}$) of 96/4 while the **8F-(*S*)-O-DAG** sulfinate ester had $dr_{R/S}$ = 11/89.

The Grignard reagent, required for the preparation of each sulfoxide enantiomer was formed from *tert*-butyldimethylsilyl-protected (TBS) 9-bromo-1-nonanol by refluxing it with magnesium in tetrahydrofuran (THF). The Grignard reagent was then added to the (*R*)- and (*S*)-sulfinyl diastereomers of the DAG sulfinate esters to generate (*S*)- and (*R*)- *tert*-butyl-[10-(8-fluoro-octane-1-sulfinyl)-decyloxy]-dimethyl-silanes. It should be noted that three equivalents of the Grignard reagent were required. This is likely owing to complexation of the reagent with the terminal fluorine atom – a phenomenon for which there is some precedence.[40] The yields of (*S*)- and (*R*)-sulfoxides in these reactions were 80 and 69% respectively, after purification by flash chromatography (60% EtOAc/hexanes).

The analytical data for the fluorine-tagged sulfoxides was in accord with their assigned structures. The mass spectrum of the dialkyl sulfoxide bearing the terminal TBS-

protected alcohol (Figure 2.11) featured a major fragment at m/z = 379 due to loss of *t*-butyl group from the protecting group suggesting success in obtaining the desired product.

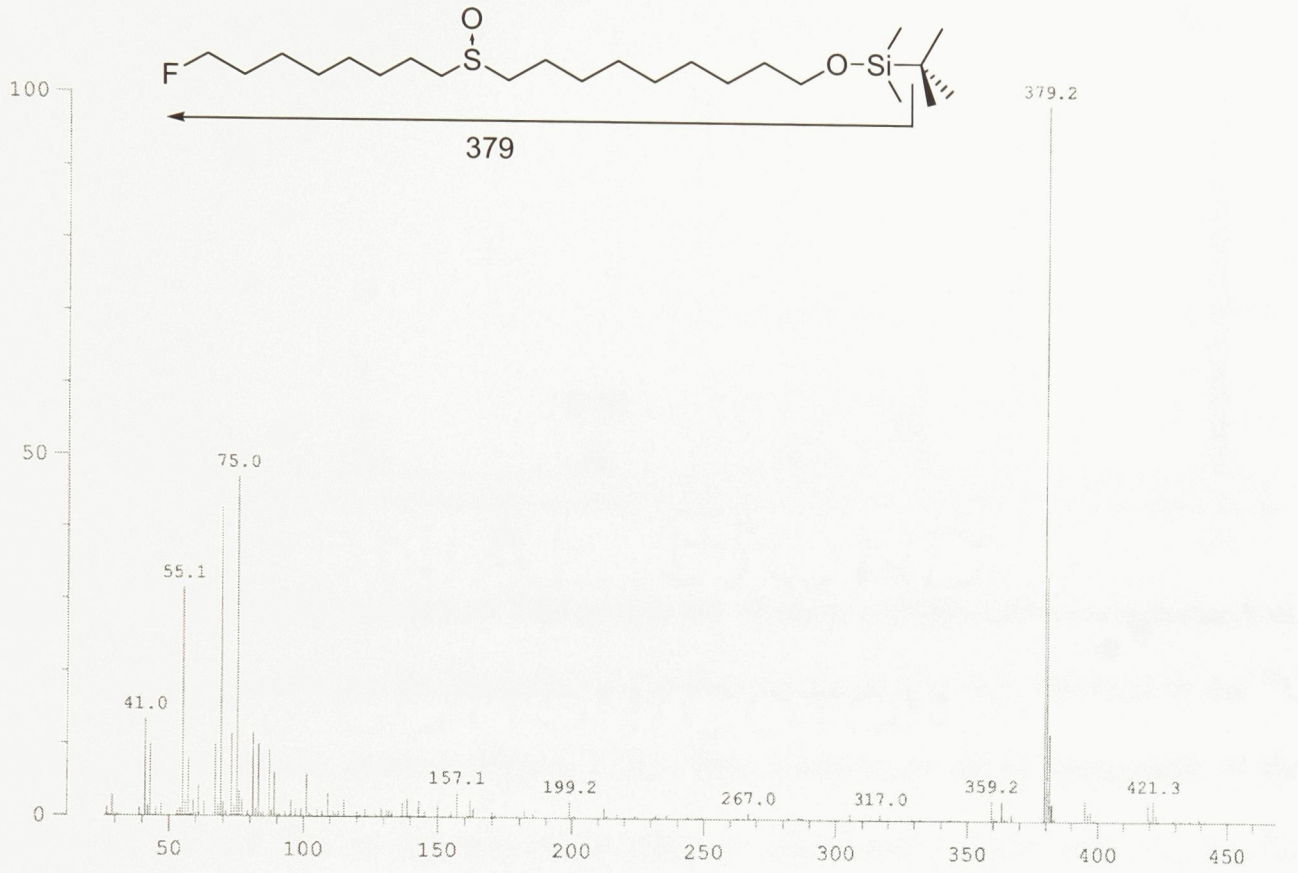

Figure 2.11 Mass spectrum of TBS-protected 18-fluoro-(10*R*)-sulfoxyoctadecan-1-ol.

One of the most notable features of the ^{1}H NMR spectrum of ω-fluorinated sulfoxides is the doublet of triplets centered around 4.43 ppm caused by the -C**H**$_2$F protons coupling both with the fluorine atom and the pair of adjacent methylene protons. Also of note is the presence of a large multiplet appearing around 2.65 ppm which is characteristic of methylene protons adjacent to a sulfoxide moiety. The complexity is derived from the overlap of signals assigned to unresolved diastereotopic protons. Evidence of the TBS protecting group is observed in the singlets at 0.88 and 0.03 ppm (methyl groups on the silicon atom and on the *t*-butyl moiety of the protecting group respectively).

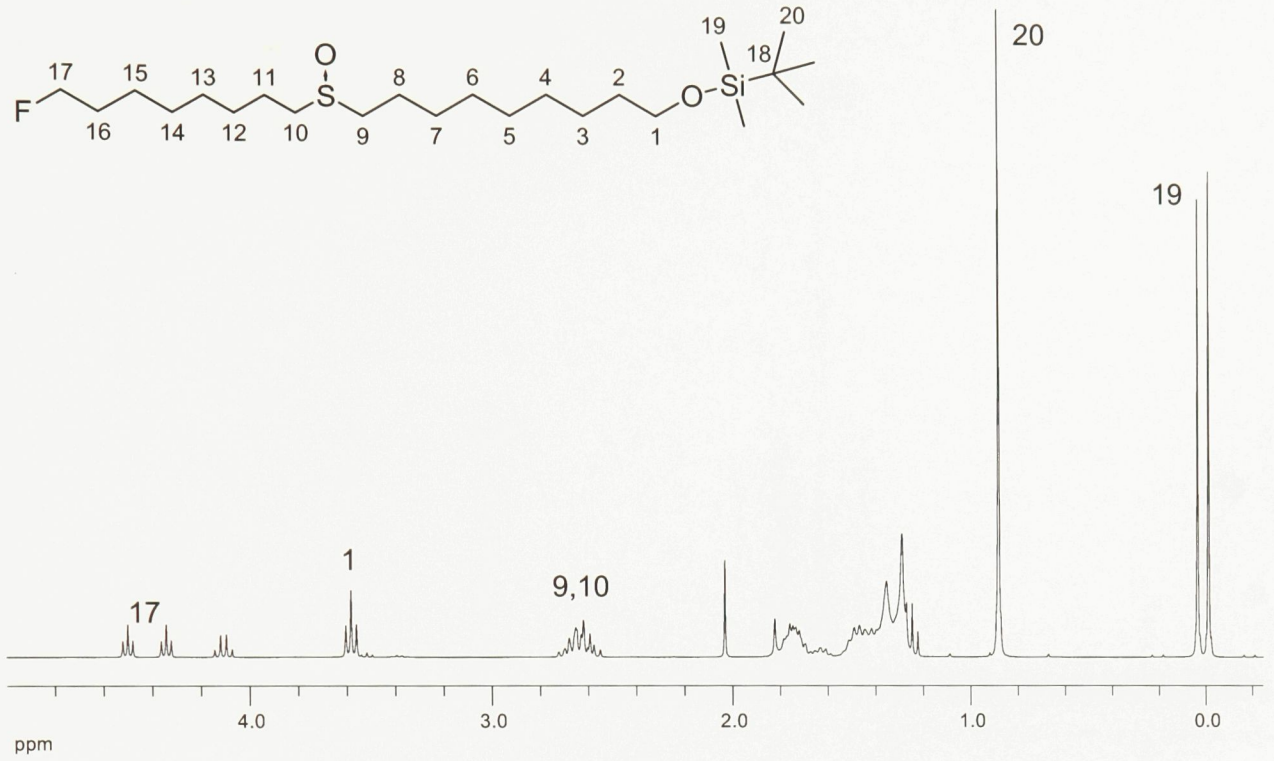

Figure 2.12 ^{1}H NMR spectrum of TBS-protected 18-fluoro-(10R)-sulfoxyoctadecan-1-ol.

Splitting caused by the presence of the fluorine atom was also observed in the ^{13}C NMR spectrum of the product (Figure 2.13). This allowed for easier assignment of the signals of C17-15 due to the long-range effect of the fluorine atoms with J^{1}_{CF} to J^{4}_{CF} coupling being observable. Two signals were also observed in the region of 52 ppm, which is indicative of alkyl carbons bonded to a sulfoxide group. The signal at -5.27 ppm shows the presence of the protecting group and is due to the methyl groups bound directly to the silicon atom.

The ^{1}H-decoupled ^{19}F NMR spectra (Figure 2.14) of the products feature a single peak at -218.36 ppm, indicating that there are no fluorinated by-products present which would be likely to interfere with further ^{19}F NMR studies to be performed. Enantiomeric excesses were determined via ^{1}H-decoupled ^{19}F NMR spectroscopy in combination with the CSA, (*R*)-AMA. The enantiomeric excesses were estimated to be 94% for **18F-(10*S*)-SO-1OTBS** and 76% for **18F-(10*S*)-SO-1OTBS**.

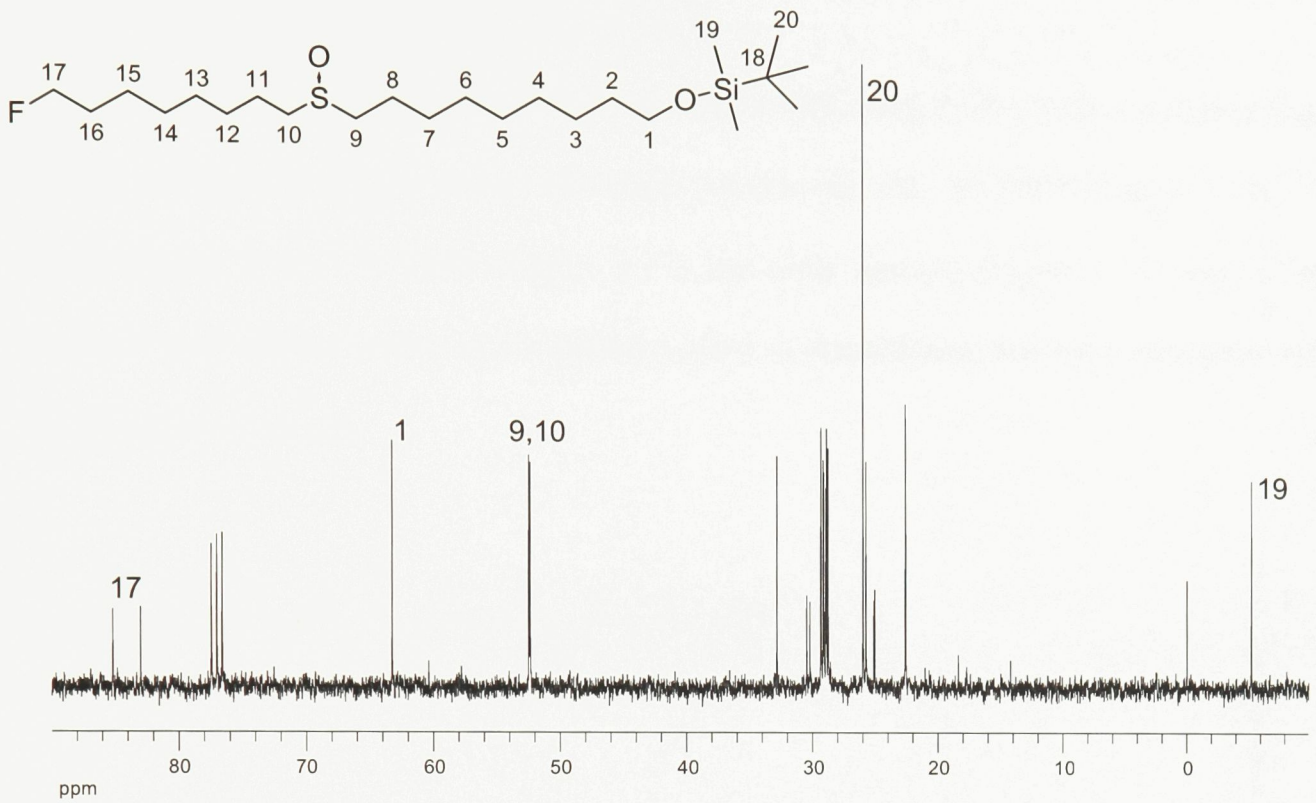

Figure 2.13 ^{13}C NMR spectrum of TBS-protected 18-fluoro-(10*R*)-sulfoxyoctadecan-1-ol.

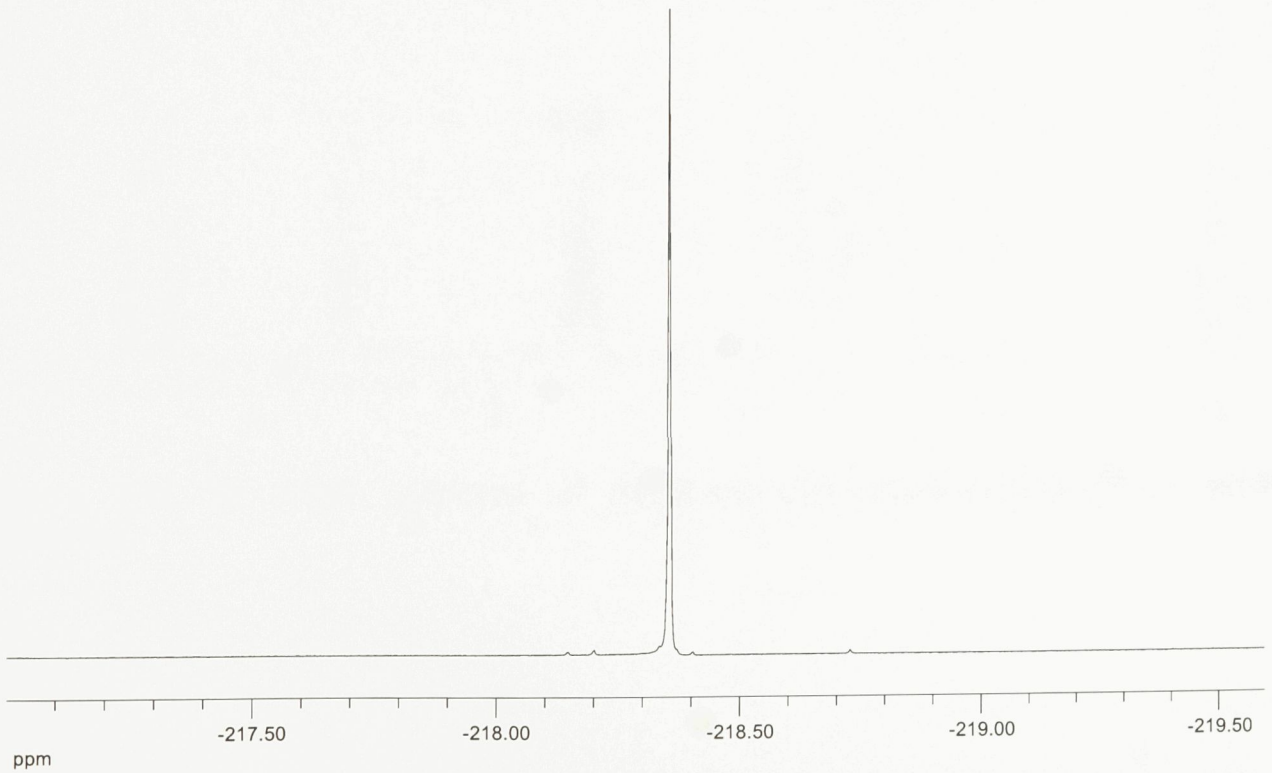

Figure 2.14 ^{1}H-decoupled ^{19}F NMR spectrum of TBS-protected 18-fluoro-(10*R*)-sulfoxyoctadecan-1-ol.

Deprotection of each enantiomer was performed using (1*S*)-(+)-10-camphorsulfonic acid in methanol at 0°C to obtain the target compounds. The ^{1}H NMR (Figure 2.15), ^{13}C NMR (Figure 2.16), ^{19}F NMR (Figure 2.17) and mass spectral (Figure 2.18) data of the products were similar to that of the products prior to deprotection and were consistent with the proposed structures.

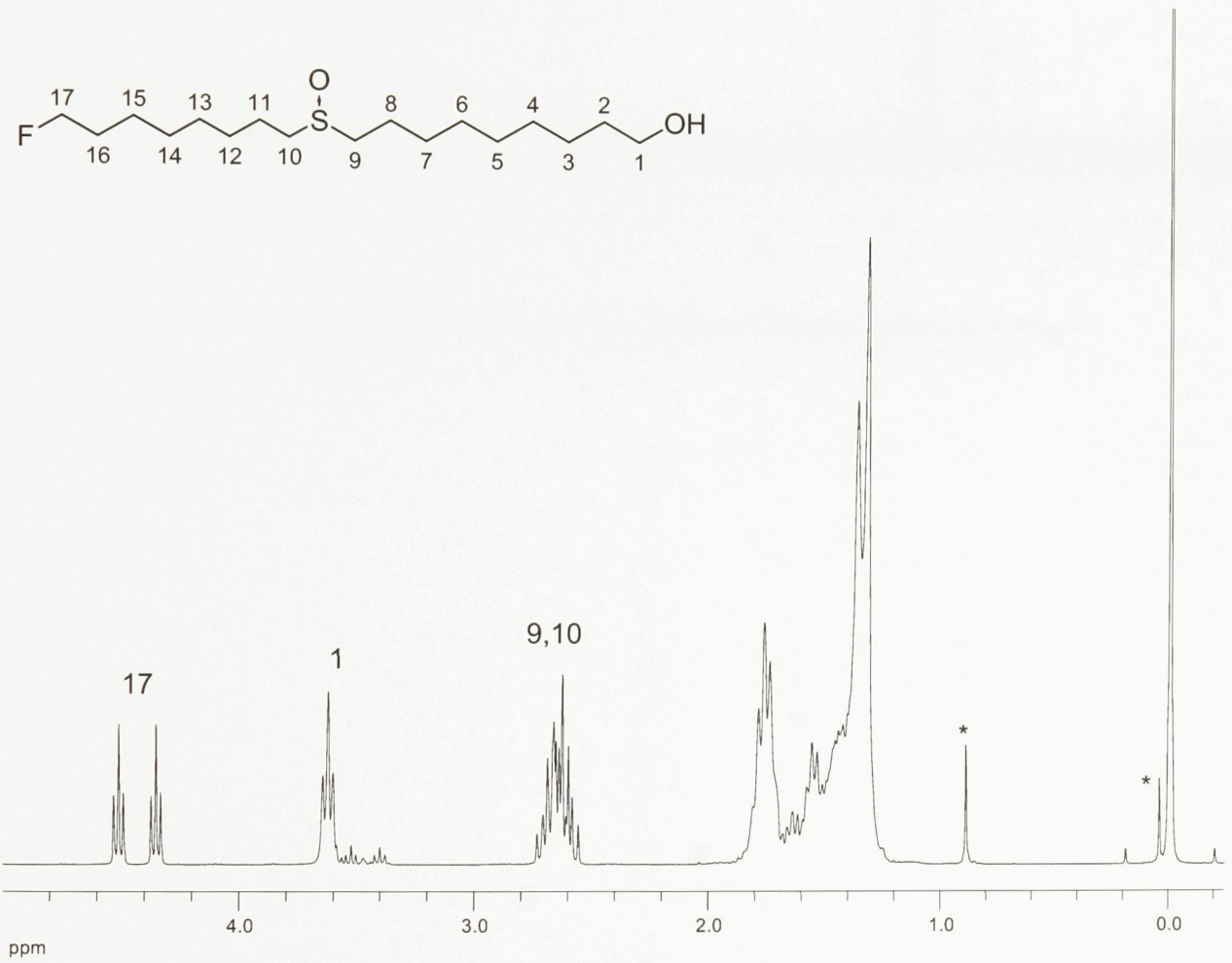

Figure 2.16 ^{1}H NMR spectrum of 18-fluoro-(10*R*)-sulfoxyoctadecan-1-ol (*TBS impurity).

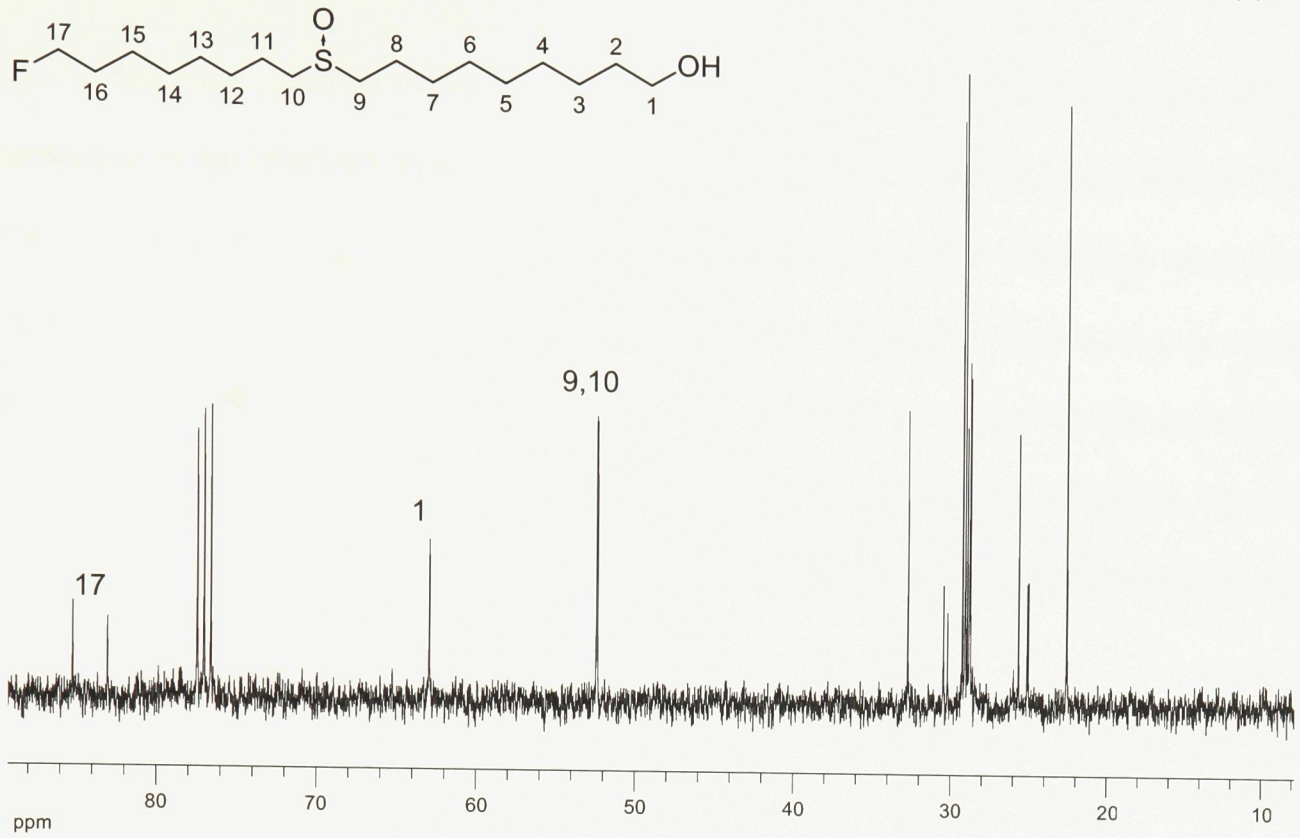

Figure 2.16 ^{13}C NMR spectrum of 18-fluoro-(10*R*)-sulfoxyoctadecan-1-ol.

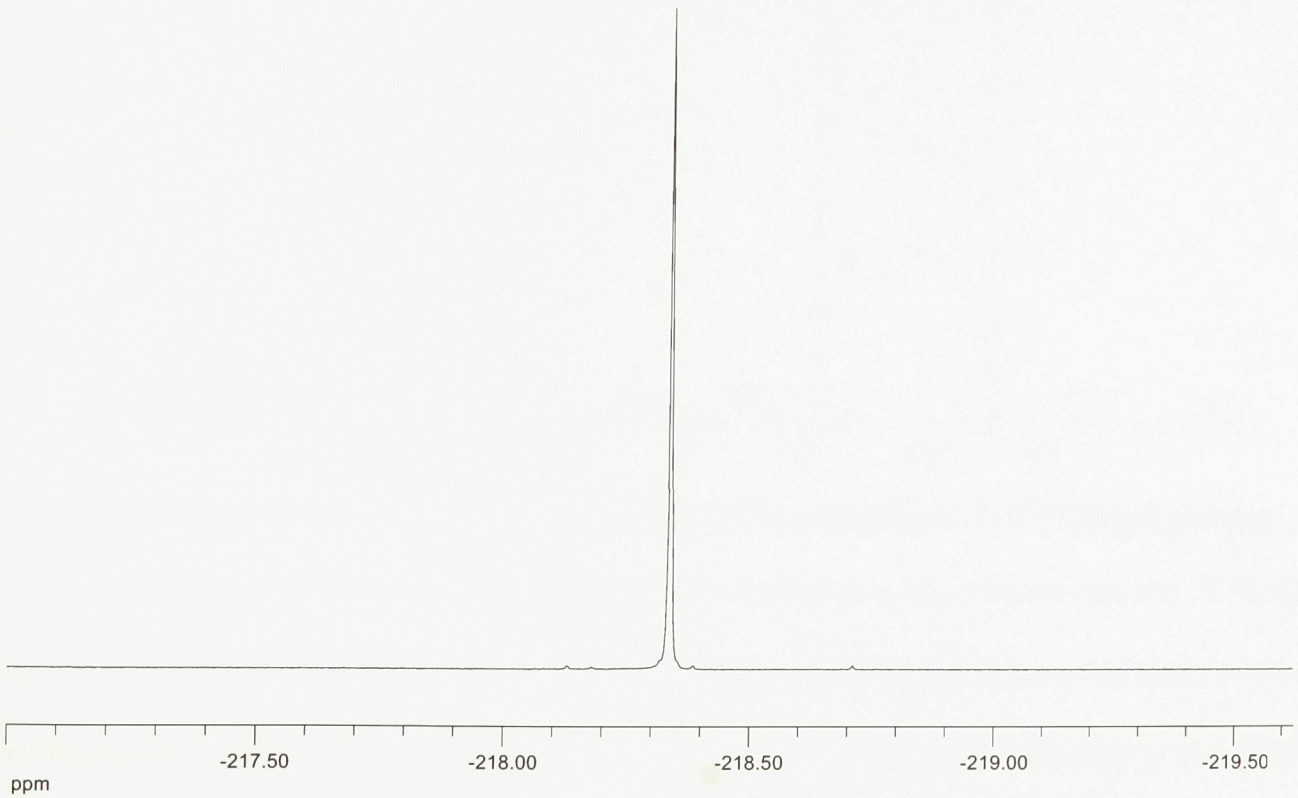

Figure 2.17 ^{1}H-decoupled ^{19}F NMR spectrum of 18-fluoro-(10*R*)-sulfoxyoctadecan-1-ol.

The mass spectrum of the product (direct probe MS) indicated that some of the silyl protecting group remained, based on the fragment with m/z = 379 due to loss of *t*-butyl from the protecting group. The prominence of this peak is somewhat misleading since this impurity is more volatile than the corresponding alcohol. The major fragment ion, however, indicates formation of the product with m/z = 305. This peak represents the loss of OH (the oxygen atom is from the sulfoxide), which is characteristic for dialkyl sulfoxides. There is also a fragment at m/z = 143 which corresponds to a cleavage between the sulfur atom and the decanol chain.

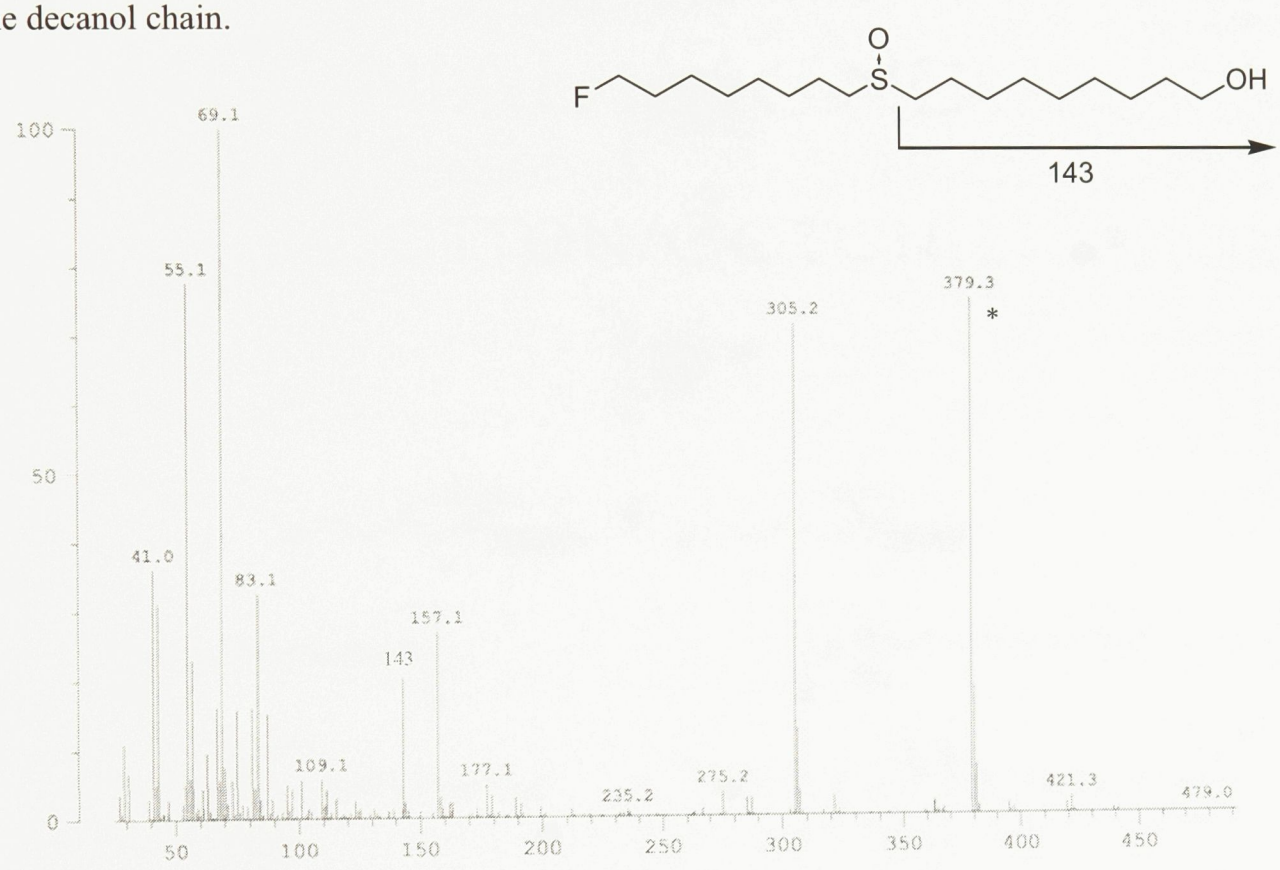

Figure 2.18 Mass spectrum of 18-fluoro-(10R)-sulfoxyoctadecan-1-ol (*TBS impurity).

Evidence of incomplete deprotection of the alcohol was also observed in the ^{1}H NMR spectrum (0.88 and 0.03 ppm). The level of protected alcohol remaining in the product was determined to be low enough (2 and 5% by ^{1}H NMR for (*S*) and (*R*) sulfoxides) to not affect subsequent stereochemical analysis by chiral NMR shift agents. The presence of this

impurity, however, does impede the determination of the enantiomeric excess of these alcohols due to subtle differences in the ^{1}H-decoupled 19F NMR shifts. The deprotection is not expected to affect the stereochemistry of the sulfur centre and thus the enantiomeric excesses are expected to mirror those of the protected alcohol, 94% for **18F-(10*S*)-SO-1-OH** and 76% for **18F-(10*R*)-SO-1-OH.**

2.1.3.2 Synthesis of (11*S*)- and (11*R*)-15-fluoro-11-sulfoxypentadecane

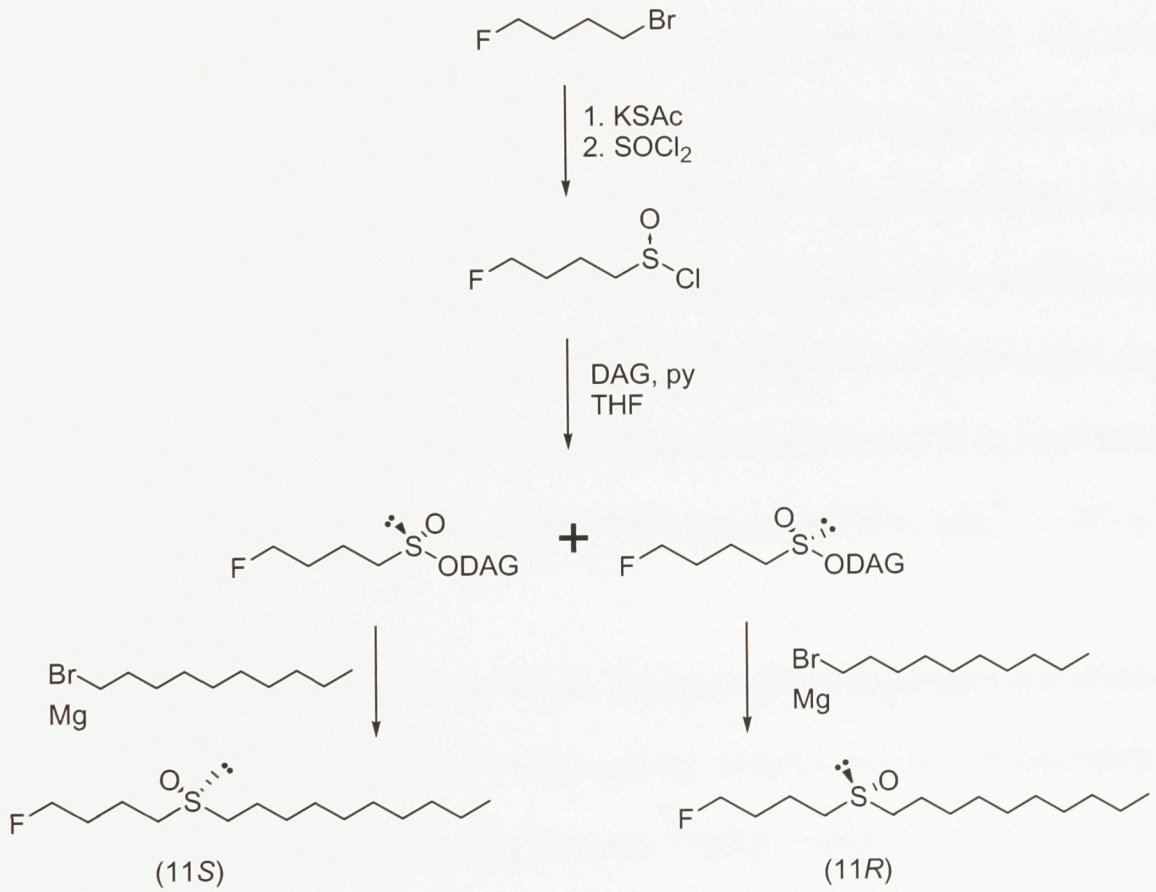

Figure 2.19 Scheme for the synthesis of (11*R*)- and (11*S*)-15-fluoro-11-sulfoxy-pentadecane.

The synthesis of both 15-fluoro-11-sulfoxypentadecane enantiomers was facilitated by the commercial availability of the starting material, 1-bromo-4-fluorobutane. The sulfinyl chloride functional group was introduced through the nucleophilic displacement of the

bromine by thiolacetate[36] (88%) followed by oxidation to the corresponding sulfinyl chloride.[37, 38]

The formation of the (*R*)-sulfinyl diastereomer of 1,2:5,6-di-*O*-isopropylidene-α-D-glucofuranosyl-4-fluorobutanesulfinate was undertaken using pyridine as a base, however the solution was allowed to come to room temperature before the reaction was completed (ca. 1.5 hours) and a mixture of the diastereomers was obtained (83% overall yield). These diastereomers were easily separated via flash chromatography (50% EtOAc/hex) to recover both the (*R*) and (*S*)-sulfinyl esters (66 and 17% yields respectively). The absolute configuration of the sulfinyl centres were assigned based on the specific rotation of the diastereomers. The **4F-(*R*)-O-DAG** sulfinate ester had a positive specific rotation of $[\alpha]_D^{21}$ = +3.91° (*c* 1.1, acetone), while the **4F-(*S*)-O-DAG** sulfinate ester had a negative specific rotation, $[\alpha]_D^{21}$ = -36.47° (*c* 1.1, acetone). The signs and magnitudes of these values correlate well with similar alkyl DAG sulfinate esters allowing the configuration to be confirmed ((*R*)-propyl sulfinate: $[\alpha]_D^{25}$ = +6.4° (*c* 1.1, acetone), (*S*)-propyl sulfinate: $[\alpha]_D^{25}$ = -33° (*c* 0.54, acetone)[26]).

As noted earlier, further support for the configurational assignments was obtained by comparing the trends in the ^{1}H and ^{13}C NMR spectra with the data for corresponding butyl and propyl sulfinate esters as found in the literature (Tables 2.1 and 2.2).[26, 39]

Diastereomeric ratios were determined through ^{19}F NMR spectroscopy, using the integration of the fluorine signals as the diastereomers featured slightly different chemical shifts. **4F-(*R*)-O-DAG** was determined to have a $dr_{R/S}$ of greater than 99/1 while **4F-(*S*)-O-DAG** had $dr_{R/S}$ = 2/98.

The target chiral fluoro sulfoxides were prepared by the modified Anderson route that was employed in the synthesis of the C18 compounds discussed previously. The required Grignard reagent was formed by treating 1-bromodecane with magnesium in refluxing THF. This reagent was then added individually to the (*R*)- and (*S*)- diastereomers of the DAG sulfinate esters to generate (*S*)- and (*R*)-1-(4-fluoro-butane-1-sulfinyl)-decane, obtained in yields of 35 and 34% yield respectively following flash chromatography (80% EtOAc/hexanes). Using ^{1}H NMR spectroscopy in combination with the chiral solvating agent (*R*)-(−)-1-(9-anthryl)-2,2,2-trifluoroethanol ((*R*)-TFAE), the enantiomeric excess of these products is estimated to be >98% and 90% for the (*S*)- and (*R*)- enantiomers.

The specific rotations of the (*S*)- and (*R*)- enantiomers were determined to be $[\alpha]_D^{25}$ +1.7 (*c* 1.1, $CHCl_3$) and $[\alpha]_D^{25}$ - 1.4 (c 1.1, $CHCl_3$) respectively. This was encouraging in that the specific rotations are of similar magnitude and opposite signs, as is expected for enantiomers.

The mass spectral (Figure 2.20), ^{1}H NMR (Figure 2.21), ^{13}C NMR (Figure 2.22) and ^{1}H-decoupled ^{19}F NMR (Figure 2.23) data for the enantiomeric products were indistinguishable from each other and were consistent with the proposed structures. The notable feature of the mass spectrum is the parent ion at 247 m/z which represents the molecular ion with the loss of OH (17), which is characteristic for dialkyl sulfoxides.[41] Also a cleavage occurs between the sulfur atom and the fluorinated alkyl group to yield a fragment having m/z = 189; cleavage on the other side of the atom produces the fluorinated-alkyl chain with a fragment mass to charge ratio of 123.

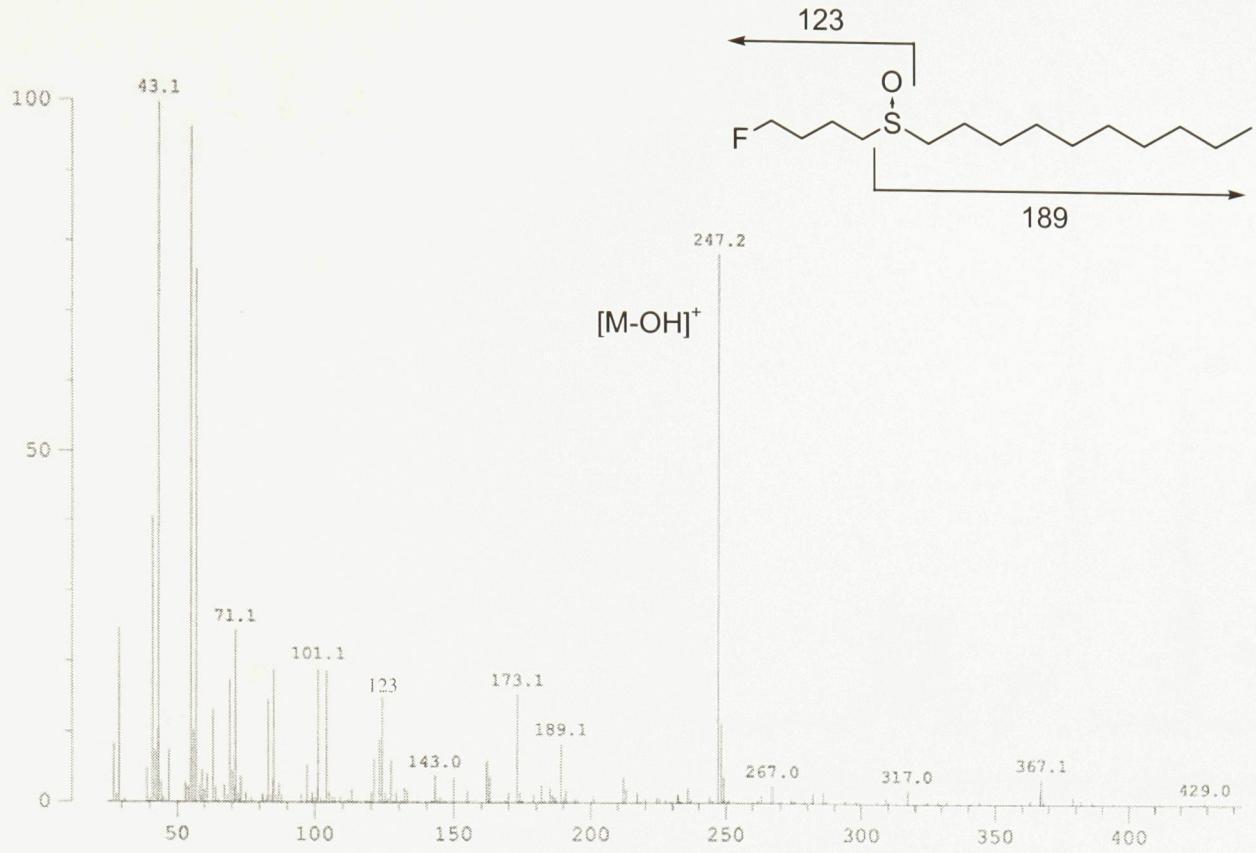

Figure 2.20 Mass spectrum of 15-fluoro-(11*S*)-sulfoxypentadecane.

The ^{1}H NMR spectrum features a doublet of triplets centered at 4.49 ppm caused by the -C**H**$_2$F methylene protons. Interestingly, each triplet displays a slightly different splitting pattern. The ^{13}C NMR spectrum features two peaks around 52 ppm that are characteristic for carbon atoms bound to a sulfoxide group. Finally, the ^{19}F NMR spectra of the products feature a single peak at -219.23 ppm. These three spectra all attest to the high purity of the fluorinated sulfoxy products.

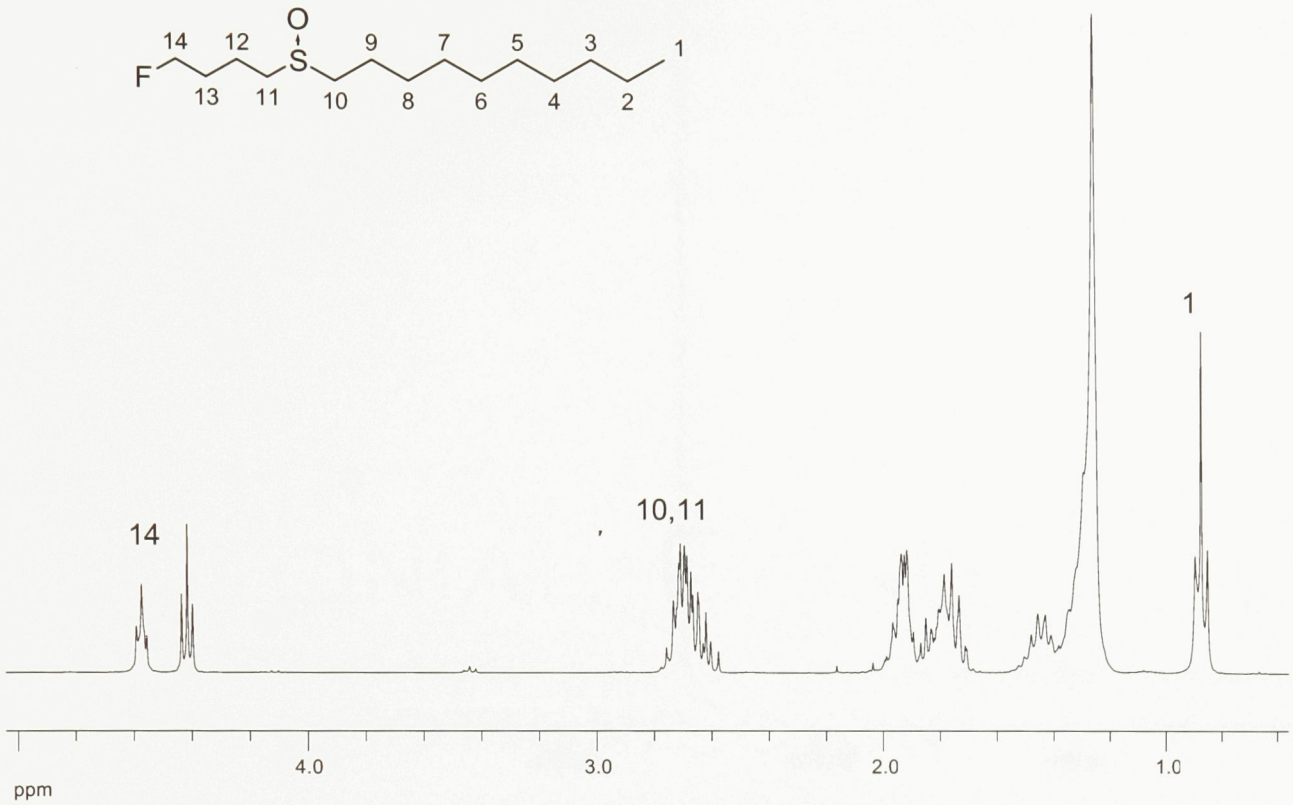

Figure 2.21 ^{1}H NMR spectrum of 15-fluoro-(11*S*)-sulfoxypentadecane.

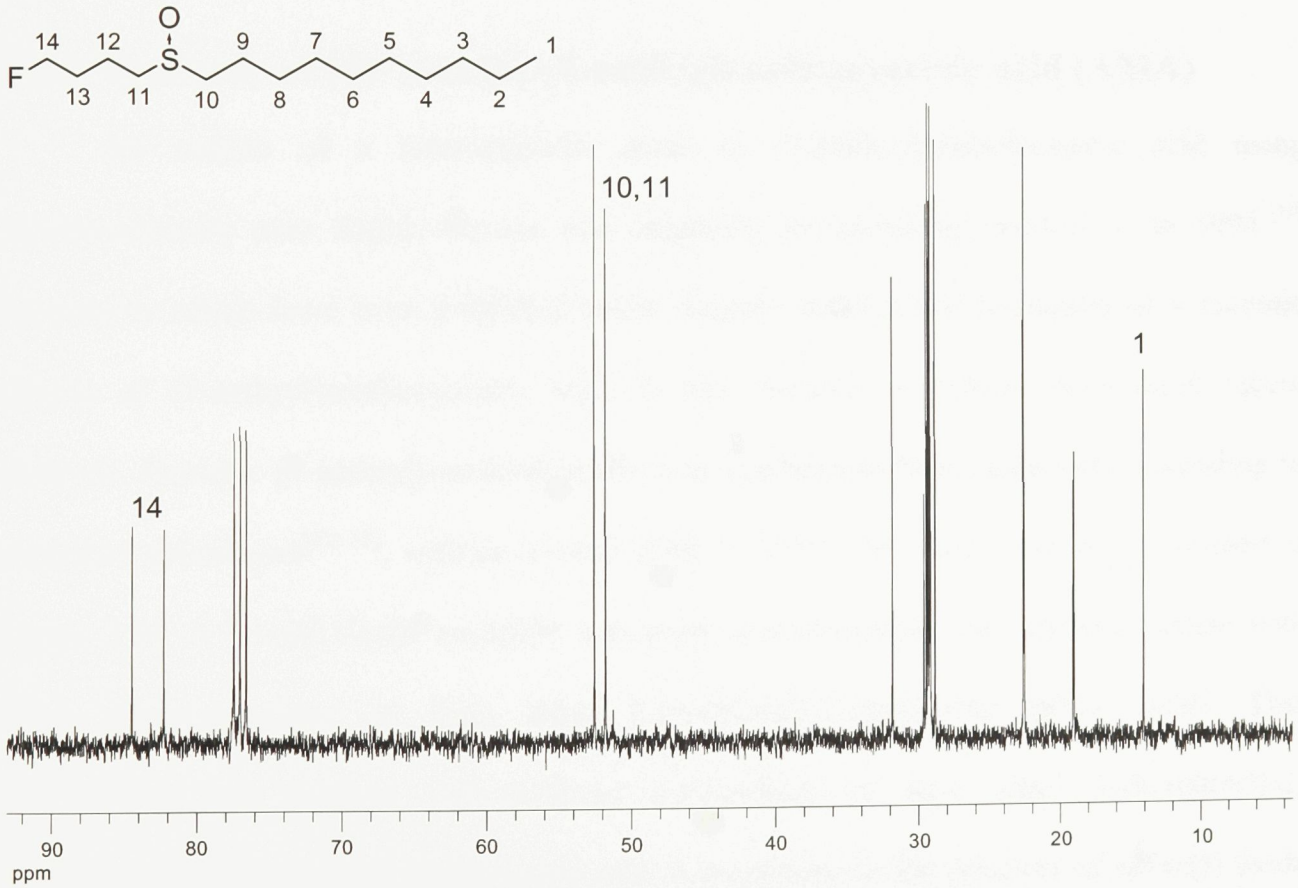

Figure 2.22 ^{13}C NMR spectrum of 15-fluoro-(11*S*)-sulfoxypentadecane.

Figure 2.23 ^{1}H-decoupled ^{19}F NMR spectrum of 15-fluoro-(11*S*)-sulfoxypentadecane.

2.1.4 Synthesis of (*R*)- and (*S*)-(9-anthryl)methoxyacetic acid (AMA)

An outline of a stereospecific route to (9-anthryl)methoxyacetic acid using enantiomerically pure Alpine-Borane was originally presented by Seco *et al* in 1994.[18] Procedures which have been published more recently involve the resolution of a racemic sample of (9-anthryl)methoxyacetic acid. It was decided to follow these more recent methods. Racemic (9-anthryl)-methoxyacetic was synthesized from anthracene according to published procedures[42, 43], with an overall yield of 32%. The route followed is outlined in Figure 2.24. A Friedel Crafts acylation was used to functionalize the aromatic system with ethyl chlorooxoacetate to form ethyl 2-(9-anthryl)-2-oxoacetate (98% yield). This intermediate was reduced with sodium borohydride to give ethyl 2-(9-anthryl)-2-hydroxyacetate (93% yield). Methylation with iodomethane in the presence of silver(I) oxide gave ethyl 2-(9-anthryl)-2-methoxyacetate (38% yield). The low yield of the methylation was

due to incomplete reaction. The product ether was isolated from the mixture by flash chromatography (DCM to 10% MeOH/DCM gradient). Finally, (9-anthryl)methoxyacetic acid was obtained through base-catalyzed hydrolysis of the ester (92%).

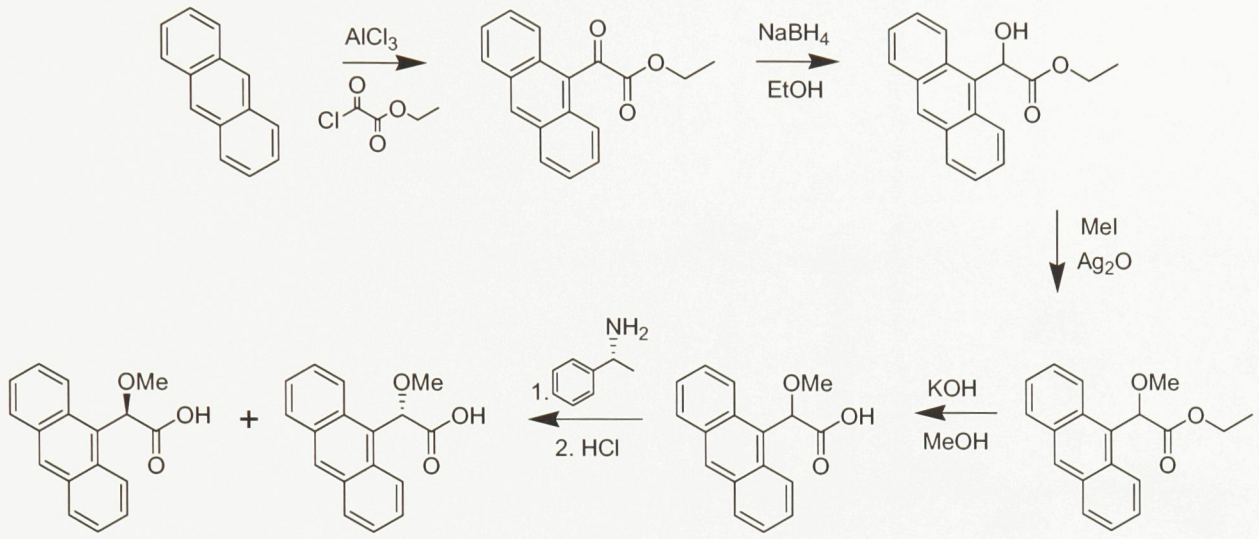

Figure 2.24 Scheme for the synthesis and resolution of both enantiomers of AMA

Mass spectral (Figure 2.25), ^{1}H NMR (Figure 2.26) and ^{13}C NMR (Figure 2.27) data were in accord with published values.[42, 43] A minor amount of an unidentified impurity was present as evidenced by the minor peaks in the aromatic region in the ^{1}H NMR spectrum.

The mass spectrum of the product features a parent ion at m/z = 266. The base peak for this spectrum is at 221 m/z. representing $[M-45]^{+}$ which is typical of an α-cleavage of an acid.

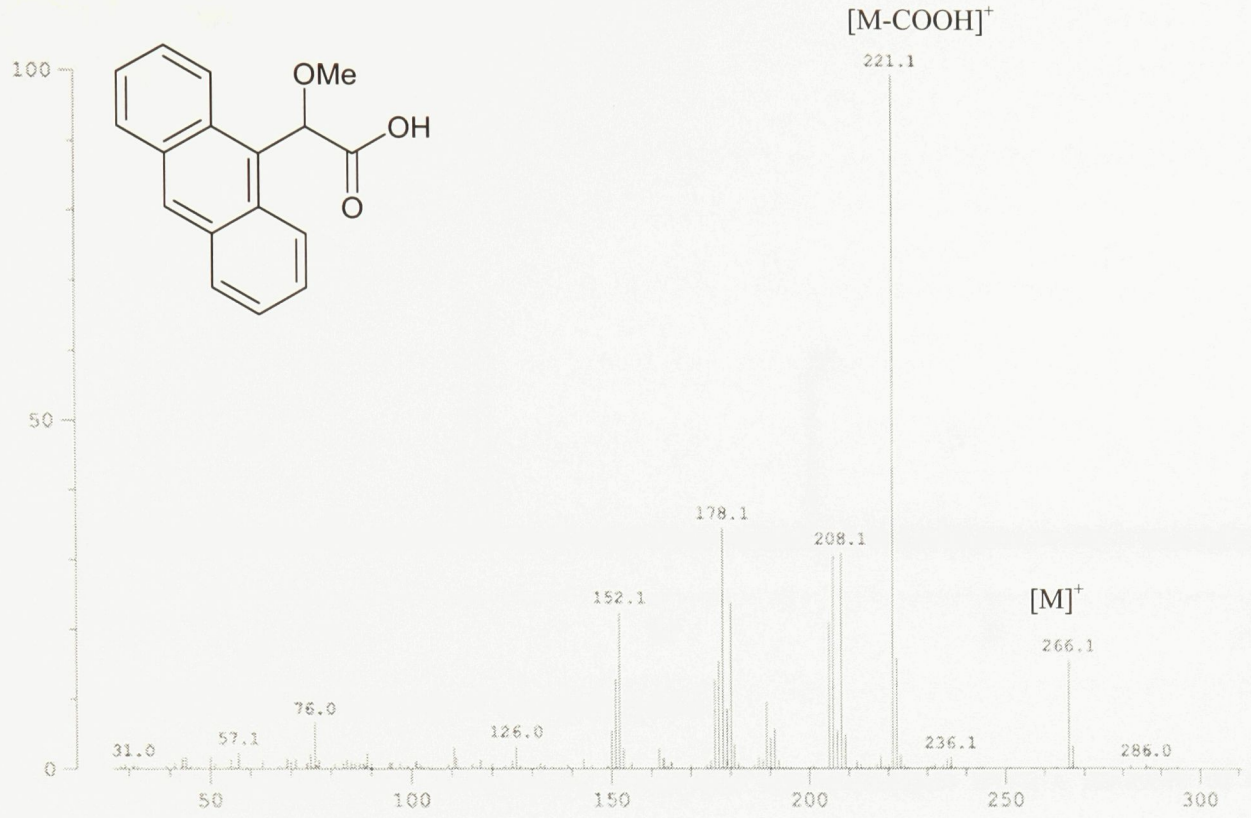

Figure 2.25 Mass spectrum of racemic AMA.

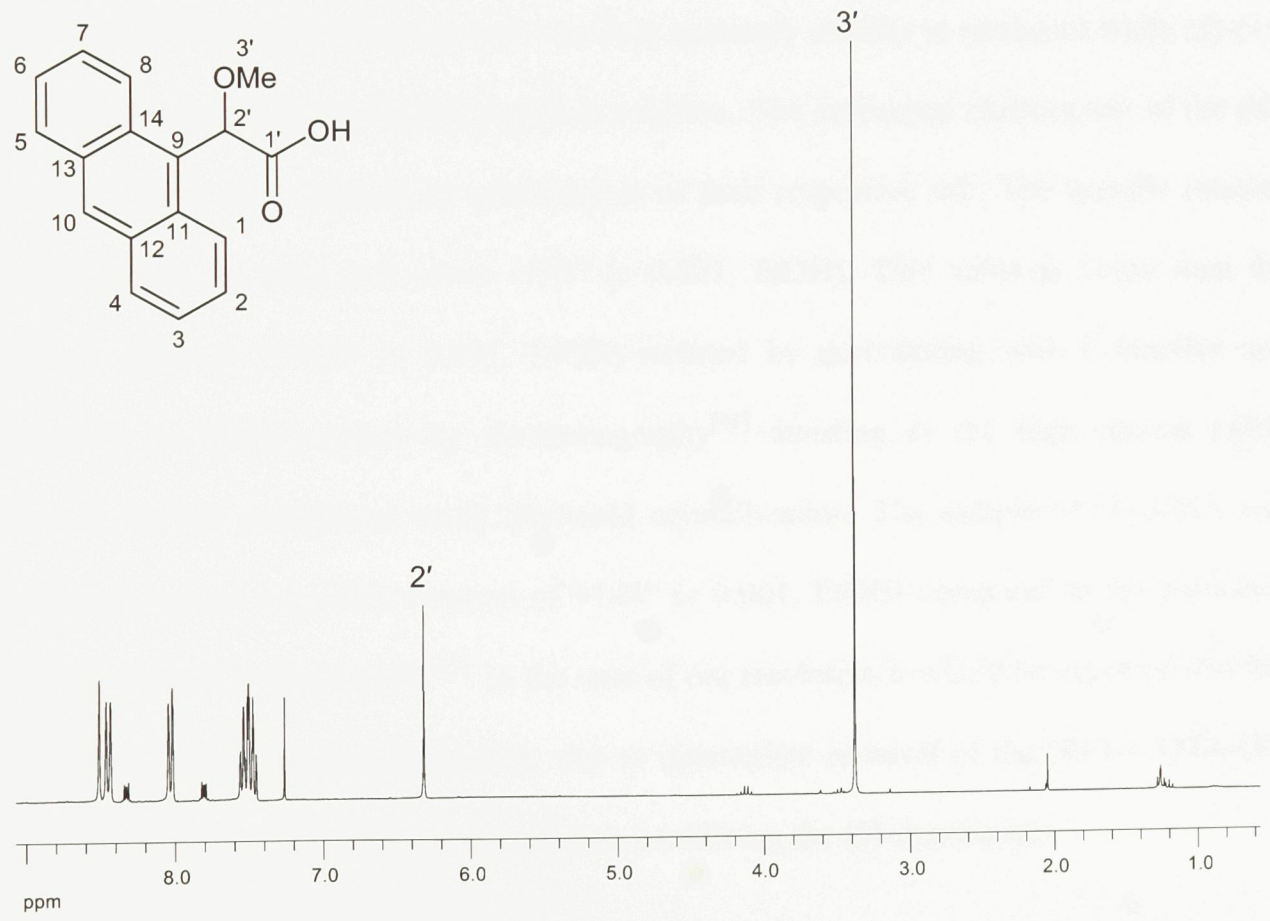

Figure 2.26 ^{1}H NMR spectrum of racemic AMA.

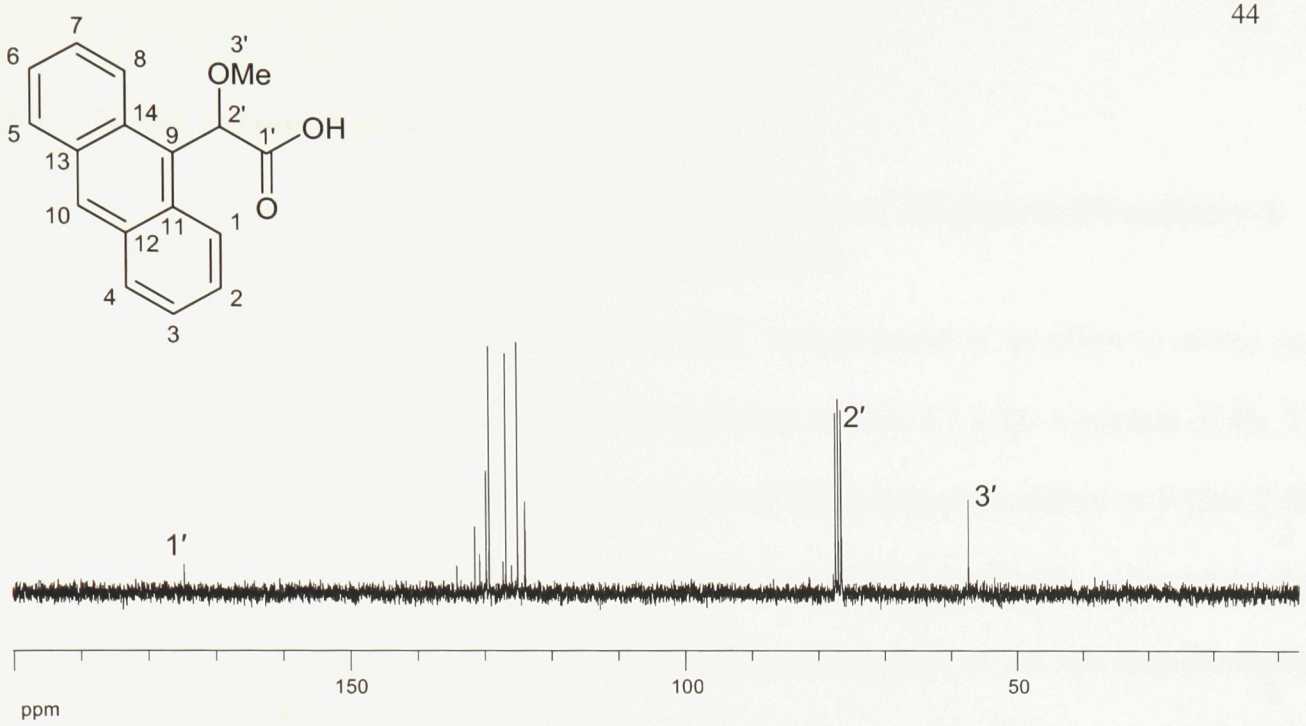

Figure 2.27 ^{13}C NMR spectrum of racemic AMA.

The enantiomers were resolved by fractional crystallization from a mixture of the diastereomeric salts formed with the addition of (*R*)-(+)-methylbenzylamine. The (*R*)-(-)-AMA-(*R*)-(+)-methylbenzylamine salt was only sparingly soluble in methanol while (*S*)-(+)-AMA-(*R*)-(+)-methylbenzylamine stayed in solution. The individual enantiomers of the title compound were then isolated by acidification of their respective salt. The specific rotation for (*R*)-AMA was measured to be -194° (c 0.001, EtOH). This value is larger than the reported value of -128.2° (c 0.001, EtOH) isolated by derivatizing with L-menthol and separating the diastereomers by chromatography[43] attesting to the high optical purity obtained for this enantiomer using fractional crystallization. The sample of (*S*)-AMA was calculated to have a specific rotation of +143° (*c* 0.001, EtOH) compared to the published value of +131° (*c* 0.001, EtOH)[43]. In the case of our resolution it would be expected that this enantiomer have a lower optical purity due to incomplete removal of the (*R*)-(-)-AMA-(*R*)-(+)-methylbenzylamine salt from the solution containing the (*S*)-enantiomer.

2.1.5 NMR experiments

2.1.5.1 Assignment of the absolute configuration of 18-fluoro-10-sulfoxy-1-octadecanol produced by a soluble Δ^9 desaturase

A 2:1 mixture of (*S*)- to (*R*) **18F-10SO-OH** was prepared in an effort to mimic the results expected from the previous biological study (see section 2.1.1.2). A portion of the ^{1}H spectrum and the ^{1}H-decoupled ^{19}F NMR spectrum of this mixture are shown in Figure 2.28 A and B respectively. The doublet of triplets of the –C**H**$_2$F group was selected as the representative diagnostic area for the ^{1}H NMR spectrum due both to the fact that the atoms would occupy approximately the same spatial relationship to the shift agent as the fluorine atom, and also because there is generally no interference caused by other peaks in the same region of the spectrum. The ^{1}H-decoupled ^{19}F NMR spectrum displays a single peak in the absence of a chiral NMR shift agent.

To this mixture of sulfoxide enantiomers was added 4 equivalents of (*R*)-AMA and the resulting ^{1}H and ^{19}F NMR spectra of this mixture in are shown in Figure 2.28 C and D. Examining the effect of the (*R*)-AMA shift agent on the selected region of the ^{1}H NMR spectrum, we see that the signal for the major (*S*) enantiomer of the sulfoxide is more shielded with respect to the (*R*) enantiomer. This result was expected based on the Pirkle-type binding model (Figure 2.4) and suggests that the binding model remains valid for ^{1}H NMR analysis of the fluorine-tagged dialkyl-sulfoxides. Examination of the ^{1}H-decoupled ^{19}F NMR spectrum (Figure 2.28 D), however shows the opposite effect, in which the major (*S*) enantiomer is less shielded than the minor (*R*) enantiomer. Similar results were obtained when the topologically equivalent (*S*)-TFAE (Figure 2.28 E and F) is used as the shift agent. As expected, when the chirality of the AMA agent is switched, the trends in shielding effects also switch. The data for these results are summarized in Table 2.3.

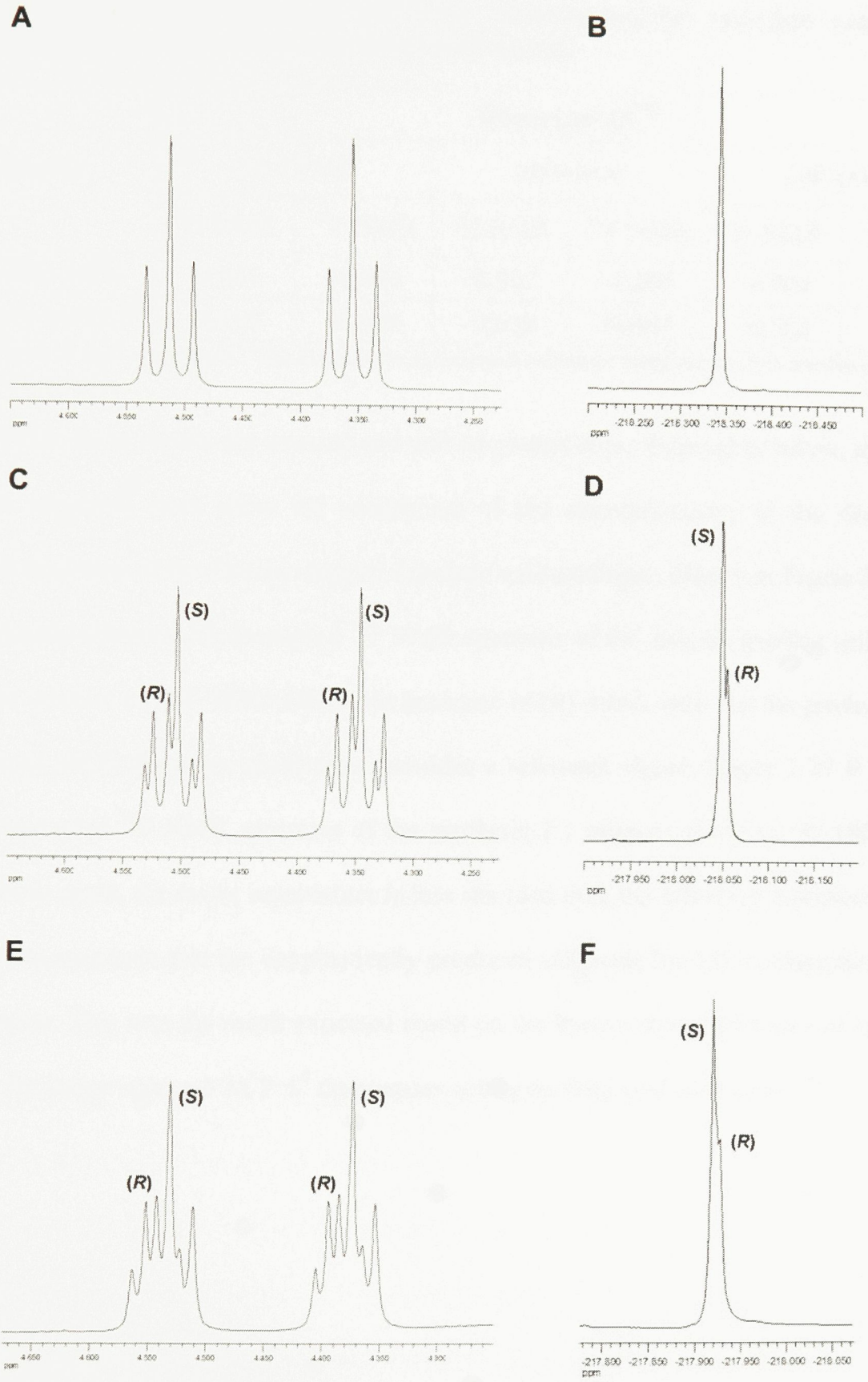

Figure 2.28 ^{1}H and ^{1}H-decoupled ^{19}F NMR spectra of a 2:1 mixture of (*S*):(*R*) 18F-10SO-OH before (A and B); after addition of 4 equivalents (*R*)-AMA (C and D); and after addition of 4 equivalents (*S*)-TFAE (E and F).

Table 2.3 Summary of observed $\Delta\delta^{S-R}$ for enantiomerically enriched samples of sulfoxides in the presence of various chiral shift agents.

Sulfoxide	Observed $\Delta\delta^{S-R}$					
	(*S*)-TFAE[a]		(*R*)-AMA[a]		(*S*)-AMA[a]	
	^{1}H NMR	^{19}F NMR	^{1}H NMR	^{19}F NMR	^{1}H NMR	^{19}F NMR
18F-10SO-1OH	-0.011	+0.006	-0.007	+0.005	+0.004	-0.002
18F-10SO-1OTBS[b]	-0.009	+0.006	-0.008	+0.005	+0.005	-0.004

[a] 4 equivalents of shift agent used; [b] The implication of the results obtained using this analyte are discussed in the following section.

While these results are unusual and will be probed more thoroughly below, the use of synthetic standards does allow the assignment of the stereochemistry of the desaturase-mediated oxidation of the fluorine-tagged thia-fatty acid analogue. Shown in Figure 2.29 A is the previously obtained ^{1}H-decoupled ^{19}F NMR spectrum of the enzyme product spiked with a racemic mixture of **18F-10SO-OH** in the presence of (*R*)-AMA such that the product signal is enhanced while the other enantiomer provides a reference signal. Figure 2.29 B features the ^{1}H-decoupled ^{19}F NMR spectrum of the synthetic 2:1 mixture of (*S*) to (*R*) **18F-10SO-OH**. In both cases, the major enantiomer is less shielded than the reference enantiomer. This allows us to conclude that the enzymatically produced sulfoxide has (*S*) configuration at the sulfur centre. This was the result expected based on the known stereochemistry of hydrogen removal for castor stearoyl-ACP Δ^{9} desaturases acting on fatty acid substrates.[19]

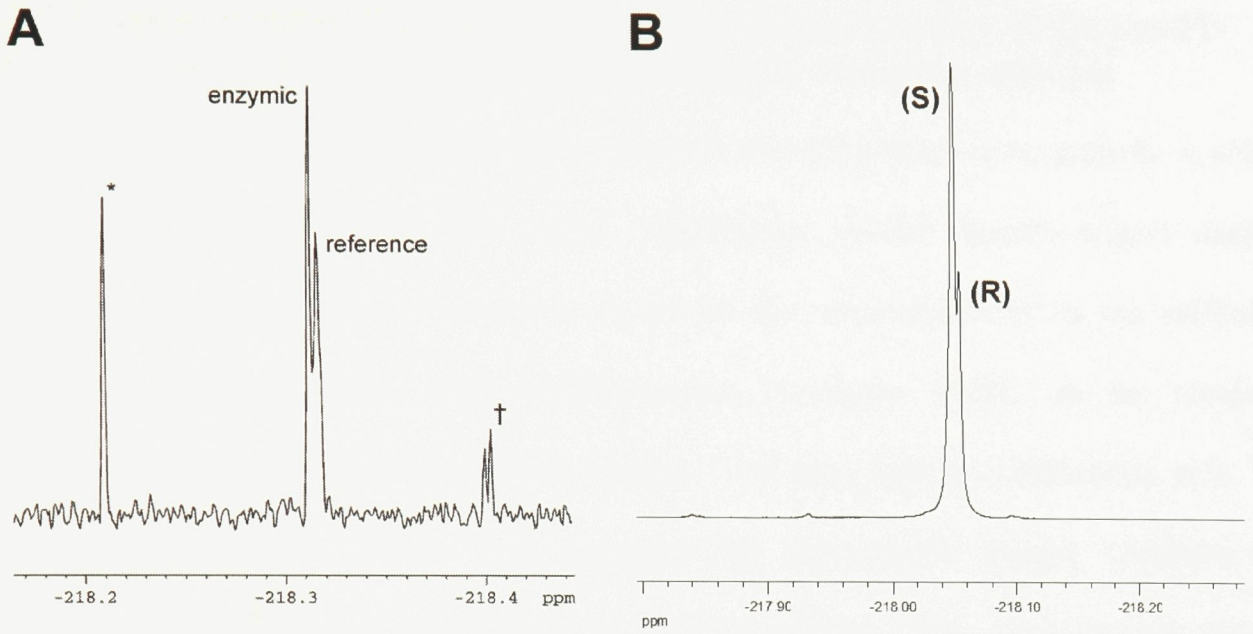

Figure 2.29 ^{1}H-decoupled ^{19}F NMR spectrum of enzymatically produced 18F-10SO-OH spiked with racemic 18F-10SO-OH and 4 equivalents (*R*)-AMA (376.5 MHz) (A); 2:1 mixture of synthetic (*S*):(*R*) 18F-10SO-OH with 4 equivalents (*R*)-AMA (282 MHz) (B). (* substrate, † unknown impurity)

2.1.5.2 Investigation of the role of the C1 hydroxyl group on the CSA induced NMR non-equivalences

The role of the terminal C1 hydroxyl group of **18F-10SO-OH** was probed to ascertain whether it would be necessary to include it in the synthesis for future experiments. The effects of the each of three different shift agents on the Δδ of the 18-fluoro-10-sulfoxy-1-octadecanols were measured before and after the removal of the protecting group. It was found that the direction of the induced chemical non-equivalence was the same for each trial for both ^{1}H NMR and ^{19}F NMR studies (Table 2.3). The difference in the magnitudes of the chemical shifts ranged from being immeasurably small to a maximum of 0.002 ppm in two cases. This difference is believed to be small enough that it should not impact the interpretation of results obtained. It was therefore deemed possible to omit the functional group at C1 in future experiments to facilitate synthesis of reference standards.

2.1.5.3 Assignment of the absolute configuration of methyl 15-fluoro-11-sulfoxypentadecanoate produced by growing *S. cerevisae* cultures

Since the functional group at the C1 position was determined to be unlikely to affect the outcome of chiral NMR shift agent experiments, simpler fluorine-tagged dialkyl sulfoxides were synthesized in order to determine the stereochemistry of the sulfoxide product obtained previously from *Saccharomyces cerevisiae* S522C. In the previous investigation, the shift agent (*S*)-MPAA (Figure 1.10) was used in combination with ^{19}F NMR spectroscopy[22] and it was reported that biosynthetic methyl 15-fluoro-11-sulfoxypentadecanoate was enriched in the (*S*) enantiomer. This determination clearly deserves greater scrutiny given the anomalous behaviour observed in the case of 18-fluoro-10-sulfoxy-octadecanols as described above (Section 2.1.5.1).

A 2:1 standard mixture of (*S*):(*R*) **15F-11-SO** was prepared and the CH_2F region of the ^1H and the ^1H-decoupled ^{19}F NMR spectra of this mixture are shown in Figure 2.30 A and B respectively. The addition of 4 equivalents of (*S*)-MPAA resulted in deshielding of the ^1H NMR signal for the C**H**$_2$F reporter group of the major enantiomer as shown in Figure 2.30 C. This result is in accord with the accepted binding model (Figure 1.10). The effect on the signal of the reporter fluorine atom in the ^1H-decoupled ^{19}F NMR spectrum resembled that obtained for the **18F-11SO-OH** sample (Section 2.1.5.1), namely that it was opposite to that observed in the ^1H NMR spectrum (Figure 2.30 D). The ^{19}F NMR signal for the (*S*) sulfoxide was more shielded than for the (*R*) sulfoxide.

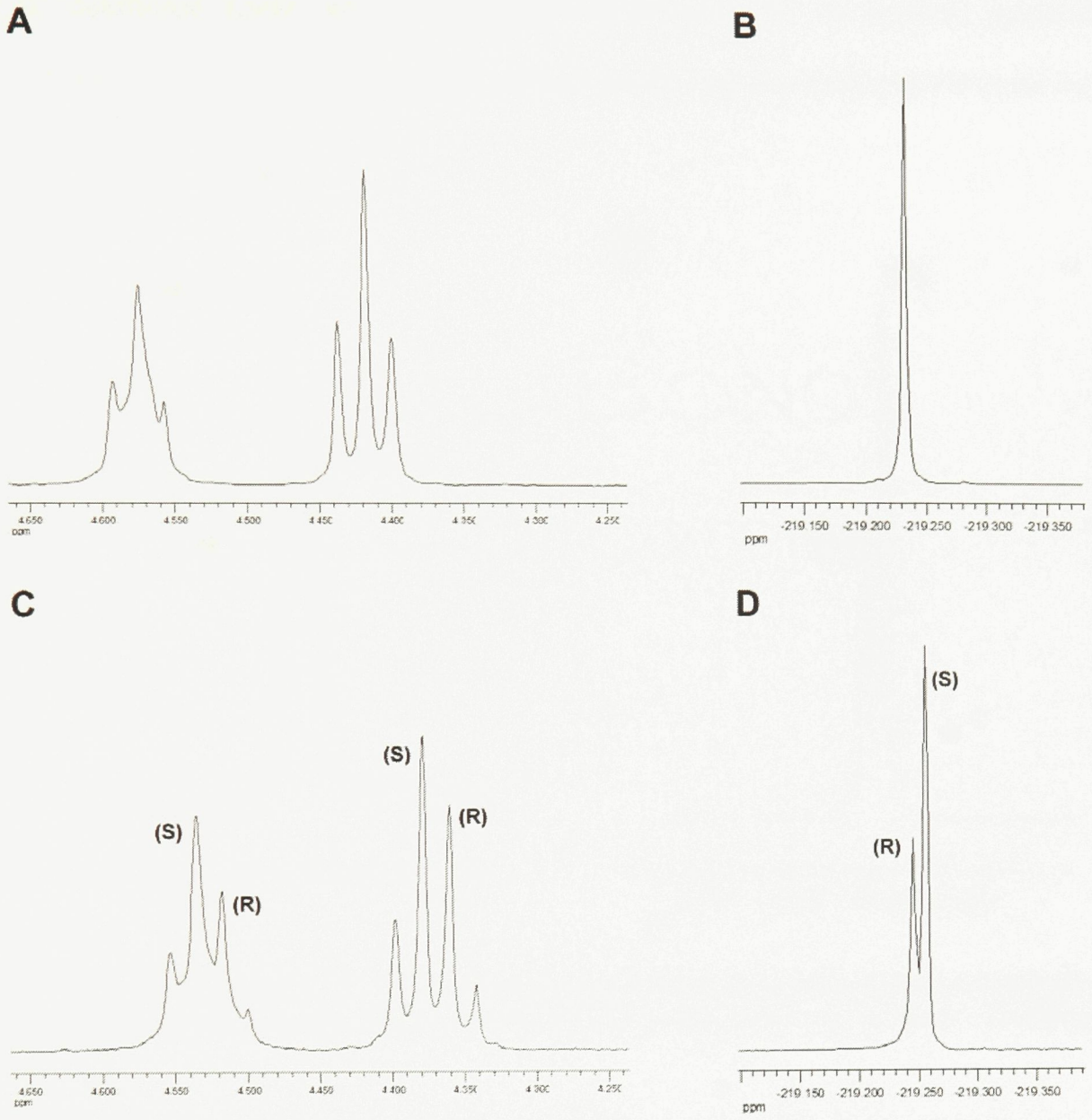

Figure 2.30 ^{1}H and ^{1}H-decoupled ^{19}F NMR spectra of a 2:1 mixture of (*S*):(*R*) 15F-11SO before (A and B) and after (C and D) the addition of 4 equivalents (*S*)-MPAA.

A comparison of the biosynthetic sample and the 2:1 synthetic sulfoxide mixture in the presence of (*S*)-MPAA is shown in Figure 2.31, A and B respectively. Based on the shielding observed in the synthetic sample, the enantiomeric composition of which has been unambiguously determined, the reported assignment[22] appears to be incorrect and the predominant enantiomer obtained biologically exhibited (*R*) configuration at the sulfur atom. This in turn implies that the corresponding 11-sulfido-C15 substrate was either misaligned in

the Δ^9 desaturase active site or underwent sulfoxidation by an oxidant unrelated to desaturases. This explanation would also account for the very low yield (<0.05%) and its low % *ee* (32%).[22]

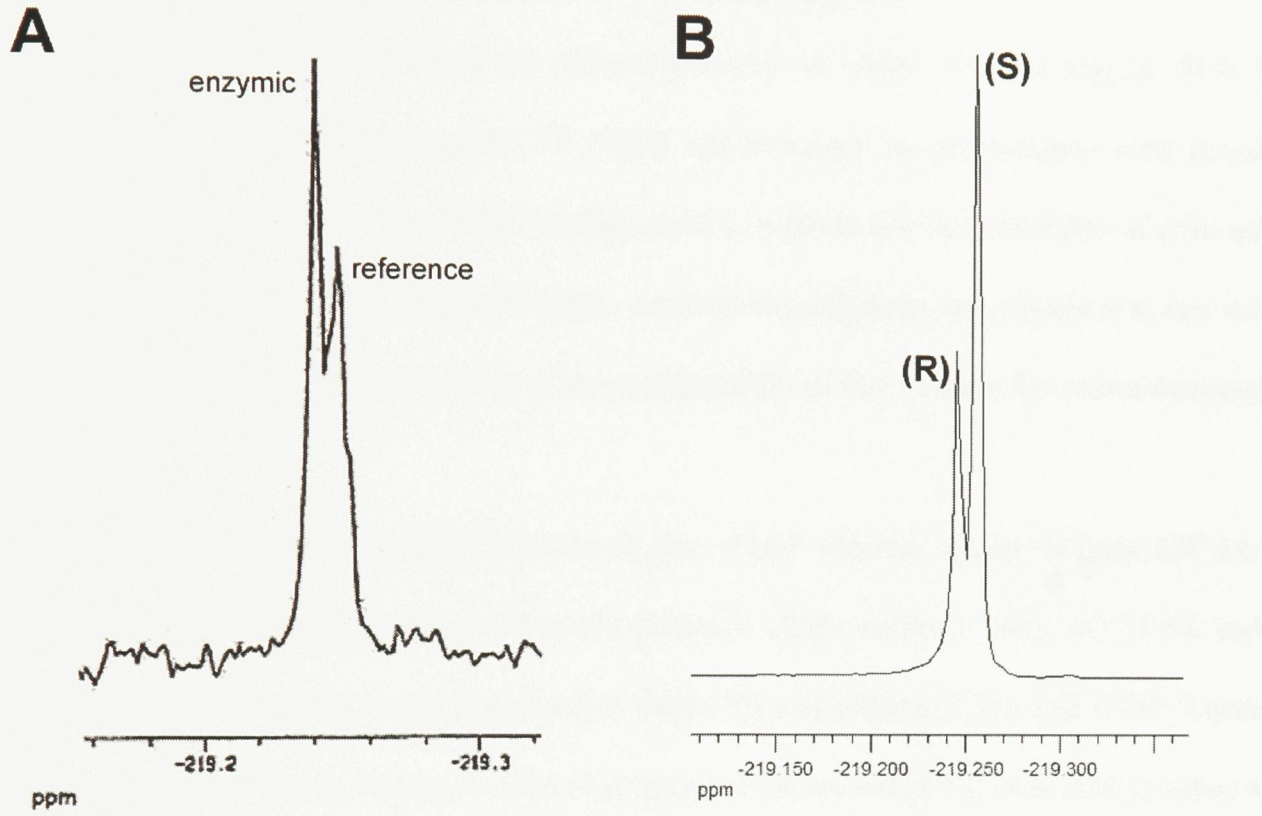

Figure 2.31 ^{1}H-decoupled ^{19}F NMR of enzymic 15-fluoro-11-sulfoxypentadecanoate (A), and 2:1 mixture of synthetic (*S*):(*R*) 15F-11SO (B), both with 4 equivalents (*S*)-MPAA.

2.1.5.4 Investigation of the effect of dilution on the direction of induced non-equivalence

To be certain that the observed effects of the chiral shift agent were not attributable to the dilution of the sample, the effects of (*S*)-MPAA on the ^{19}F NMR shifts were measured at both a 15 millimolar and a 40 nanomolar scale, the latter corresponding to the conditions of the analysis of the biosynthetic product.[22] In both cases, 4 equivalents of (*S*)-MPAA was used and the volume of $CDCl_3$ was approximately 0.9 ml. The $\Delta\delta^{S-R}$ for both dilutions was negative, confirming that concentration of analyte was not important with respect to the

direction of induced-non equivalence in the ^{1}H-decoupled ^{19}F NMR results. The magnitudes of the $\Delta\delta^{S-R}$ were -0.010 and -0.007 for the concentrated and diluted samples respectively.

2.1.5.5 A study of the direction of induced non-equivalence in ^{1}H and ^{1}H-decoupled ^{19}F NMR for various chiral solvating agents

In the course of identifying the stereochemistry of chiral fluorine-tagged dialkyl sulfoxides using ^{1}H and ^{1}H-decoupled ^{19}F NMR spectroscopy in combination with chiral NMR shift agents, the use of the Pirkle binding model in predicting the direction of induced non-equivalence was found to be problematic. Further investigation was required to test the generality of the results obtained and thus the predictability of this method for stereochemical determination.

The chemical shift non-equivalences of the $-CH_2F$ reporter group of both **18F-11-SO-1OH** and **15F-10SO** were observed in the presence of the anthryl CSAs, (*S*)-TFAE and (*R*)-AMA, the results of which are presented in Table 2.4 and Figures 2.33a and 2.33b. These agents were selected based on reports that shift agents with an anthryl system will produce a larger $\Delta\delta$ than a corresponding benzyl shift agent.[17, 18] Figure 2.32 shows the predicted effect of each CSA on the NMR signals of the $-CH_2F$ reporter group. In all cases, it is predicted that the reporter signal for the (*S*)-sulfoxides will be shielded with respect to the (*R*)- enantiomers.

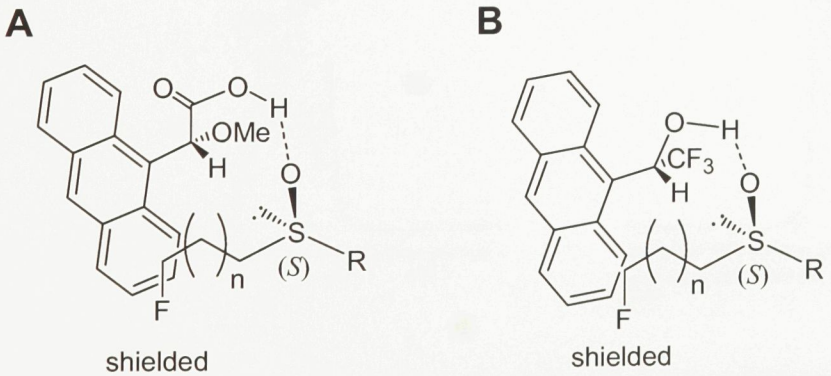

Figure 2.32 Pirkle binding model of (*R*)-AMA (A), and (*S*)-TFAE (B) with an ω-fluoro (*S*) sulfoxide.

Table 2.4. Summary of the direction of the induced non-equivalence of the (*S*)-sulfoxide with respect to (*R*)-sulfoxide in the presence of two chiral anthryl NMR shift agents.

		Observed			
		18F-10SO-1OH		15F-11SO	
	Predicted	(*R*)-AMA	(*S*)-TFAE	(*R*)-AMA	(*S*)-TFAE
^{1}H NMR	shielded	shielded	shielded	shielded	shielded
^{19}F NMR	shielded	deshielded	deshielded	deshielded	shielded

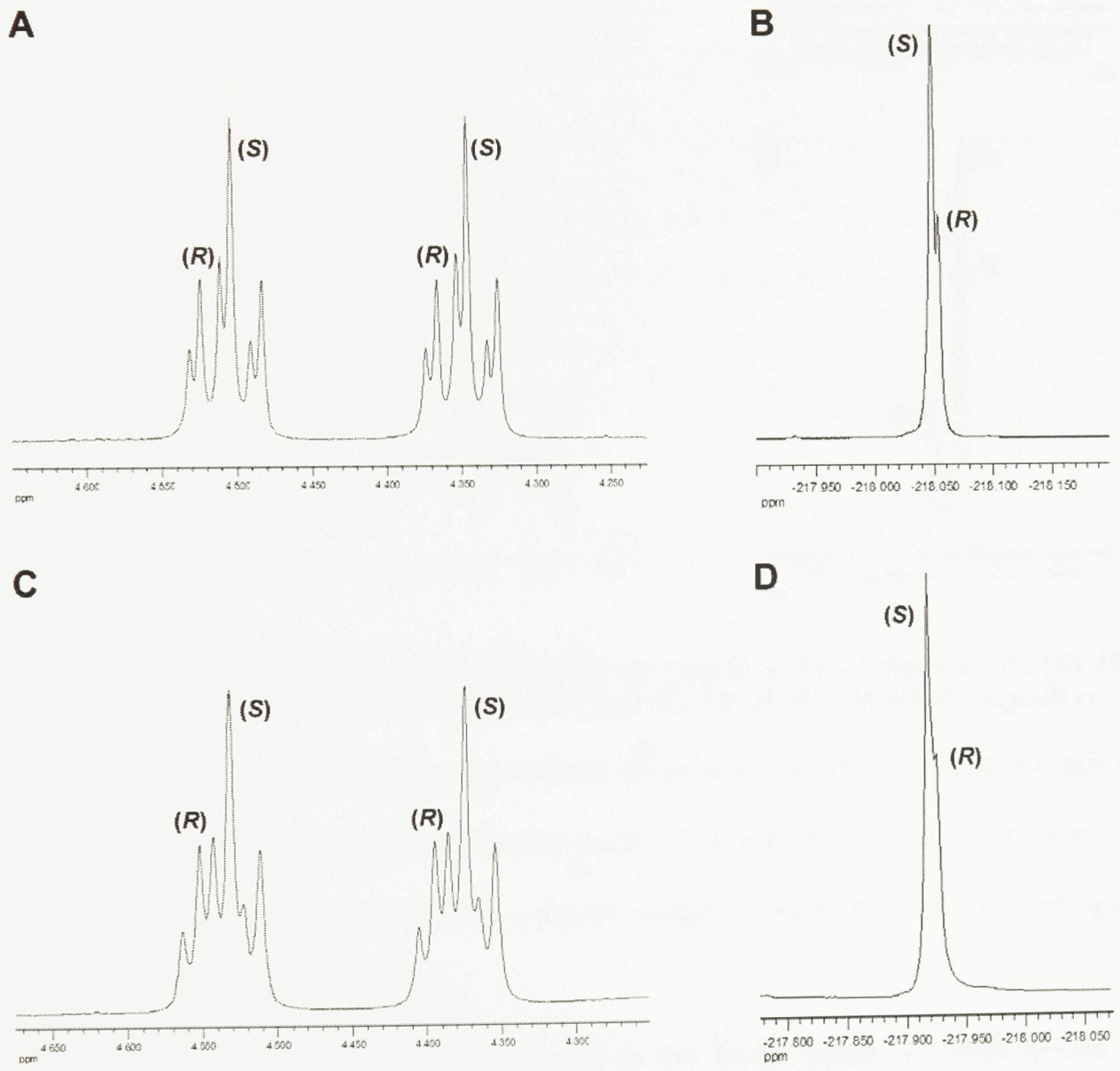

Figure 2.33a ^{1}H and ^{1}H-decoupled ^{19}F NMR spectra of a 2:1 mixture of (*S*):(*R*) 18F-10SO-1OH with 4 equivalents (*R*)-AMA (A and B) and (*S*)-TFAE (C and D).

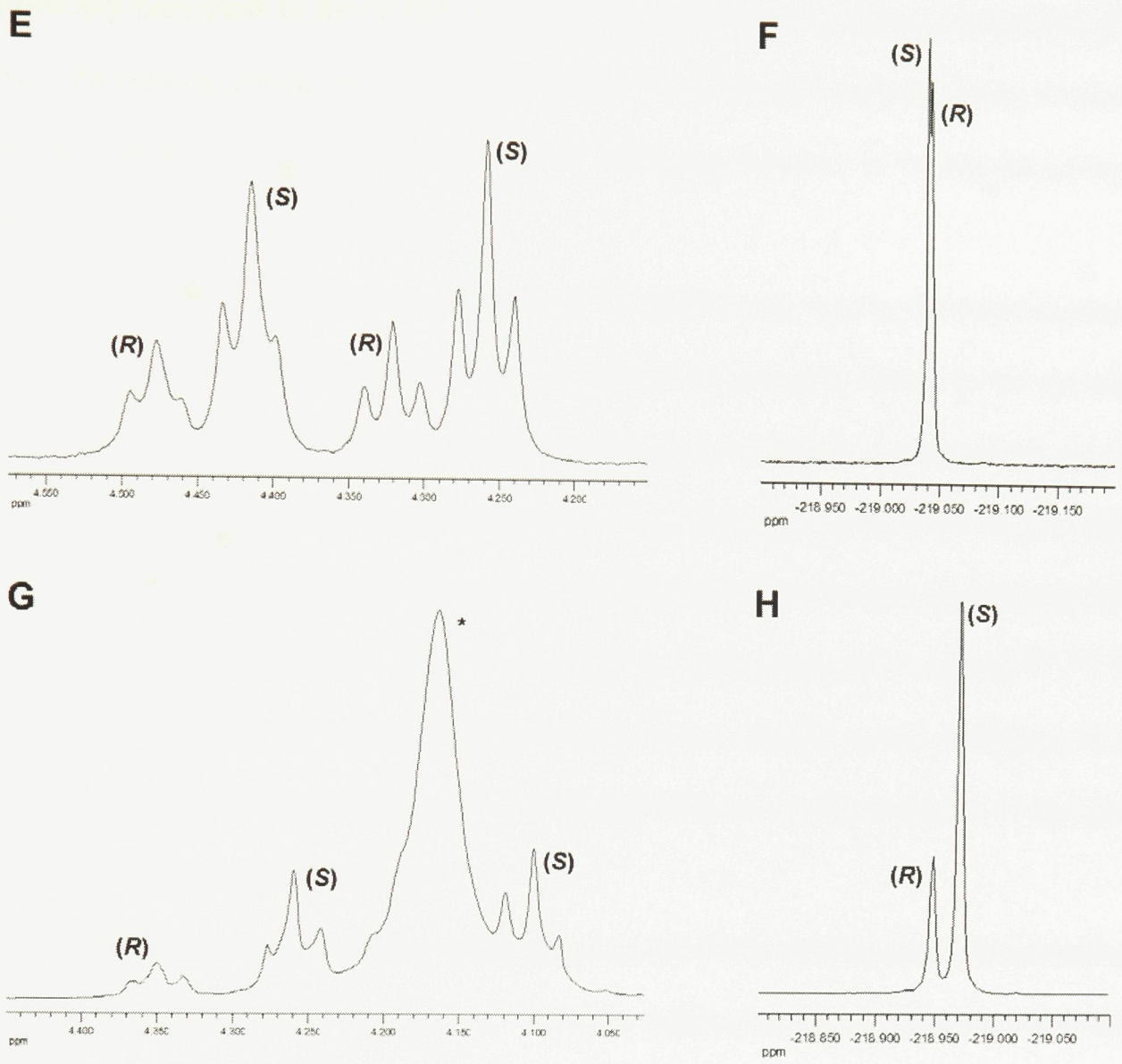

Figure 2.33b ^{1}H and ^{1}H-decoupled ^{19}F NMR spectra of a 2:1 mixture of (*S*):(*R*) 15F-11SO with 4 equivalents (*R*)-AMA (E and F) and (*S*)-TFAE (G and H). (* Impurity)

In all cases, the induced non-equivalence observed in the ^{1}H NMR spectra match the predicted results based on the Pirkle binding model. This suggests that this model may still be an appropriate representation for the collision complex formed between the shift agents and the sulfoxides presented herein.

The induced non-equivalences observed in the ^{1}H-decoupled ^{19}F NMR spectra are opposite to those observed in the ^{1}H NMR spectra, with the exception of the case of **15F-11SO** in the presence of (*S*)-TFAE. That the signals of the fluorine reporter behave

differently than those of the –C**H**$_2$F protons in the presence of a CSA is unexpected given that both reporter groups should reside in similar shielding environments, being bonded to the same freely rotating carbon atom. Just as surprising, however, is the non-generality of the ^{1}H-decoupled ^{19}F NMR results.

There are examples in the literature of ^{19}F NMR being used in the determination of absolute configuration,[44] however these are found to be primarily limited to the use of the fluorine atom on the chiral shift agent and are therefore not readily comparable to our case with a remote fluorine reporter. Nevertheless, it is noted that examples of the fluorine signal behaving anomalously using this method are very few, and the cases bear no similarity to the situation presented herein (i.e. large cyclic systems, lanthanide shift reagents).[44, 45] The method of measuring an induced shift difference of the fluorine signals belonging to the chiral solvation agent, (*S*)-TFAE could not be applied to our compounds due to the quasi-symmetrical nature of the sulfoxides.

Preliminary computational studies based on the Pirkle binding model have predicted possible anomalies in the behaviour of ^{19}F NMR chemical shifts of fluorinated sulfoxides complexed to MPAA.[46] Given the sensitivity of ^{1}H-decoupled and ^{19}F NMR, there may be anisotropic effects occurring which hinder the facile prediction of the direction of induced non-equivalence. Further experimental and computational studies in this area are necessary to determine to what extent the direction of non-equivalence can be predicted when using ^{19}F NMR.

2.1.6 Conclusions and future directions

In this work, a general and efficient procedure for preparing synthetic fluorine-tagged chiral dialkyl sulfoxides was developed using DAG methodology. 18-fluoro-(10*S*)-sulfoxy-1-

octadecanol, 18-fluoro-(10*R*)-sulfoxy-1-octadecanol, 15-fluoro-(11*S*)-sulfoxypentadecane, and 15-fluoro-(11*R*)-sulfoxypentadecane were prepared.

These compounds were used in the stereochemical analysis of enzymatically produced sulfoxides arising from the introduction of fluorine-tagged thia fatty acid analogues to a soluble and a membrane-bound Δ^9 desaturase. Introduction of an 18-fluoro-10-thia fatty acid analogue to castor stearoyl-ACP Δ^9 desaturase resulted in the oxidation of the thia moiety to an (*S*)-configured sulfoxide. This is in accord with the stereochemistry expected based on isotope-labeling experiments.[19] The oxidation of a 15-fluoro-11-thia fatty acid analogue by a membrane-bound *Saccharomyces cerevisiae* S522C Δ^9 desaturase resulted in a sulfoxide with (*R*) configuration. This result is not altogether surprising given that C-11 does not correspond to a desaturase-accessible position.

Further to these investigations, we have found that the Pirkle binding model is successful for predicting the direction of induced non-equivalence of fluorine-tagged dialkyl sulfoxide enantiomers by ^{1}H NMR using the chiral solvating agents AMA, MPAA and TFAE. The observed non-equivalence of ^{19}F NMR signals of these sulfoxides under the same conditions is dependent on the nature of the CSA used. Preliminary computational studies have to some extent predicted this phenomenon[46], however, to our knowledge, this is the first experimental result to demonstrate the NMR nucleus-dependent switch in observed induced non-equivalence of NMR signals. Further experimental and computational studies may shed more light on the origins of this behaviour.

The use of chiral solvating agents in the study of the stereochemistry of the oxidation of thia fatty acid analogues by desaturase enzymes using ^{1}H-decoupled ^{19}F NMR is an

attractive option for use at the analytical level. Confirmation of stereochemical assignments via synthetic standards is required when using ^{19}F NMR spectroscopy.

2.2 Study of the catalytic diversity of an acyl-ACP desaturase mutant

2.2.1 Introduction

Mutagenesis experiments are a useful tool for determining structure-function relationships in enzymes. In the case of soluble desaturase enzymes, experiments have shown that the substitution of only a few amino acids can lead to changes in the regioselectivity of a desaturase with respect to the introduction of a double bond, a change in substrate chain lengths specificity or both.[47] Membrane-bound desaturases have shown more diversity on reaction outcome and mutants have been engineered that increase the amount of hydroxylated product, based on comparison studies with a hydroxylase.[48]

While progress has been made towards the rational mutation of desaturases, it is limited by the absence of greater structural characterization for membrane-bound desaturases and also by the limited reactivity of soluble desaturases, which to date have been shown to only catalyze dehydrogenation reactions with normal substrates. To this end, the team of John Shanklin at Brookhaven National Laboratories in Upton, New York has engineered a new triple mutant, T117R/G188L/D280K of the castor Δ^9 acyl-ACP desaturase, herein referred to as "the mutant".

The soluble acyl-ACP Δ^4 desaturase isolated from *Hedera helix* shows 74% homology with the amino acid sequence of castor stearoyl-ACP Δ^9 desaturase.[6] The aim in the design of the mutant was to rationally produce a Δ^4 desaturase from the Δ^9 desaturase based on a comparison of the active sites of these two enzymes. The mutant featured two

mutations in the lining of the substrate cavity and one near the acyl-ACP binding site (Figure 2.34).

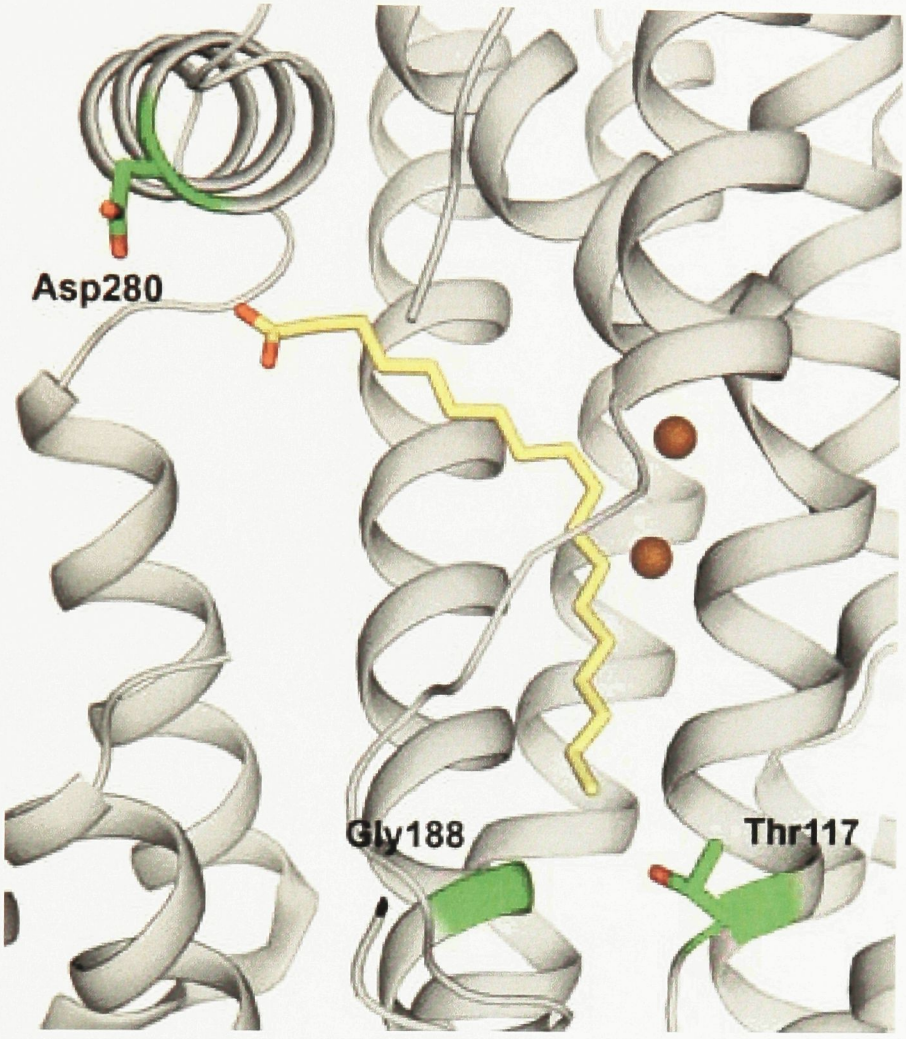

Figure 2.34 Model of the triple mutant of the castor Δ^9 acyl-ACP desaturase with mutations shown in green, diiron as brown spheres and stearate substrate in yellow.

When the mutant was incubated with the stearoyl-ACP derivative, desaturation occurred at the 9th position (Peak 2 in Figure 2.35 B), as was observed in the wild-type enzyme and contrary to the aim of the project. Interestingly, however, at longer incubation times, the unsaturated product disappeared based on GC/MS analysis (Figure 2.35 C). Silylation of the product mixture prior to GC/MS showed that an alcohol was being produced (Figure 2.35 D). Figure 2.35 E and F show the mass spectra of the product peaks labelled 3 and 4. The molecular ion and the mass of the major fragment of these products indicated that

the product was an unsaturated alcohol, with the major fragment resulting from cleavage between the 8th and 9th positions consisting of the methyl terminus and both the trimethylsilyl (TMS) alcohol and alkene moieties.

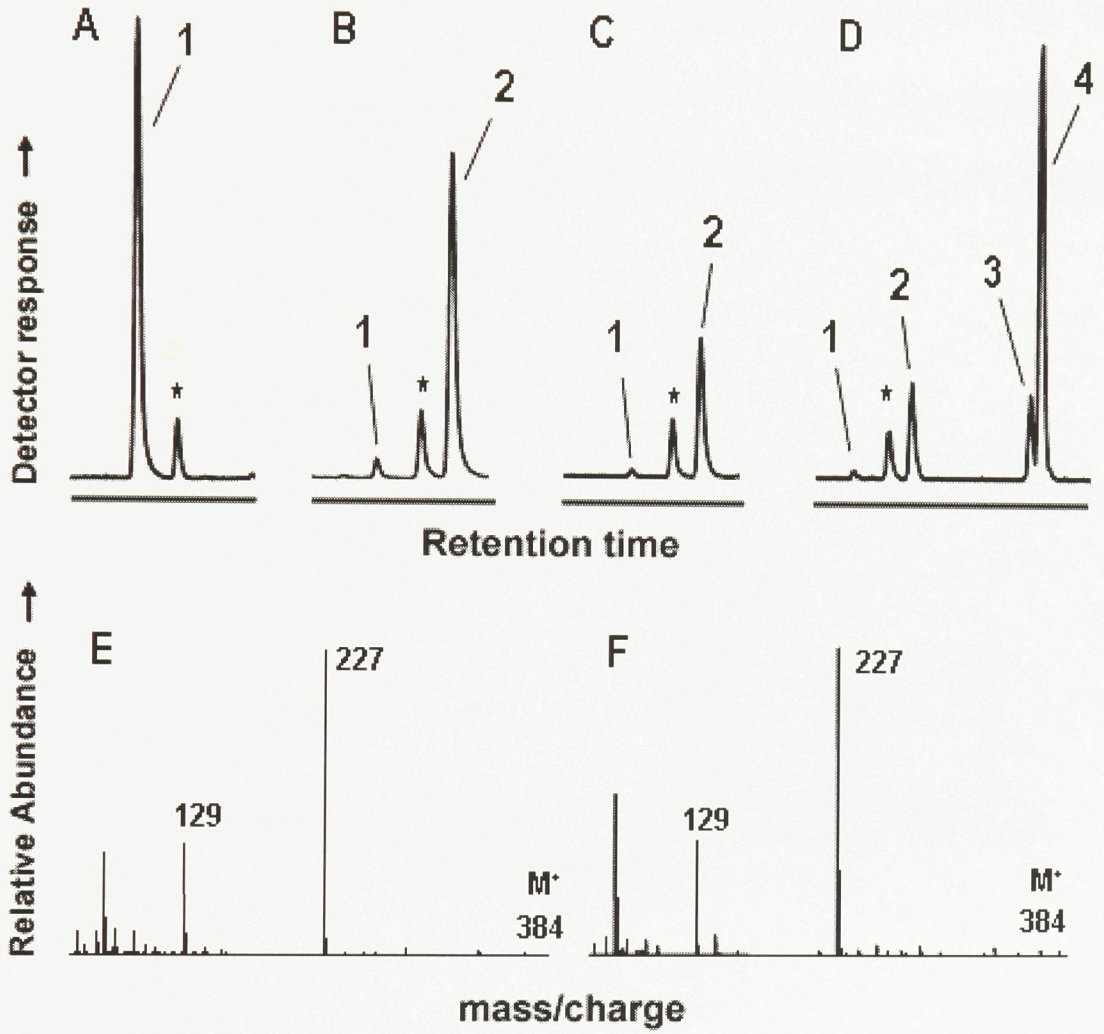

Figure 2.35 GC analysis of the products obtained from the incubation of stearoyl-ACP with the mutant desaturase at reaction time, t = 0 (A), T = 0.5 h (B) and t = 5 h (C and D). E and F feature the mass spectra of the allylic alcohol product peaks labelled 3 and 4 respectively. (1, substrate; 2, methyl 9-octadecenoate;* contaminant)

With the disappearance of the original Δ^9 unsaturated product, which is not a substrate for the wild-type enzyme, a new incubation experiment was performed using 9*Z*-octadecenoate (oleate) as a substrate. The same product profile was obtained as with the unsaturated substrate indicating that the oleate was being produced and then acting as a substrate for the mutant enzyme.

Given the novelty of the mutant enzyme accepting unsaturated substrate, the *E* isomer of oleate, elaidate was introduced to the enzyme to see whether it could also serve as a substrate. While it was a poorer substrate than the *Z* configured oleate, it was converted to a near equal mixture of allylic alcohol and dienoic fatty acid products (Figure 2.36). The allylic alcohols shared identical mass spectra to those obtained from the 9*Z* substrate. The mass spectrum of the pyrrolidine derivative of the diene product (Figure 2.36 D) showed that it was a C18-9,11 conjugated dienoic acid.

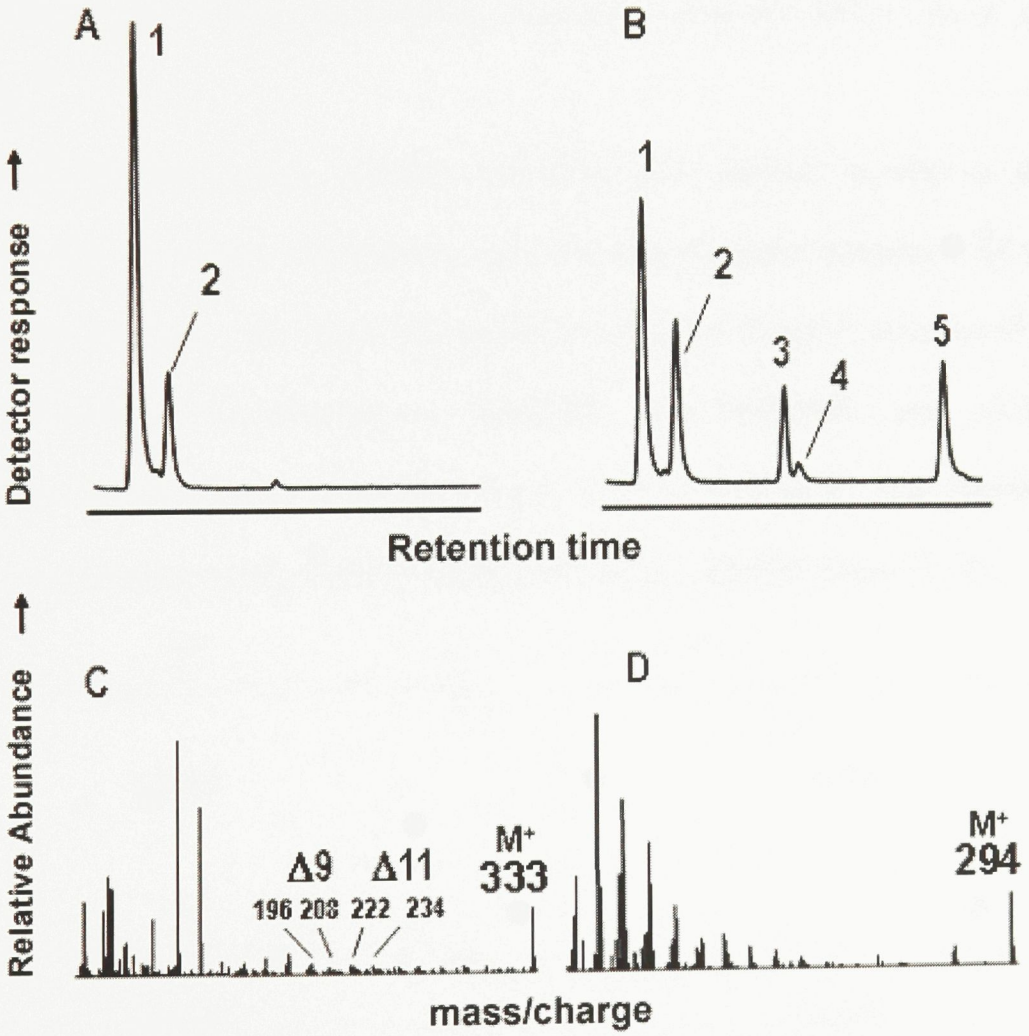

Figure 2.36 GC analyses of the TMS derivatives of elaidyl-ACP before (A) and after the addition of the mutant desaturase (B). Mass spectrum of the pyrrolidine derivative of 5 (C) and the corresponding parent methyl ester (D). (1, substrate; 2, unidentified; 3 and 4, allylic alcohols; 5, diene).

2.2.2 Project goals

The aim of this project was to gain a better understanding of how these unusual products arise from the mutant desaturase enzyme. This could be achieved in part by identifying the location of the hydroxyl group and the double bond in the allylic alcohols produced by the mutant desaturase, as well as determining the stereochemistry of the double bonds of the allylic alcohols and the diene product obtained from this enzyme. This information could give a better understanding of the structure-function relationship by providing some idea of how the different substrates fit in the active site of the mutant desaturase.

To achieve these goals, synthetic standards were required in order to identify the products by GC co-elution experiments and to assign the stereochemistry of the double bond(s) in the products. The target molecules included the *Z* and *E* isomers of the allylic alcohols, 9-hydroxy-10-octadecenoate (**9OH10*Z*** and **9OH10*E***) and 11-hydroxy-9-octadecenoate (**11OH9*Z*** and **11OH9*E***) (Figure 2.37) as well as all four stereoisomers of methyl 9,11-octadecadienoate: **9*Z*11*E***, **9*E*11*Z***, **9*Z*11*Z*** and **9*E*11*Z*** (Figure 2.38).

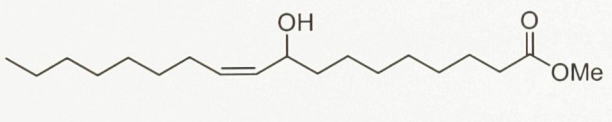

9OH10Z

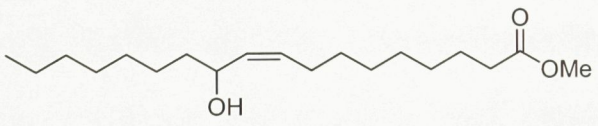

11OH9Z

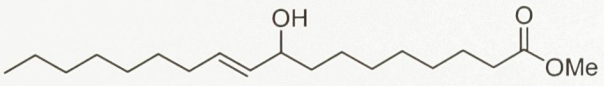

9OH10E

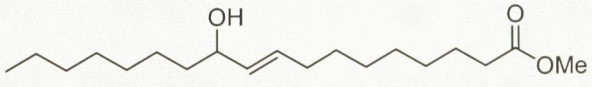

11OH9E

Figure 2.37 Target allylic alcohols, methyl (10*Z*) and (10*E*) 9-hydroxy-10-octadecenoate and methyl (9*Z*) and (9*E*) 11-hydroxy-9-octadecenoate.

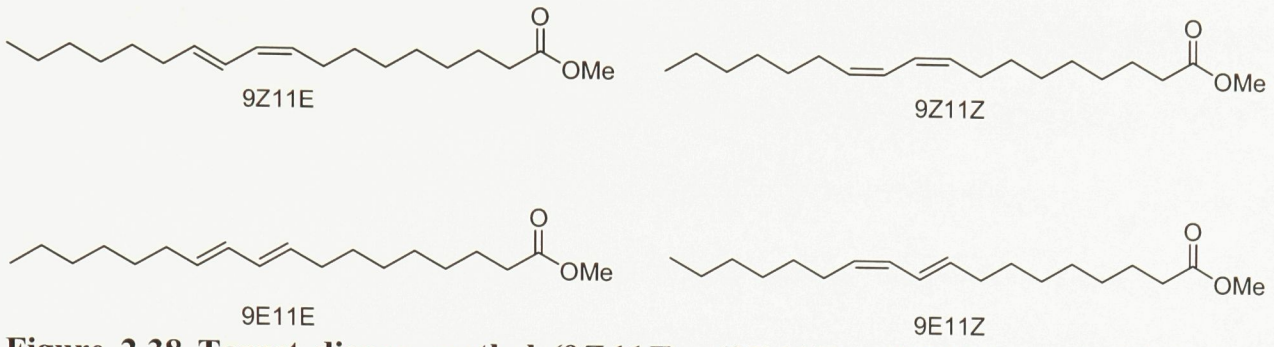

Figure 2.38 Target dienes, methyl (9*Z*,11*E*)-, (9*E*,11*E*)-, (9*Z*,11*Z*)- and (9*E*,11*Z*) 9,11-octadecadienoate.

2.2.3 Synthesis of allylic alcohol fatty acid methyl ester standards

There are several different routes involving well known methods which can be used for synthesis of allylic alcohols. These include the addition of a terminal alkene or alkyne to an aldehyde, the addition of a Grignard reagent to an enal, or the reduction of an enone. For the target compounds, the required starting enals and enones were not commercially available and thus it was decided to add alkenes and alkynes to aldehydes and obtain the desired stereochemistry either through the starting material, or through the reduction of an intermediate. Allylic alcohols are stable to equilibration in the absence of strong acid and thus both stereoisomers of the allylic alcohols should be obtainable.

A *Z* double bond is introduced quite easily through the reduction of the corresponding triple bond of a propargylic alcohol using Lindlar's catalyst. The *E* double bond, though thermodynamically more stable, is not as easily obtained through reduction. However, it has been found that in some cases, a small amount of *E* product can occur with the Lindlar reduction of an alkyne.[49] It is necessary for this study, that the two stereoisomers are synthesized; however if a sufficient amount of the *E* product is obtained while producing the *Z* stereoisomer, only one synthesis would be required for the two target compounds.

While the ideal scenario involves obtaining the corresponding *E* stereoisomer as a by-product, it may be required to synthesize them directly. In this case, a convenient route would be to add a terminal *E*-alkyl halide to the aldehyde. This would permit us to use the same starting aldehyde as for the formation of the *Z* stereoisomer. The appropriate alkyl halide was not commercially available in either case, however terminal *E* vinyl iodides can be obtained from the corresponding terminal alkynes through the use of the Schwartz reagent, $HZrCp_2Cl$.[50] This reagent is produced *in situ* from $ZrCp_2Cl_2$ and DIBAL-H.[50] The zirconium reagent is first added to the acetylene to produce a vinylzirconium(IV) intermediate. Iodolysis is then performed, and occurs with retention of configuration (Figure 2.39).[51]

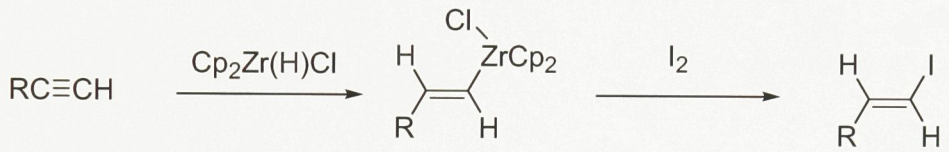

Figure 2.39 The trans-iodonation of a terminal alkyne.

2.2.3.1 Synthesis of methyl (10*Z*)- and (10*E*)-9-hydroxy-10-octadecenoate

The synthesis of (10*Z*)- and (10*E*)- methyl 9-hydroxy-10-octadecenoate was performed with overall yields of 17% and 14% respectively starting with commercially available mono-methyl azelate (Figure 2.40). The aldehyde was first formed from azelaic acid, mono-methyl ester through a borane reduction of the acid to an alcohol (26% yield) followed by pyridinium chlorochromate (PCC) oxidation of the alcohol to the aldehyde (78% yield).[52] 1-nonyne was added to the aldehyde after lithiation with n-butyllithium (n-BuLi) to form the intermediate propargyl alcohol (89% yield). Methyl (10*Z*)-9-hydroxy-10-octadecanoate was obtained by the Lindlar-catalyzed reduction of the propargylic intermediate (93% yield). The spectral data of this compound was similar to that reported

previously.[53] The spectra showed a clean reduction of the triple bond to the *Z* isomer and thus the 10*E* isomer had to be made using another method.

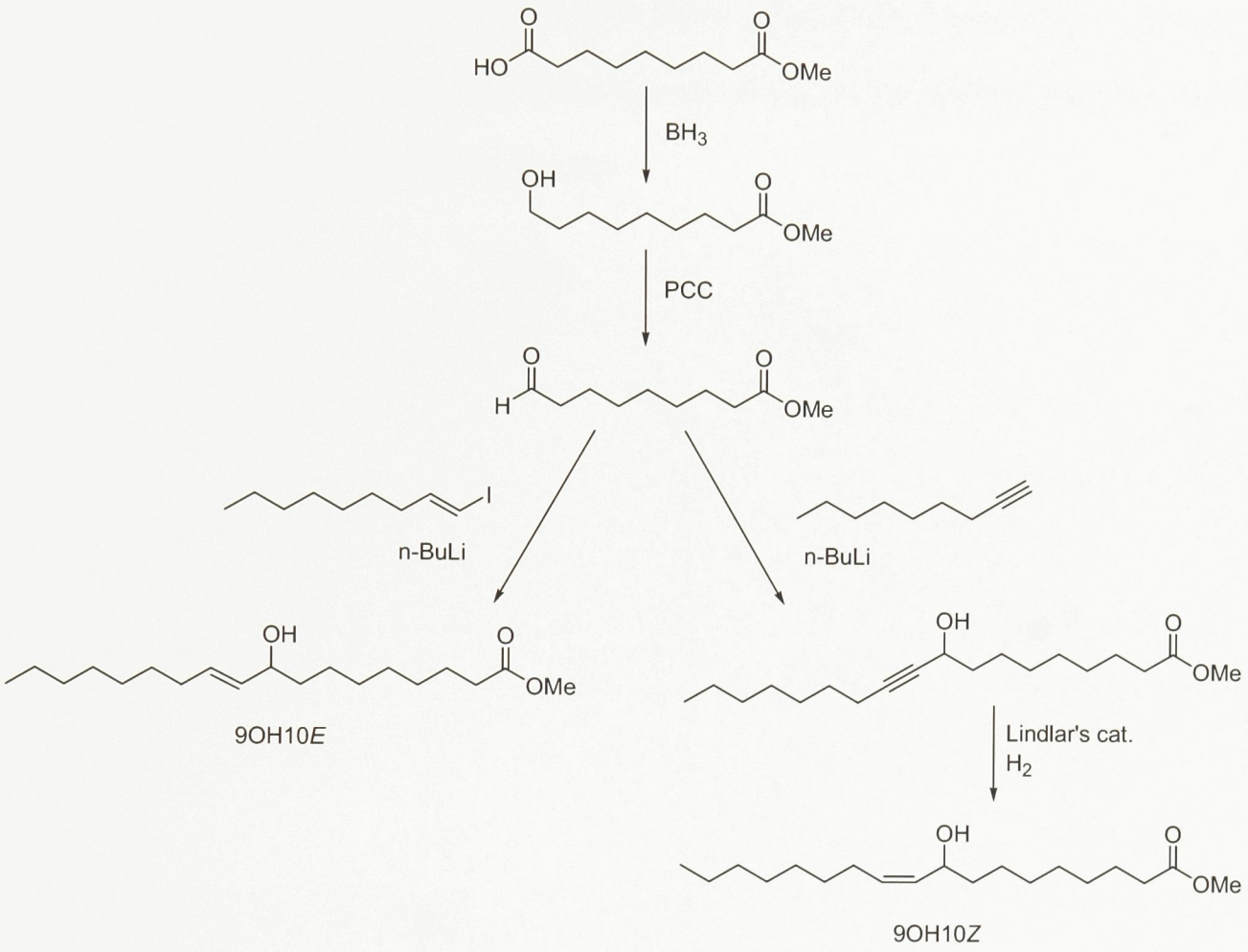

Figure 2.40 Scheme for the synthesis of (10*Z*)- and (10*E*) methyl 9-hydroxy-10-octadecenoate.

The *E* iodo-alkene required, 1,1*E*-iodononene was made from commercially available 1-nonyne. $ZrCp_2Cl_2$ was first converted to the Schwartz reagent, $HZrCp_2Cl$ using diisobutylaluminum hydride (DIBAL-H). Iodolysis was then performed to obtain the vinyliodide with a 76% yield. The stereochemistry of this compound was confirmed by ^1H and ^{13}C NMR data which was similar to that previously reported.[54] The vinyliodide was lithiated using n-BuLi and methyl 9-oxononanoate was added to obtain (10*E*) methyl 9-hydroxy-10-octadecanoate (7% yield).

The assigned structures of the products were confirmed using mass spectra, ^{1}H and ^{13}C NMR. The structural data for both compounds were similar to that previously reported.[53] The mass spectra of the trimethylsilyl ether these compounds were nearly identical and featured a major fragment having m/z of 227 due to cleavage between the 8th and 9th carbons of the fatty acid (Figure 2.41).

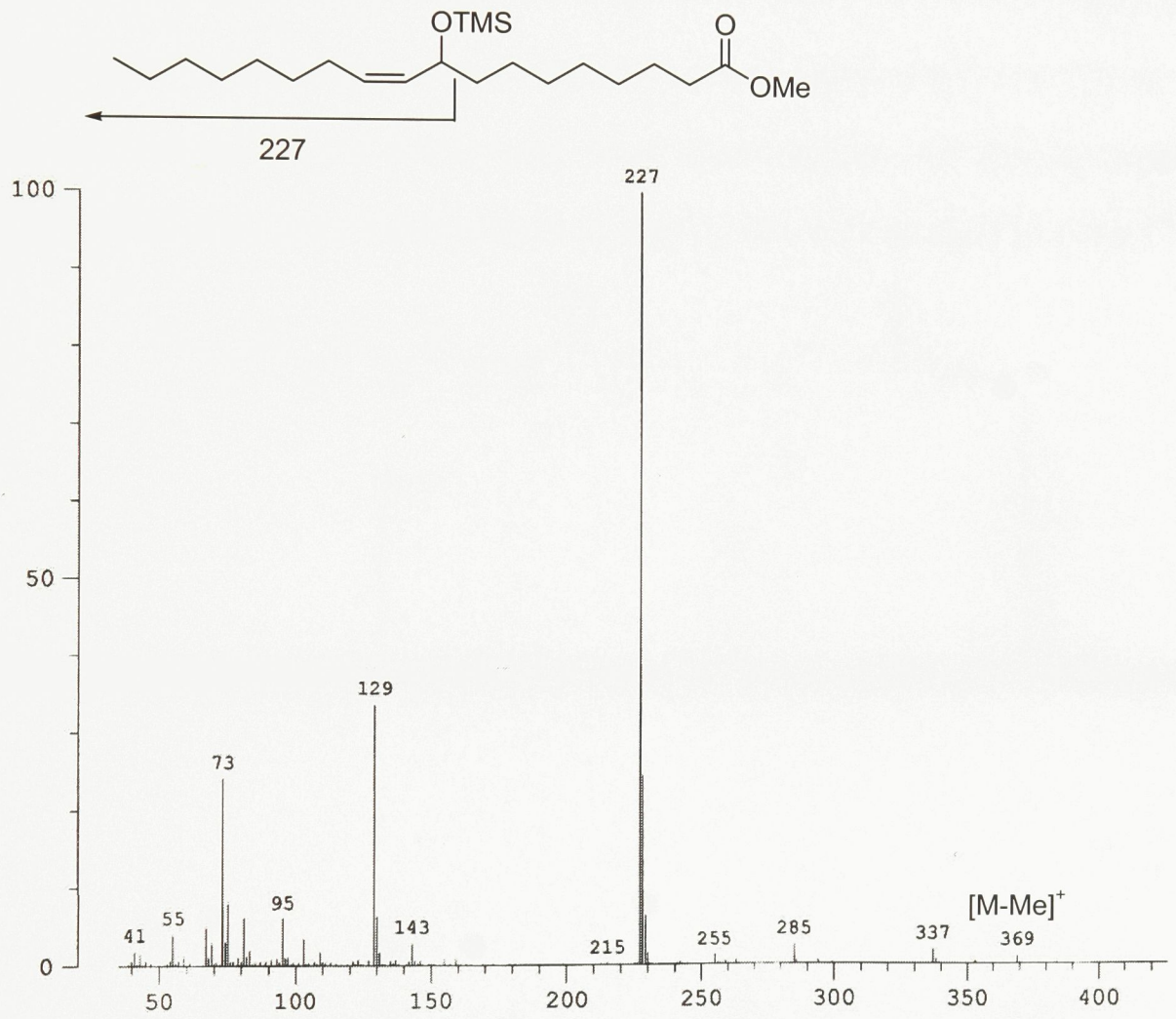

Figure 2.41 Mass spectrum of methyl (10*Z*)-9-hydroxy-10-octadecenoate.

The ^{13}C NMR spectrum of the 9-OH-10-ene products are shown in Figures 2.42, 2.43 and Table 2.5. The most characteristic signals of note is the appearance of the 9th carbon at either 67.68 or 73.16 ppm and of the 12th carbon at 27.71 or 32.17 ppm depending on whether they are adjacent to a *Z* or a *E* double bond respectively. The ^{1}H NMR shifts

(Figures 2.44, 2.45 and Table 2.6) of the 9th, 10th and 11th positions are also characteristic depending on the stereochemistry of the double bond, as well as the coupling constant between the vinylic protons. In the case of the *Z* double bond, the carbon in the 9th position (labeled 'a' in Table 2.6) appears at 4.41 ppm versus 4.03 ppm when adjacent to the *E* double bond. The shifts of the vinyl protons H10 and H11 (b and c in Table 2.6) appear to be more shielded for the *Z* double bond coming at 5.36 and 5.49 versus 5.43 and 5.61 respectively. More significant is the coupling constant between these two protons which is 10.7 Hz for a *Z* double bond and 15.3 for a *E* double bond. These values correlate well with the expected values for these bonds, where *Z* protons have a typical *J* value of 10 Hz and *E* of 16 Hz.[55]

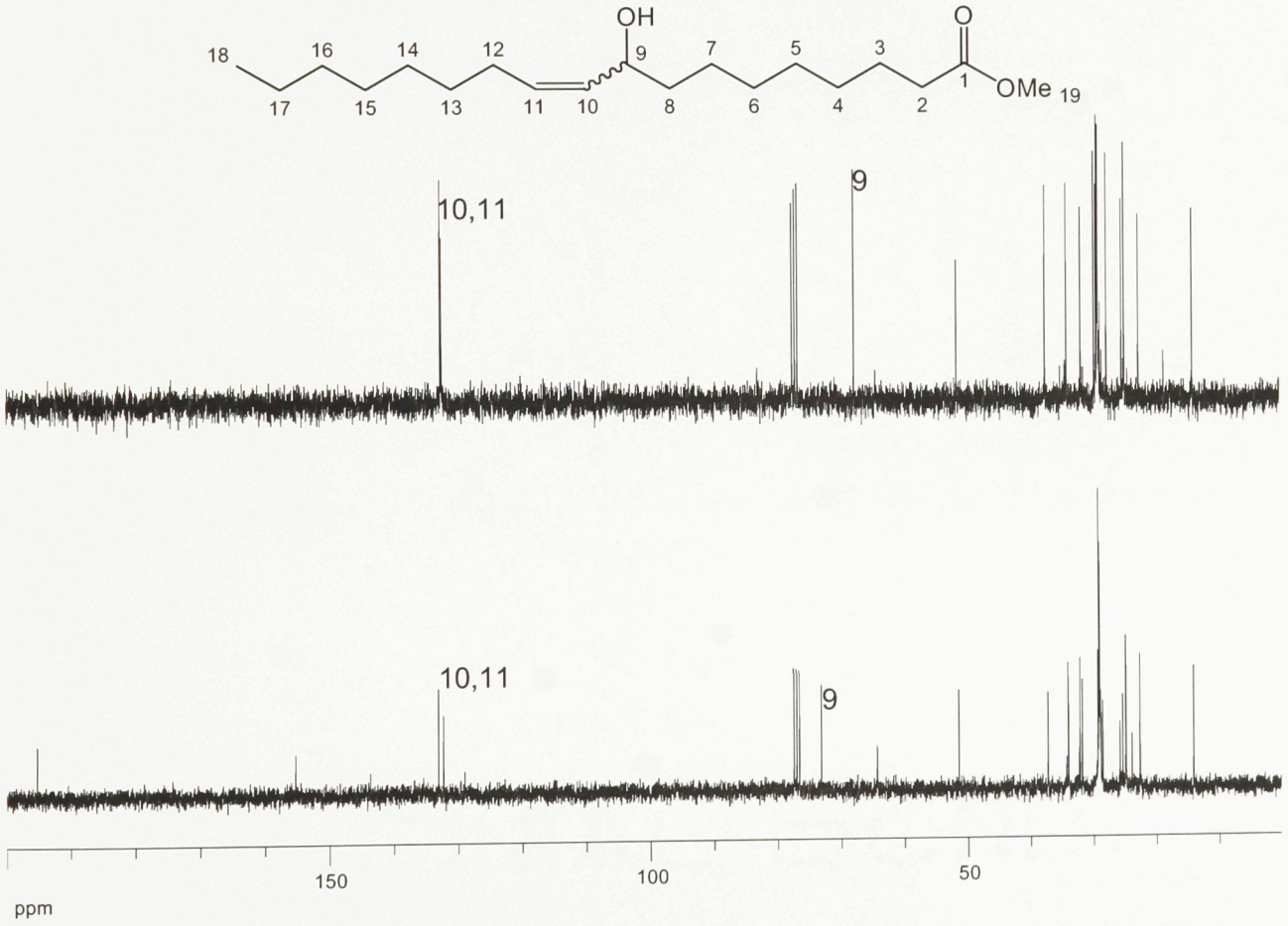

Figure 2.42 ^{13}C NMR spectra of methyl (10*Z*)- (above) and (10*E*)- (below) 9-hydroxy-10-octadecenoate.

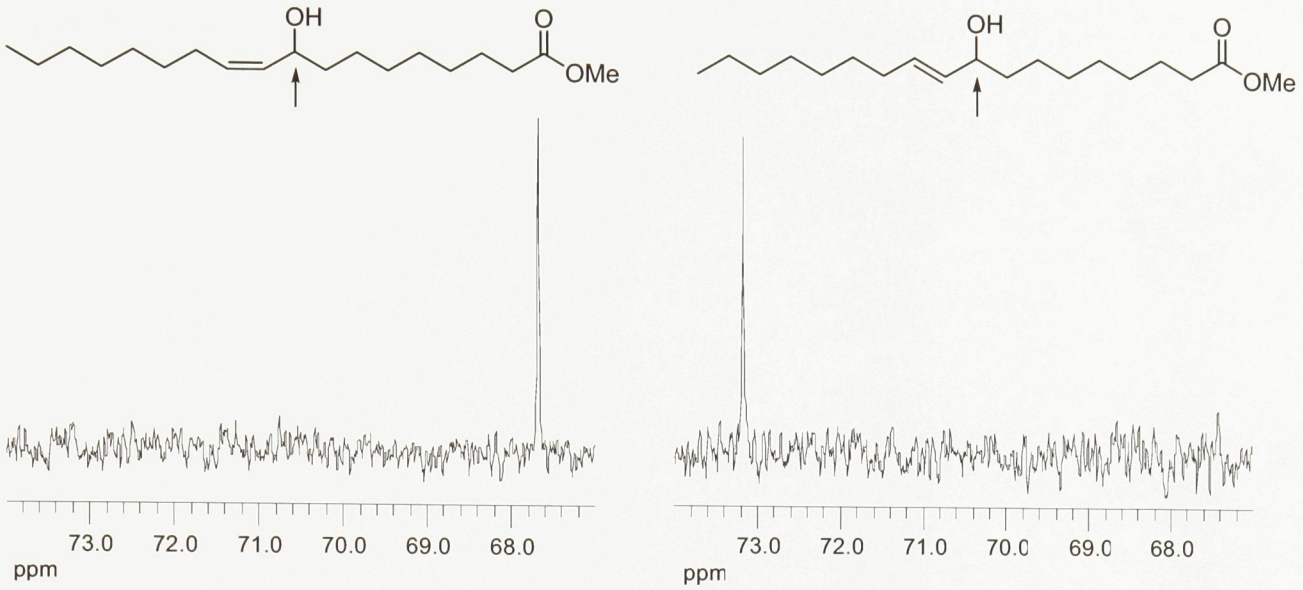

Figure 2.43 ^{13}C NMR of the C(OH) carbons in (10*Z*)- (right) and (10*E*)- (left) 9-hydroxy-10-octadecenoate.

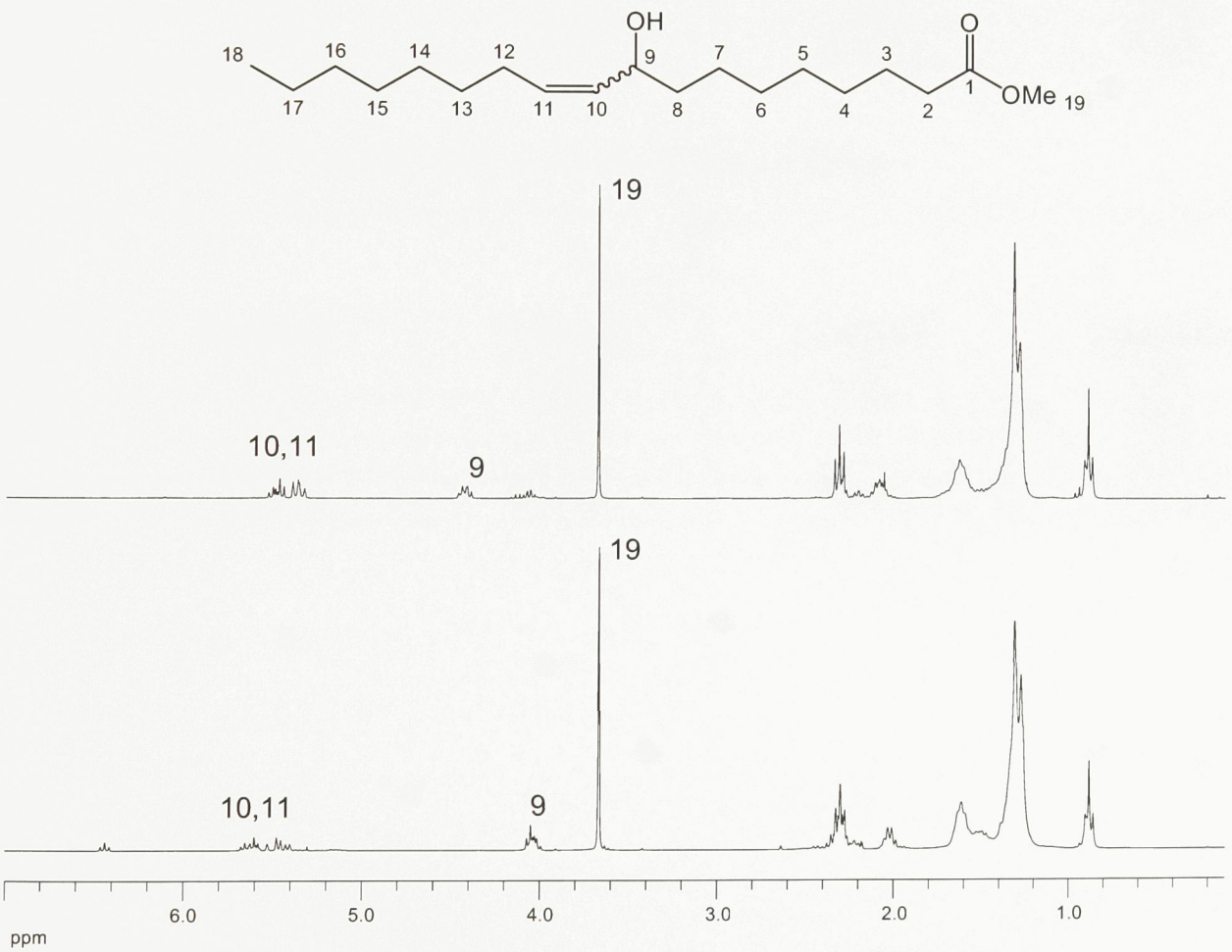

Figure 2.44 ^{1}H NMR spectra of methyl (10Z)- (above) and (10E)- (below) 9-hydroxy-10-octadecenoate.

Table 2.5 Selected ^{13}C NMR shifts of allylic alcohol products.

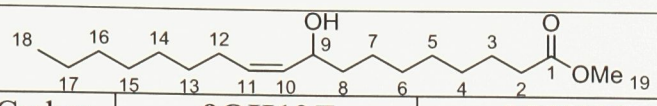

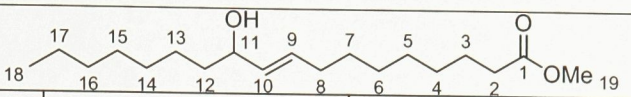

Carbon	**9OH10*Z***	**9OH10*E***	**11OH10*Z***	**11OH10*E***
1	174.32	174.30	174.31	174.31
2	34.08	34.06	34.06	34.06
3	24.92	24.89	24.90	24.90
7	25.32	25.39	na	na
8	37.47	37.26	27.66	32.13
9	67.68	73.16	132.73	133.16
10	132.39	132.21	132.16	132.01
11	132.55	132.98	67.72	73.21
12	27.71	32.17	37.55	37.36
13	na	na	25.40	25.50
16	31.82	31.82	31.82	31.82
17	22.65	22.64	22.66	22.66
18	14.10	14.09	14.09	14.08
19	51.45	51.44	51.45	51.45

*na = not assigned

Table 2.6 Selected ^{1}H NMR shifts of allylic alcohol products.

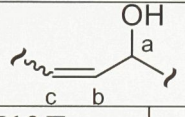

Proton	**9OH10*Z***	**9OH10*E***	**11OH10*Z***	**11OH10*E***
a	4.41	4.03	4.42	4.03
b	5.36	5.43	5.37	5.46
c	5.49	5.61	5.46	5.62
J_{bc}	10.7 Hz	15.3 Hz	11.0 Hz	15.3 Hz

2.2.3.2 Synthesis of methyl (9*Z*)- and (9*E*)- 11-hydroxy-9-octadecenoate

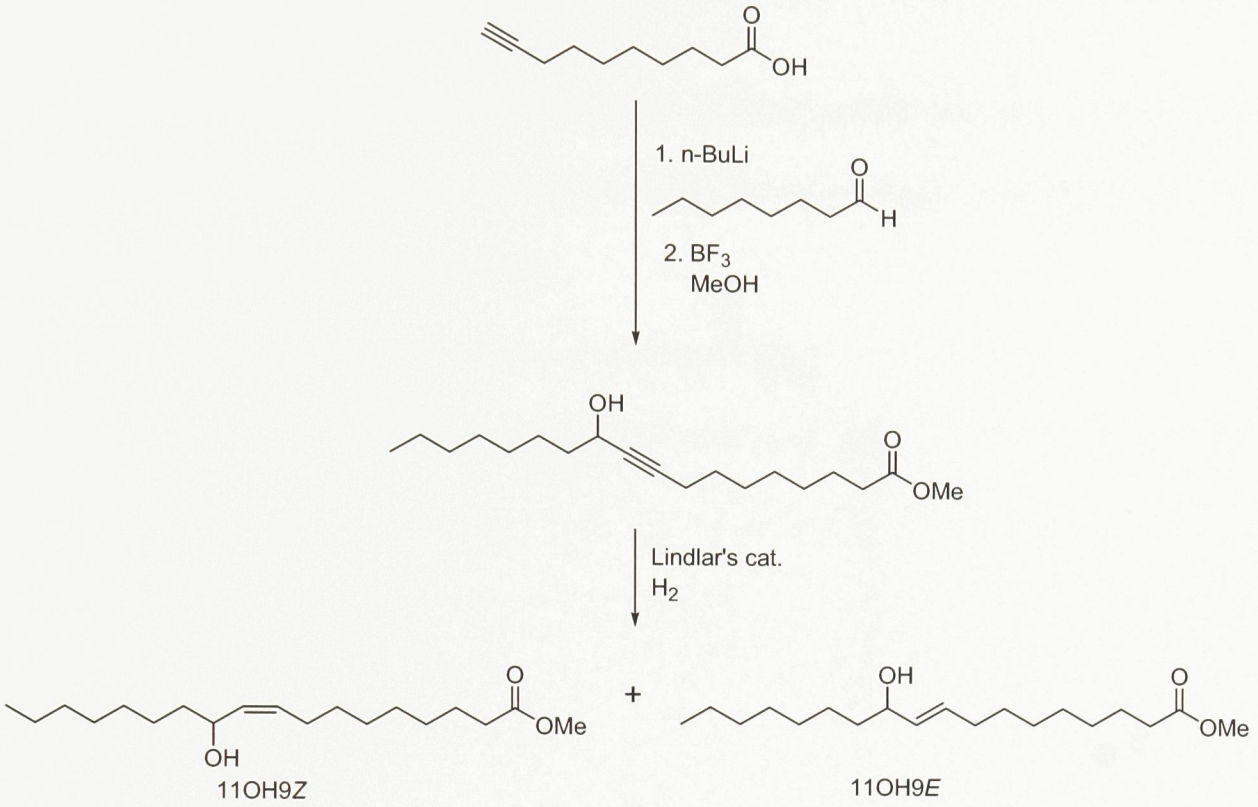

Figure 2.45 Scheme for the synthesis of methyl (9Z)- and (9E)-11-hydroxy-9-octadecenoate.

(9*Z*)- and (9*E*) Methyl 11-hydroxy-8-octadecanoate were prepared starting with 9-decynoic acid which had previously been prepared through the acetylenic displacement of 8-bromooctanoic acid.[56] Both stereoisomers were obtained in the same synthesis, with the (9*E*) product present as minor product (Figure 2.45). The overall yields based on the starting alcohol for the (9*Z*) and (9*E*) allylic alcohols were 7 and 1 % respectively based on 9-decynoic acid. 9-Decynoic acid was deprotonated with two equivalents of n-BuLi and then added to octanal to form the intermediate propargyl alcohol. This intermediate was then methylated using borontrifluoride diethyl etherate (BF_3)[57] before being purified by flash chromatography (10% yield). Methyl (10*Z*)-9-hydroxy-10-octadecanoate was obtained by the Lindlar catalyzed reduction of the propargylic intermediate (93% yield). Accompanying this product was also a small amount (7%) of the methyl (10*E*)-9-hydroxy-10-octadecanoate. The

spectral data of these compounds was similar to that reported for the 9-OH-10-ene positional isomer.

The GC/MS of the trimethylsilyl ether of these compounds were virtually identical and featured a major fragment having m/z of 285 due to cleavage between the 11th and 12th carbons of the fatty acid (Figure 2.46).

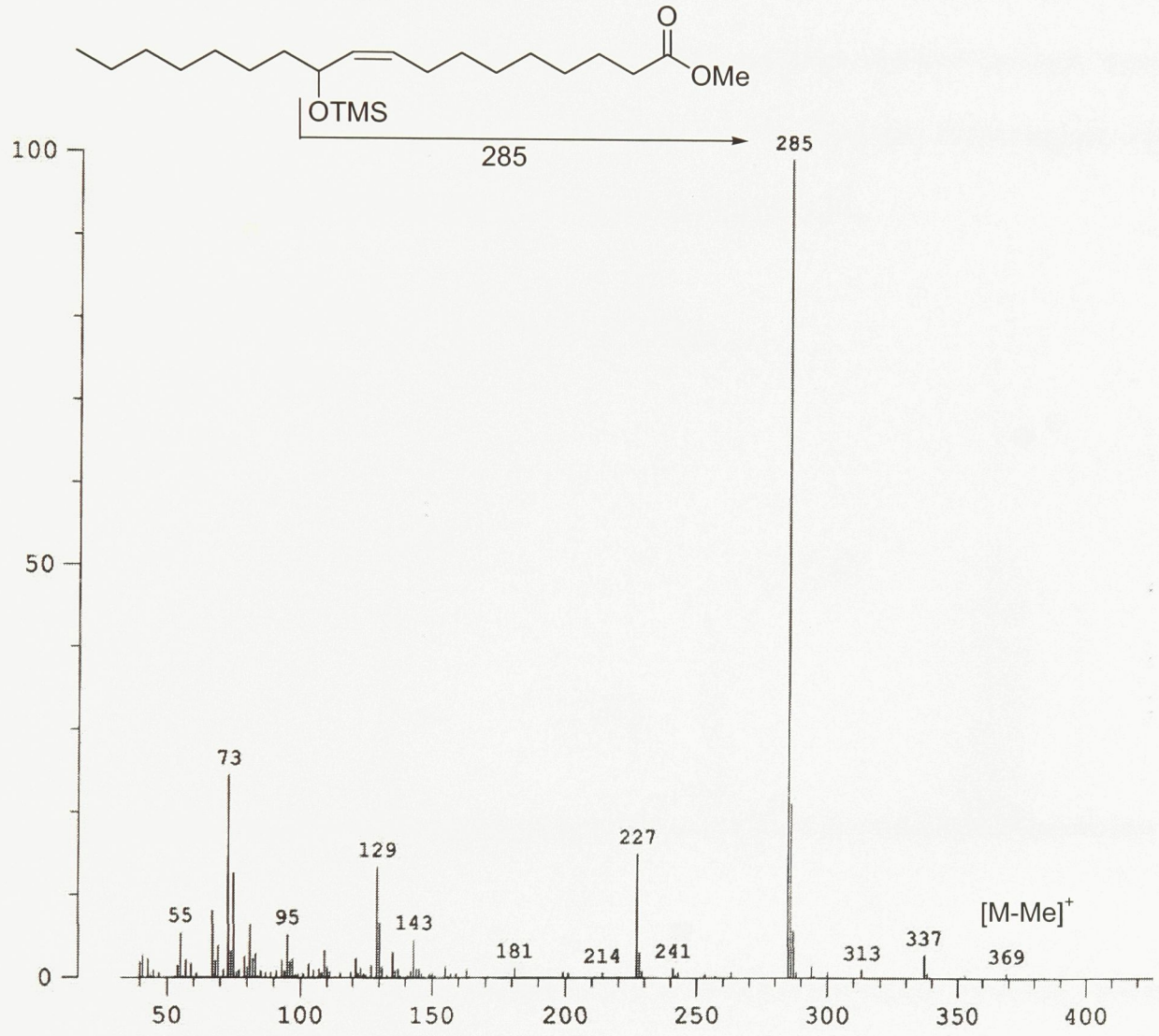

Figure 2.46 Mass spectrum of methyl 11-hydroxy-(9*Z*)-octadecenoate.

The ^{13}C NMR shifts of the 11-OH-9-ene products are shown in Table 2.5 and Figures 2.47 and 2.48. The most characteristic shifts of note is the appearance of the 11th carbon at either 67.72 or 73.21 ppm and of the 8th carbon at 27.66 or 32.13 ppm depending on whether they are adjacent to a *Z* or a *E* double bond respectively. The ^{1}H NMR shifts of the 9th, 10th

and 11th positions are also characteristic depending on the stereochemistry of the double bond, as well as the coupling constant between the vinylic protons. In the case of the *Z* double bond, the carbon in the 11th position (labeled 'a' in Table 2.6) appears at 4.42 ppm versus 4.03 ppm when adjacent to the *E* double bond. The proton shifts of the vinyl protons H9 and H10 (b and c in Table 2.6) appear more shielded for the *Z* double bond coming at 5.37 and 5.46 versus 5.46 and 5.62 respectively. The coupling constant between these two protons is 11.0 Hz for a *Z* double bond and 15.3 for a *E* double bond, which agrees with the expected values.[55] The ^{1}H NMR spectra is shown in Figure 2.49.

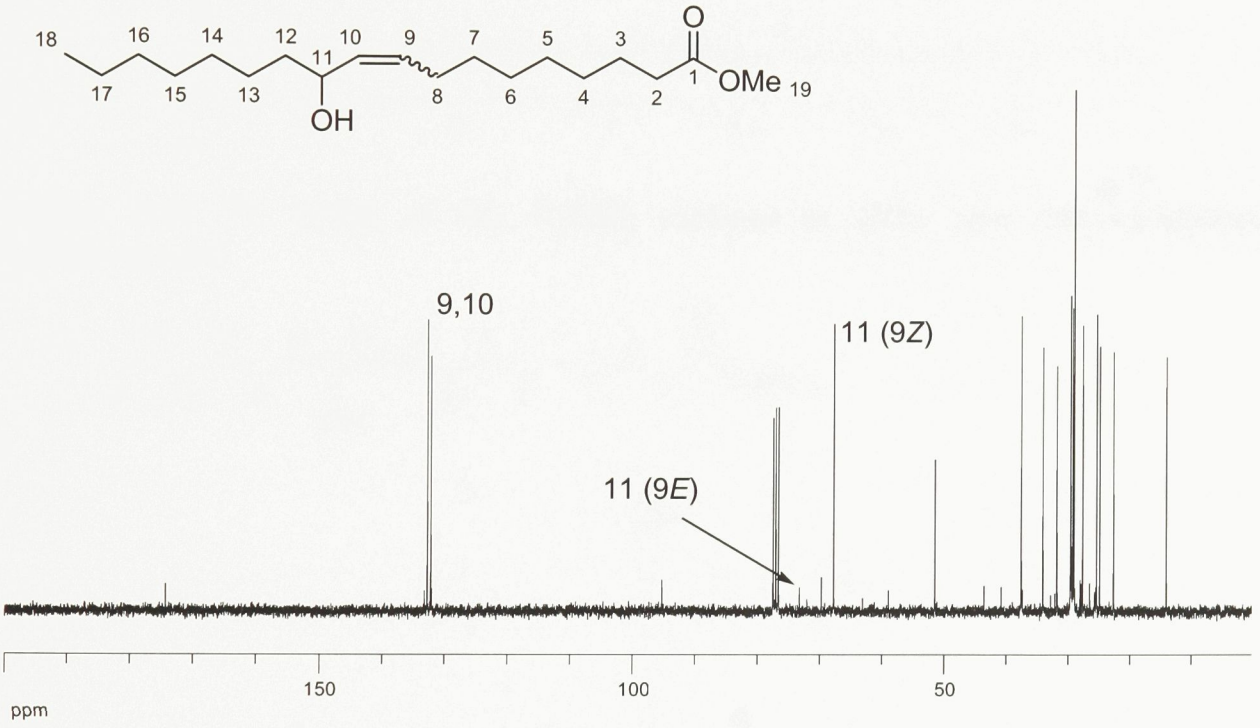

Figure 2.47 ^{13}C NMR spectrum of methyl (9*Z*)- and (9*E*)-11-hydroxy-9-octadecenoate.

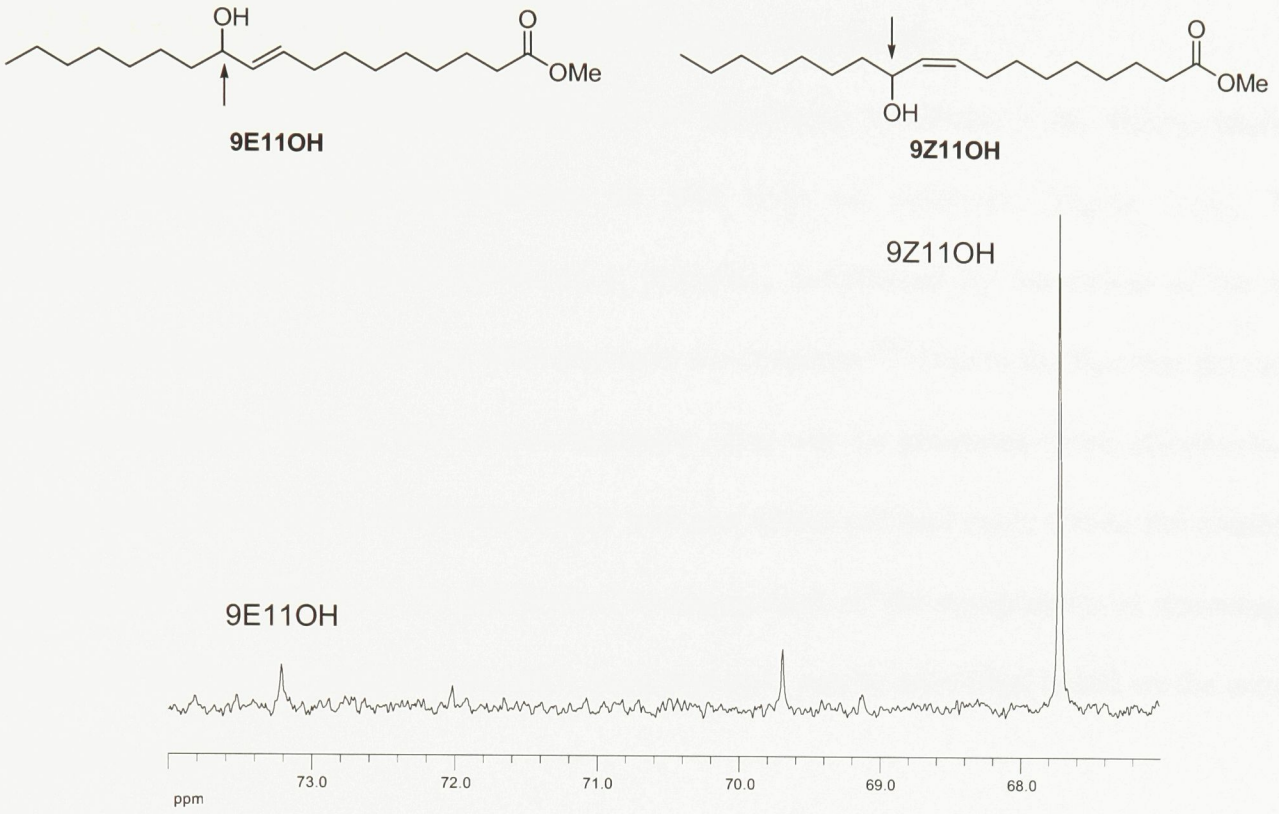

Figure 2.48 ^{13}C NMR of the C(OH) carbons in (9*Z*)- and (9*E*)-11-hydroxy-9-octadecenoate.

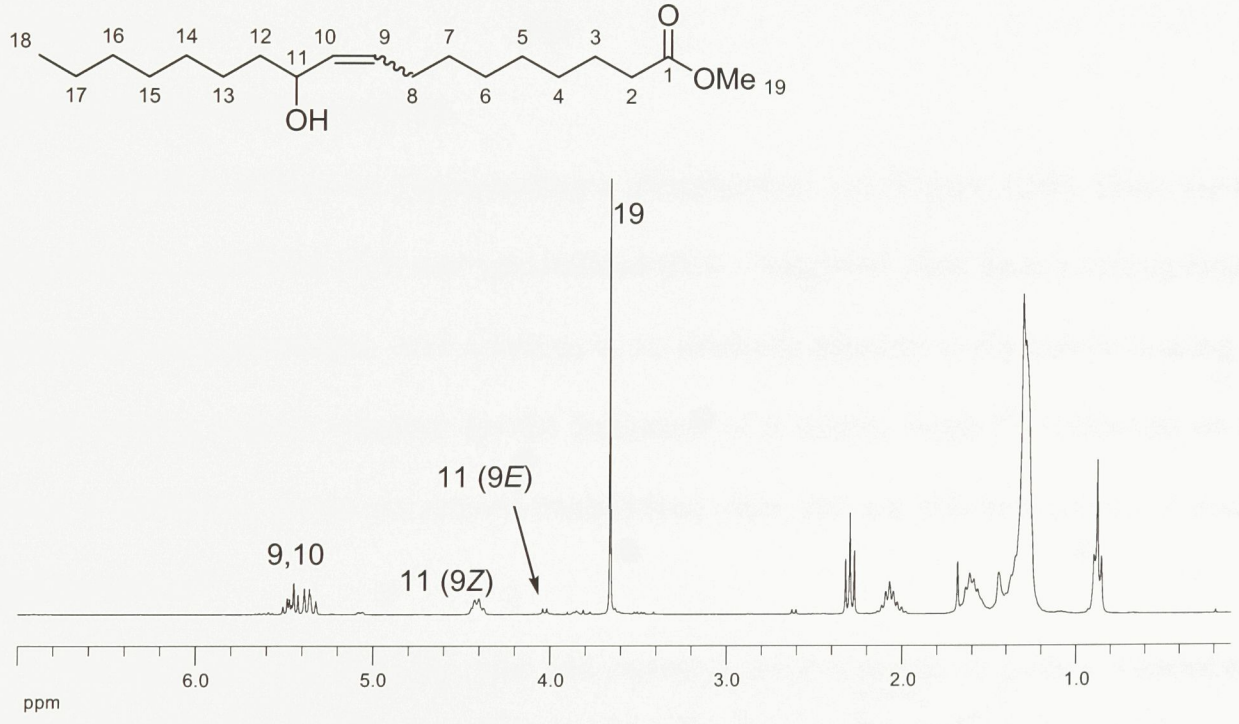

Figure 2.49 ^{1}H NMR spectrum of methyl (9*Z*)- and (9*E*)-11-hydroxy-9-octadecenoate.

2.2.4 Synthesis of dienoic acid methyl ester standards

One of the most important methods for producing an alkene is the Wittig reaction. The alkene is produced by reacting an ylid with an aldehyde (Figure 2.50). The stereochemistry of the alkene produced is primarily determined by the nature of the ylid substituent, however mixtures of stereoisomers are common.[58] Due to the fact that the target compounds differ only in their stereochemistry, they can be produced more effectively by using only two routes to obtain one major and one minor product each. Given the nature of the GC-MS experiments to be performed, isolating each of the components is unnecessary provided they can be produced in ratios such that they can be identified based on the area of their GC peaks.

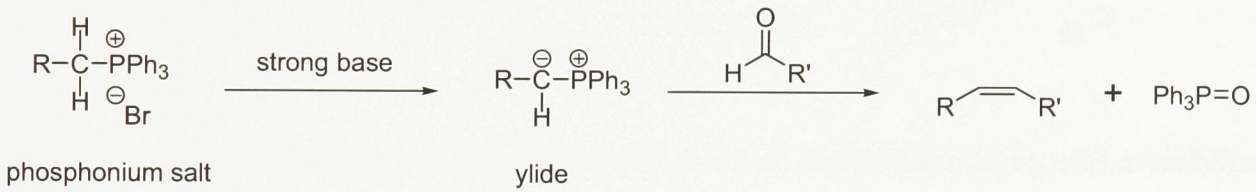

Figure 2.50 The Wittig reaction.

An ylid is formed by deprotonating a phosphonium salt (Figure 2.50). There are two types of ylids, stabilized ylids and unstabilized ylids. Stabilized ylids have a conjugating or anion-stabilizing substituent, such a ketone or an aldehyde adjacent to the carbon bearing the negative charge and are selective for the formation of *E* double bonds.[58] Ylids that do not feature a stabilizing group are termed unstabilized ylids and are selective for the *Z* double bond formation.[59]

In the Wittig reaction, the ylid and carbonyl come together to form a 4-membered ring oxaphosphetane intermediate. With an unstabilized ylid, this occurs in such a manner to keep the large substituents apart, resulting in a *Z* double bond (Figure 2.51).[58] When a

stabilized ylid is used, the formation of the intermediate is reversible and the more stable *anti* oxaphosphetane determines the stereochemistry of the product to be *E*.

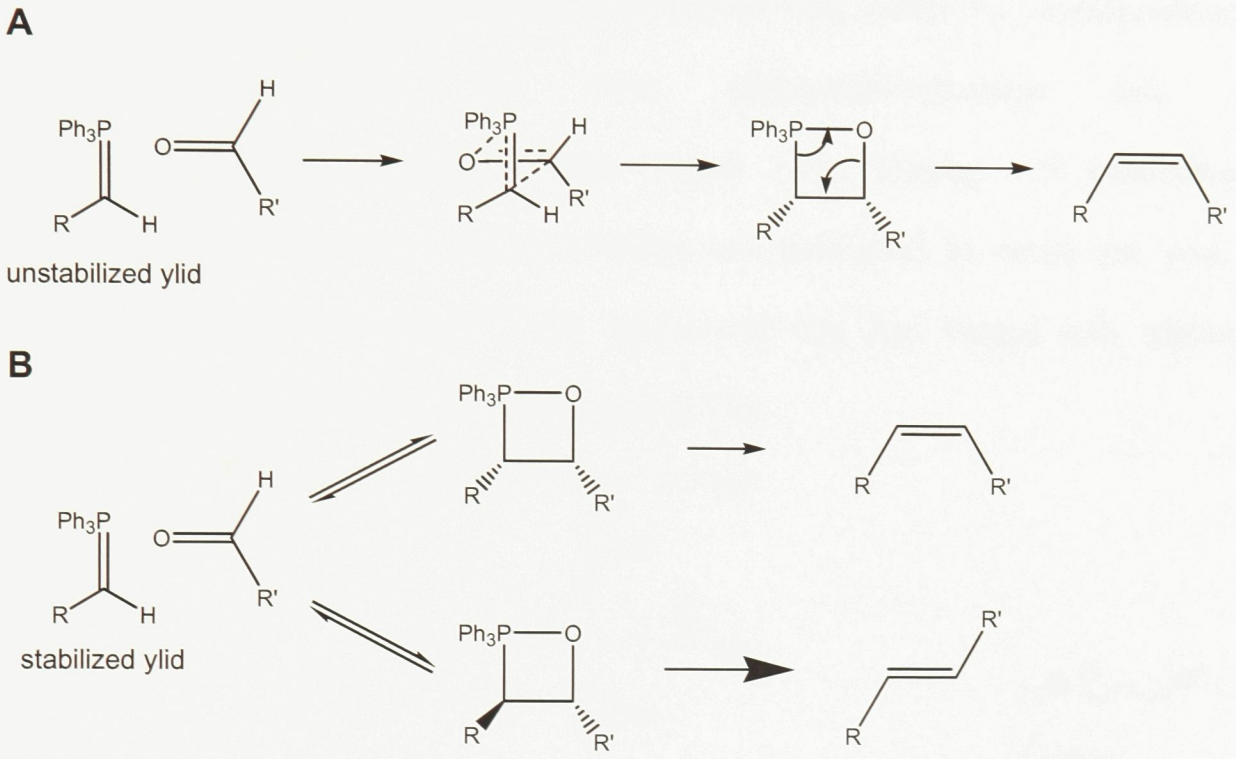

Figure 2.51 Mechanisms for the Wittig reaction of an unstabilized (A) and a stabilized ylid (B).

More efficiency can be had in obtaining the title compounds if a common phosphonium salt can be used in the synthesis of both major enantiomers. For the ease of obtaining suitable α,β-unsaturated aldehydes, it was decided to include the carboxylic acid group in the Wittig reagent to form the double bond between the 9th and 10th carbons and introduce the other unsaturated bond via the aldehyde.

2.2.4.1 Synthesis of (9*Z*,11*E*)-, (9*E*,11*E*)-, (9*Z*,11*Z*)- and (9*E*,11*Z*)- methyl 9,11-octadecadienoate

All four stereoisomers of the conjugated linoleic acid, methyl 9,11-octadecadienoate were synthesized from the same triphenylphosphonium salt, (8-carboxyoctyl)triphenylphosphonium bromide (Figure 2.52). Starting with commercially available 9-bromo-1-nonanol, a Jones oxidation was performed to obtain the acid, 9-bromononanoic acid (93% yield).[60] The bromo-acid was then treated with triphenyl-phosphine, converting it into the salt with a yield of 72%.

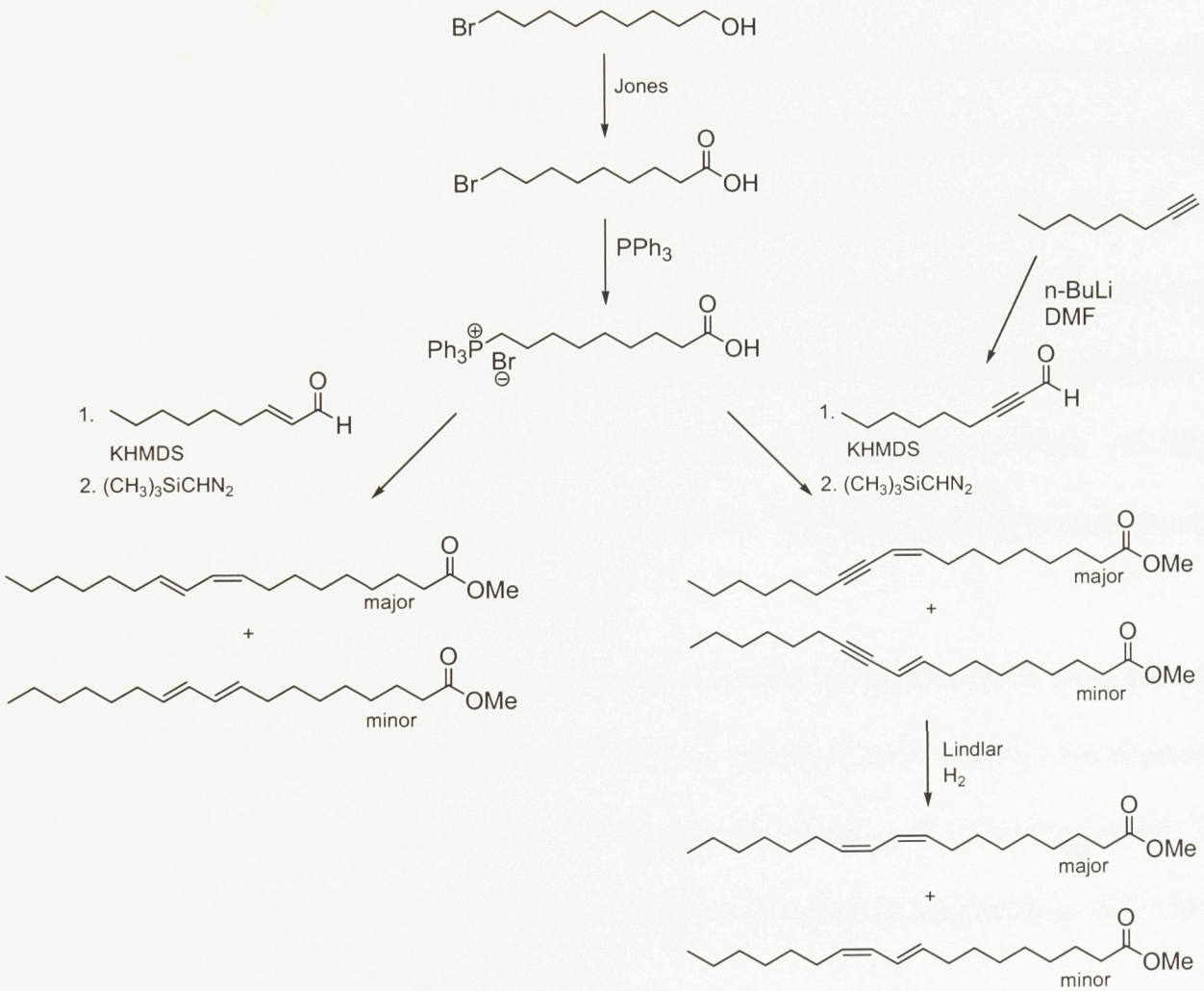

Figure 2.52 Scheme for the synthesis of all four stereoisomers of methyl 9,11-octadecadienoate.

The synthesis of methyl 9*Z*,11*E*-octadecadienoate with a minor component of methyl 9*E*,11*E*-octadecadienoate was performed by first reacting the Wittig reagent with *E*-2-nonanal using potassium bis(trimethylsilyl)amide (KHMDS) as the base.[60] The intermediate acid product was then methylated with (trimethylsilyl)diazomethane[61] before purification by flash chromatography for a combined yield of 65% over the two steps. The stereoisomers were produced in a 9:1 ratio.

The *Z*- aldehyde required for the synthesis of the other stereoisomers was not commercially available and thus an alkyne/reduction route was planned. 2-Nonynal was prepared by deprotonating 1-octyne with n-BuLi and adding it to dimethylformamide (DMF) (79% yield).[62] This aldehyde was added to the Wittig reagent again using KHMDS at the base, followed by (trimethylsilyl)diazomethane methylation[61] and purification by flash chromatography to obtain methyl 9*Z*-11-octadecenynoate as the major product with a minor component of methyl 9*E*-11-octadecenynoate (90% yield, 3:1 ratio). The enynoic fatty acid was reduced using Lindlar's catalyst[63] to obtain a (58:11:31) mixture of 9*Z*,11*Z*-octadecadienoate with a minor component of methyl 9*E*,11*Z*-octadecadienoate as well as unreduced enyne staring material (45% yield).

The mass spectra of each of the dienes are virtually indistinguishable from each other. The mass spectrum for the 9Z,11E product is shown in Figure 2.53. A parent ion is present at m/z = 294, as well as a signal at m/z = 263 representing the loss of a methoxy group. These values are in accord with the proposed chain length and degree of unsaturation of the dienoic fatty acid methyl esters.

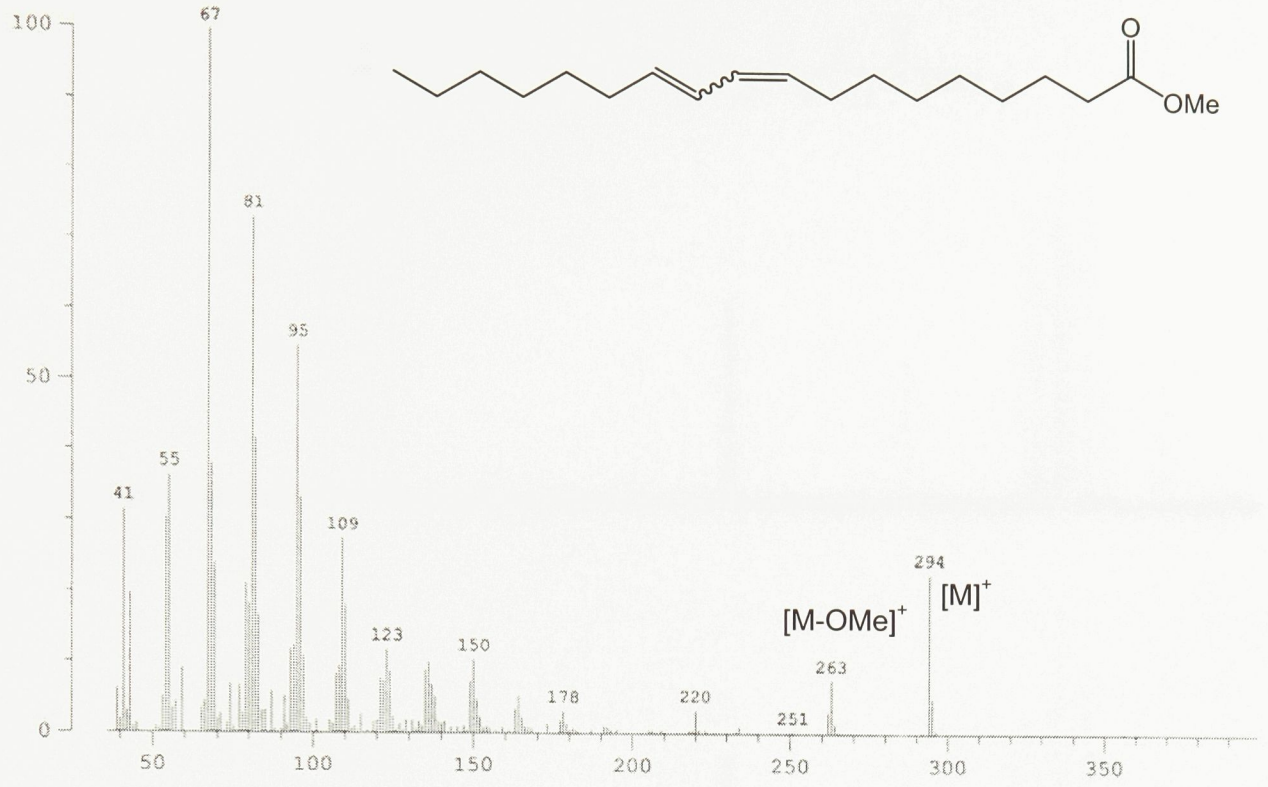

Figure 2.53 Mass spectrum of methyl (9*Z*,11*E*)-octadecadienoate.

The stereochemistry of the products was confirmed by ^{13}C NMR (Figures 2.54). The assigned chemical shifts of the 9,11-diene products are shown in Table 2.7. These values agree with those reported for these compounds.[64] Most significantly, the shifts of the 9th, 10th, 11th and 12th carbons are unique for each of the stereoisomers (Figure 2.55). Also of interest is the value of the chemical shifts of the 8th and 13th carbons which fall either between 27 and 28 ppm or 32 and 33 ppm depending on whether they are adjacent to a *Z* or a *E* double bond respectively. The ^{1}H NMR shifts of the 9th, 10th, 11th and 12th positions are also characteristic depending on the stereochemistry of the double bond. These values are shown in Table 2.8 and Figures 2.56 and 2.57 and correlate well with the reported values for these shifts.[64]

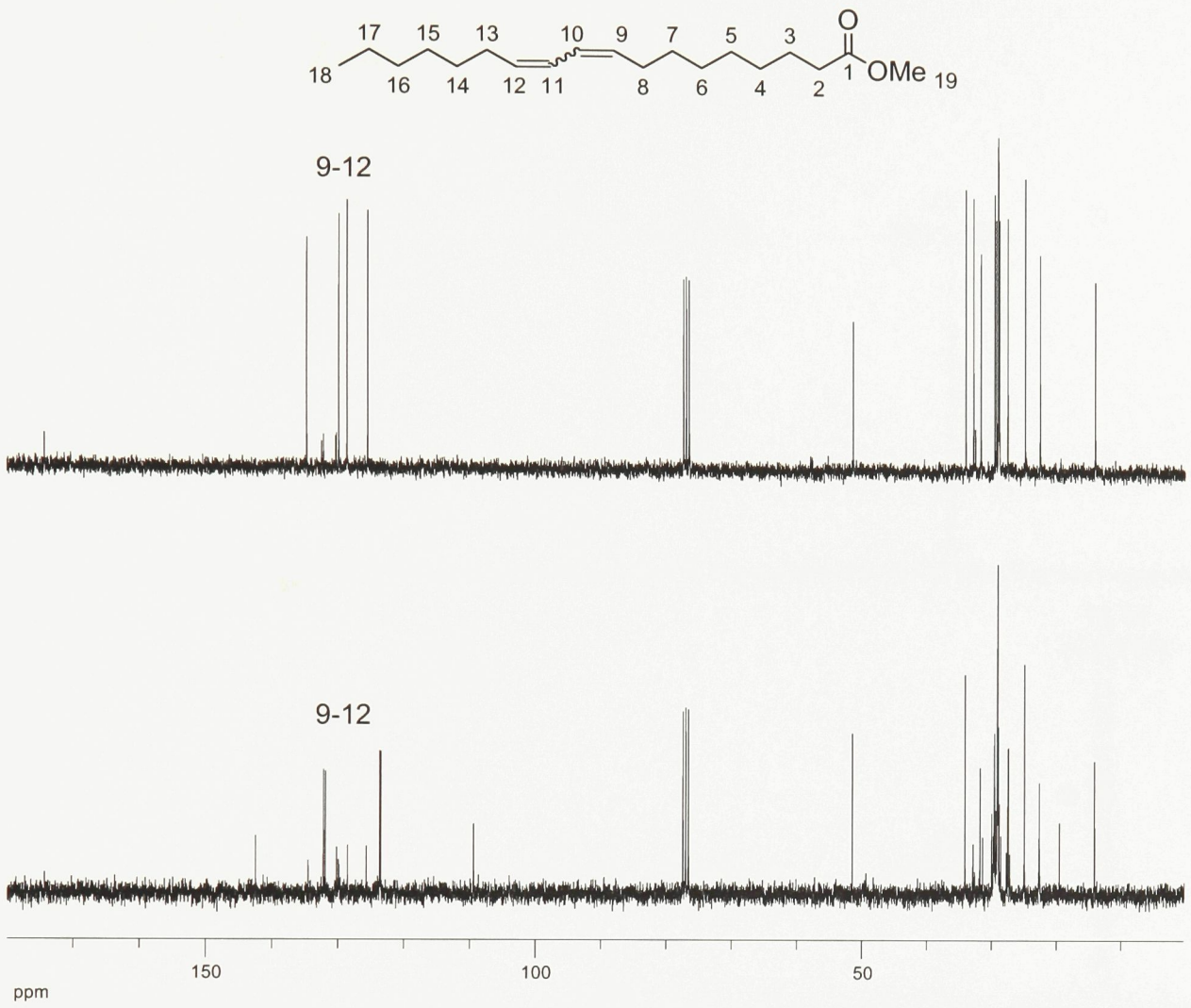

Figure 2.54 ^{13}C NMR spectra of methyl (9*Z*,11*E*)- and (9*E*,11*E*)-octadecadienoate (above) and methyl (9*Z*,11*Z*)- and (9*E*,11*Z*)-octadecadienoate (below).

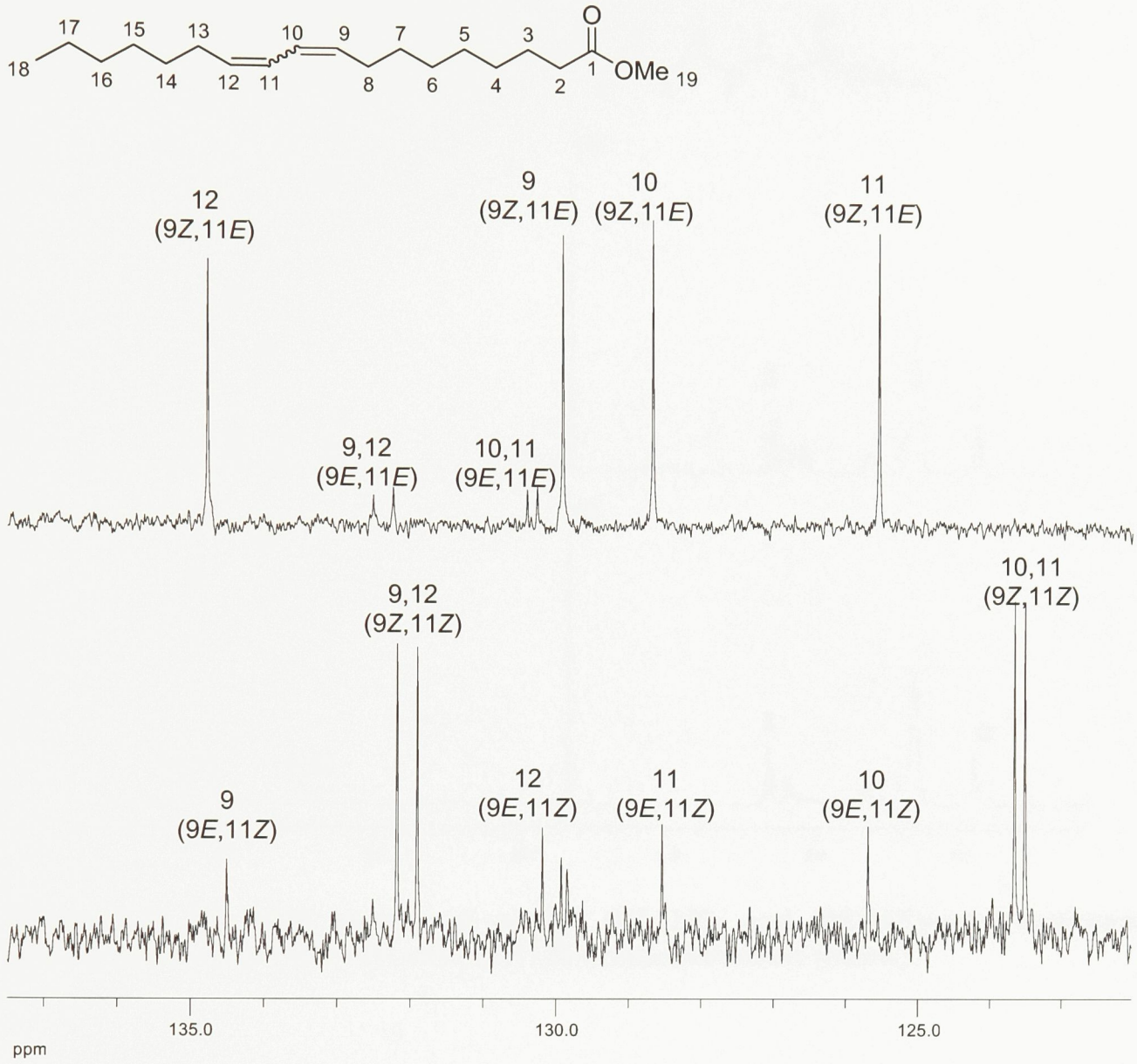

Figure 2.55 ^{13}C NMR spectra of the olefinic region of methyl (9*Z*,11*E*)- and (9*E*,11*E*)-octadecadienoate (above) and methyl (9*Z*,11*Z*)- and (9*E*,11*Z*)-octadecadienoate (below).

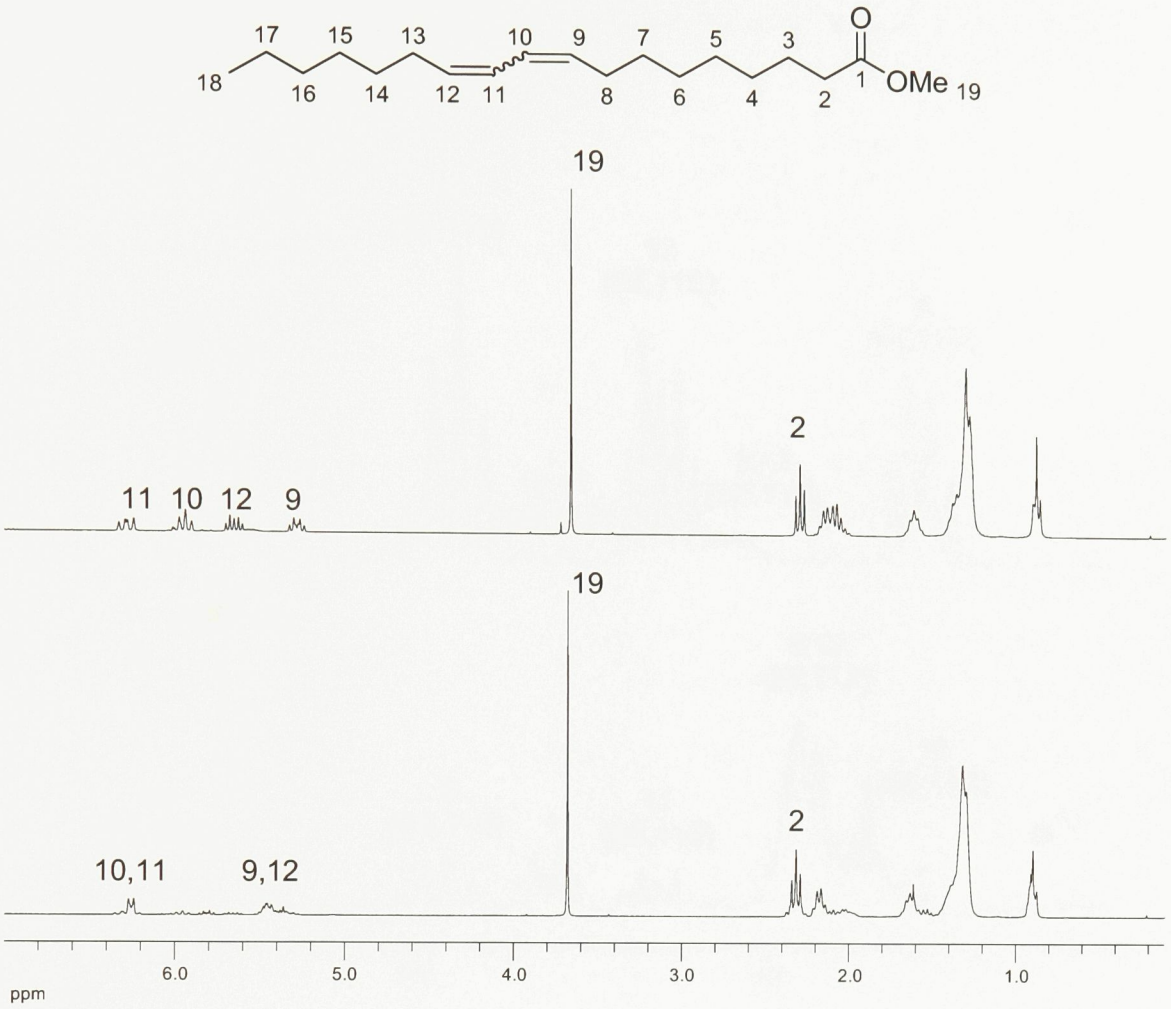

Figure 2.56 ^{1}H NMR spectra of methyl (9*Z*,11*E*)- and (9*E*,11*E*)-octadecadienoate (above) and methyl (9*Z*,11*Z*)- and (9*E*,11*Z*)-octadecadienoate (below).

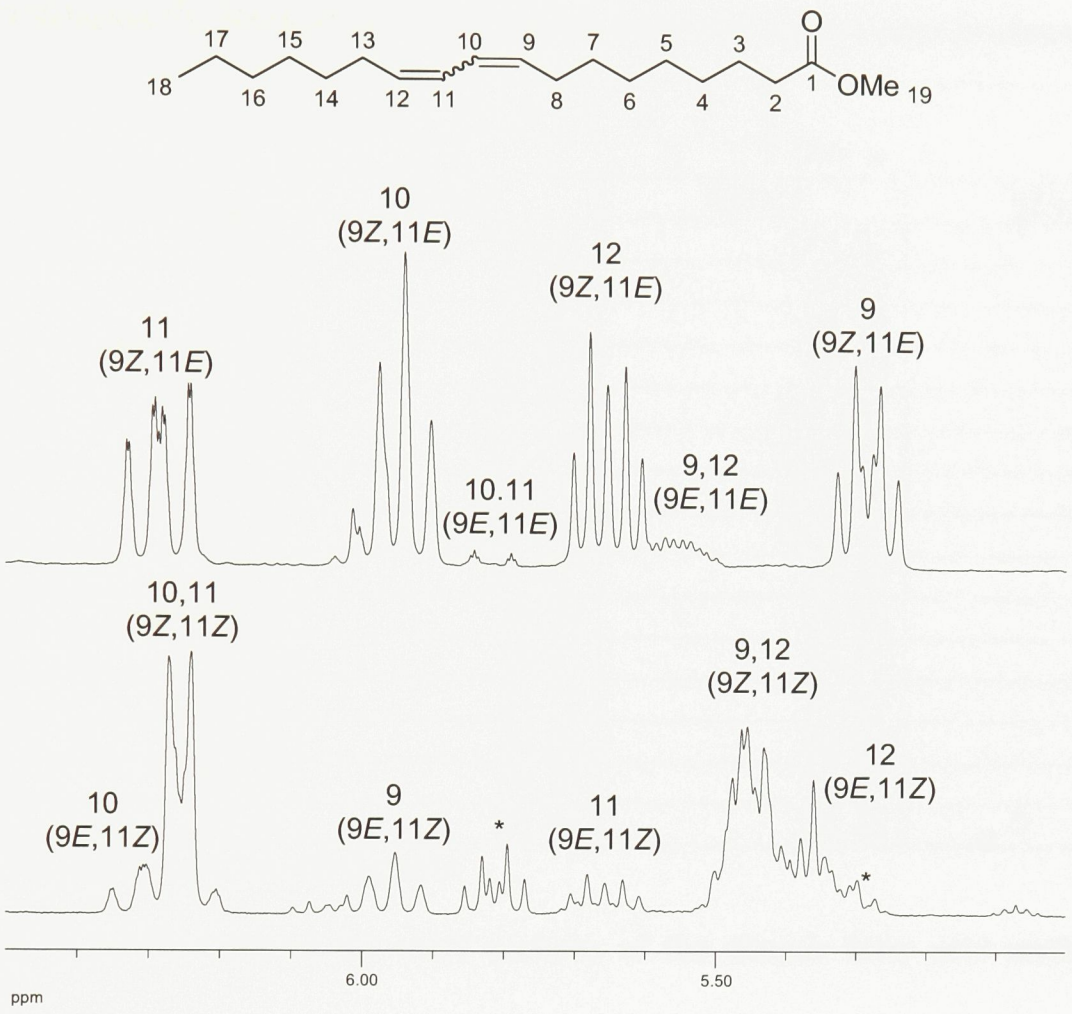

Figure 2.57 ^{1}H NMR spectra of the olefinic region of methyl (9*Z*,11*E*)- and (9*E*,11*E*)-octadecadienoate (above) and methyl (9*Z*,11*Z*) and (9*E*,11*Z*)-octadecadienoate (below). (* enyne impurity)

Table 2.7 Selected ^{13}C NMR shifts of the dienoic fatty acid methyl ester products.

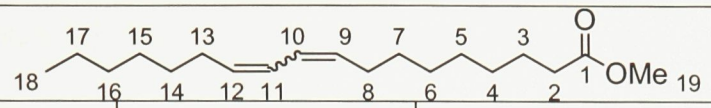

Carbon	***9Z11E***	***9E11E***	***9Z11Z***	***9E11Z***
1	174.31	174.31	174.32	174.32
2	34.10	34.10	34.10	34.10
3	24.94	24.94	24.94	24.94
8	27.65	32.56[a]	27.43	32.85
9	129.92	132.25[b]	131.91[d]	134.51
10	128.68	130.28[c]	123.66[e]	125.70
11	125.56	130.41[c]	123.52[e]	128.55
12	134.78	132.52[b]	132.19[d]	130.19
13	32.91	32.63[a]	27.50	27.72
14	29.39	29.39	29.63	29.72
15	28.93	28.93	29.06	28.97
16	31.75	31.75	31.80	31.75
17	22.63	22.63	22.64	22.64
18	14.11	14.11	14.11	14.11
19	51.44	51.44	51.45	51.45

a-a, b-b, c-c, d-d, e-e are interchangeable

Table 2.8 ^{1}H NMR shifts of the vinyl carbons of the dienoic fatty acid methyl ester products.

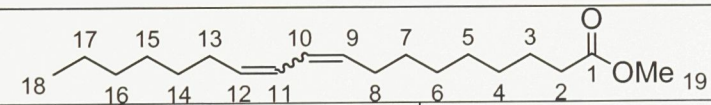

Proton	***9Z11E***	***9E11E***	***9Z11Z***	***9E11Z***
9	5.30	5.56	5.45	5.95
10	5.95	5.78-6.05	6.25	6.19-6.36
11	6.30	5.78-6.05	6.25	5.65
12	5.67	5.56	5.45	5.36

2.2.5 GC/MS experiments

2.2.5.1 Identification of the allylic alcohol positional isomer

Identification of the position of the hydroxyl group in the major allylic alcohol product obtained by incubating the mutant enzyme with either stearic or oleic acid was first performed using mass spectrometry. A different fragmentation pattern for the different positional isomer standards is obvious by inspection of Figures 2.41 and 2.46. The TMS derivative of the 9-OH-10-ene allylic alcohol standards had a major fragment of 227 amu, while the major fragment of the TMS derivative of the 11-OH-9-ene positional isomer featured a major fragment of 285 amu due in both cases to cleavage between the carbon bearing the TMS ether and the adjacent methylene carbon. The TMS-derivative of the enzymic product featured a major fragment of 227 amu indicating that this compound is a 9-OH-10-ene allylic alcohol. Figure 2.58 shows a comparison of these spectra.

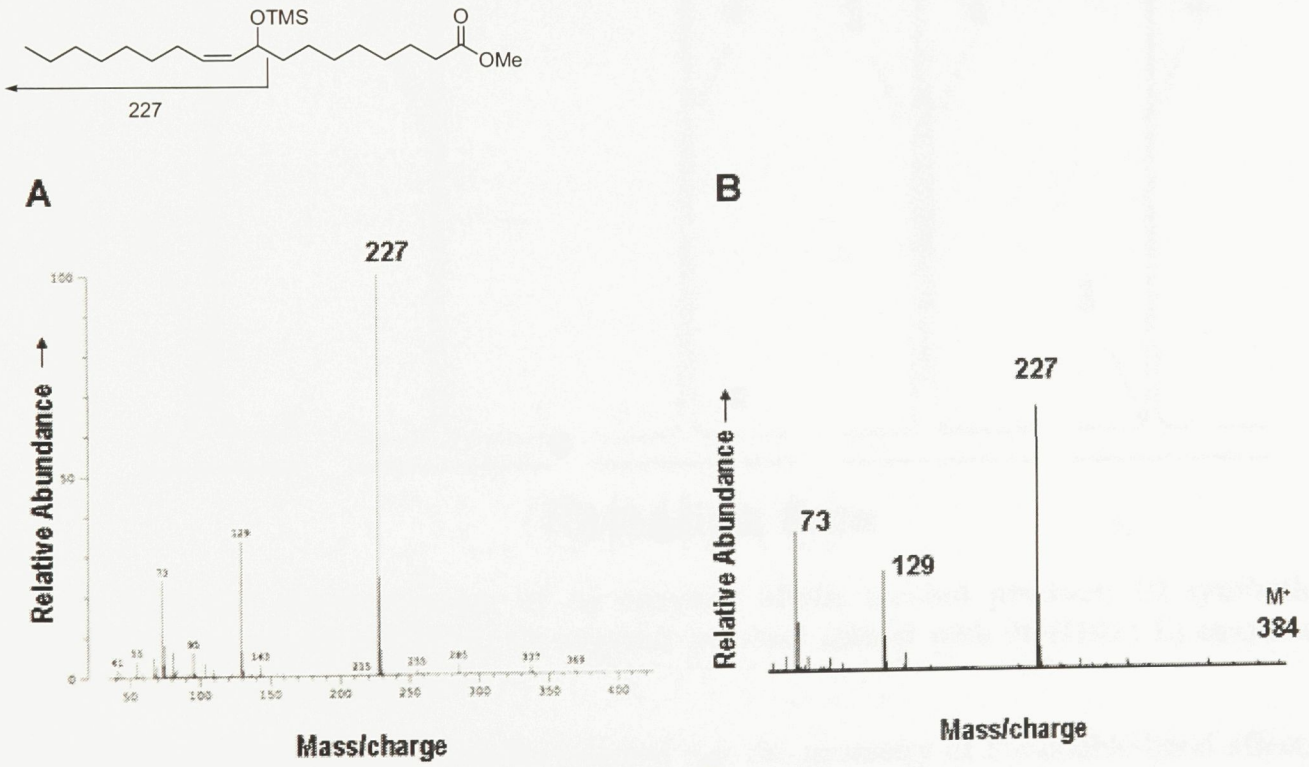

Figure 2.58 Mass spectrum of TMS-derivatives of 9OH10*Z* methyl ester standard (A) and enzymic allylic alcohol product (B).

2.2.5.2 Determination of the double bond stereochemistry of allylic alcohol products obtained from the incubation of oleate with mutant desaturase

GC co-elution experiments were performed using the allylic alcohol standards in combination with the enzymic product. The resulting GC chromatograms are shown in panels A-E of Figure 2.59 A) the enzyme product profile featuring a small peak followed by a major component, both sharing similar mass spectra; B) **9OH10Z** standard; C) **9OH10*E*** standard; D) the result of a spiking experiment of the enzymic product with **9OH10*E*** which resulted in an enhancement of the major peak; E) the enhancement of the minor peak when spiked with the **9OH10*Z*** standard. These results allowed for the positive identification of the major reaction product of the enzyme incubated with stearate as **9OH10*E*** with a minor component of **9OH10*Z***.

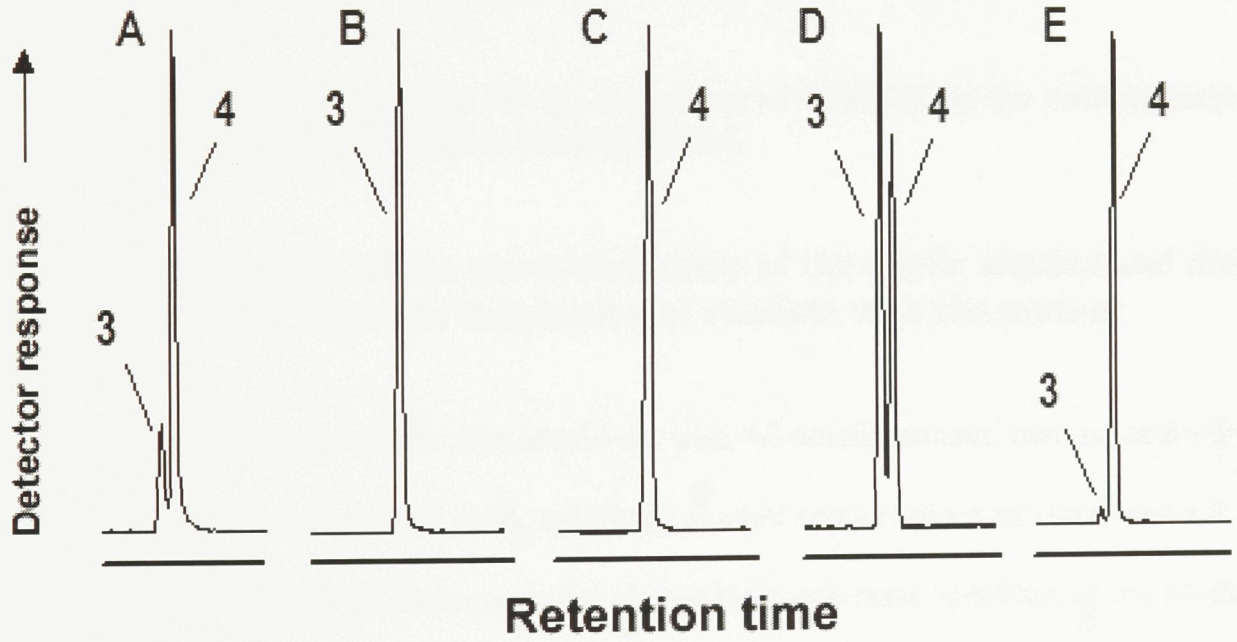

Figure 2.59 GC chromatogram of A) enzymic allylic alcohol product; B) synthetic 9OH10*Z*; C) synthetic 9OH10*E*; D) enzymic product spiked with 9OH10*Z*; E) enzymic product spiked with 9OH10*E*.

Based on this result, it can be inferred that the geometry of the double-bond affects the positioning of the substrate in the active site. In Figure 2.60 a possible scenario is shown.

The initial hydrogen abstraction for the wild type enzyme occurs at the 10th position. In the unsaturated substrate, the proton on the 10th carbon would be both energetically and sterically less accessible. A proposed mechanism for the mutant-enzyme catalyzed oxidation begins with an initial hydrogen abstraction at the 11th position with a subsequent rearrangement to obtain the *E* double bond stereochemistry observed in the major product and finally a hydroxyl rebound to the 9th position.

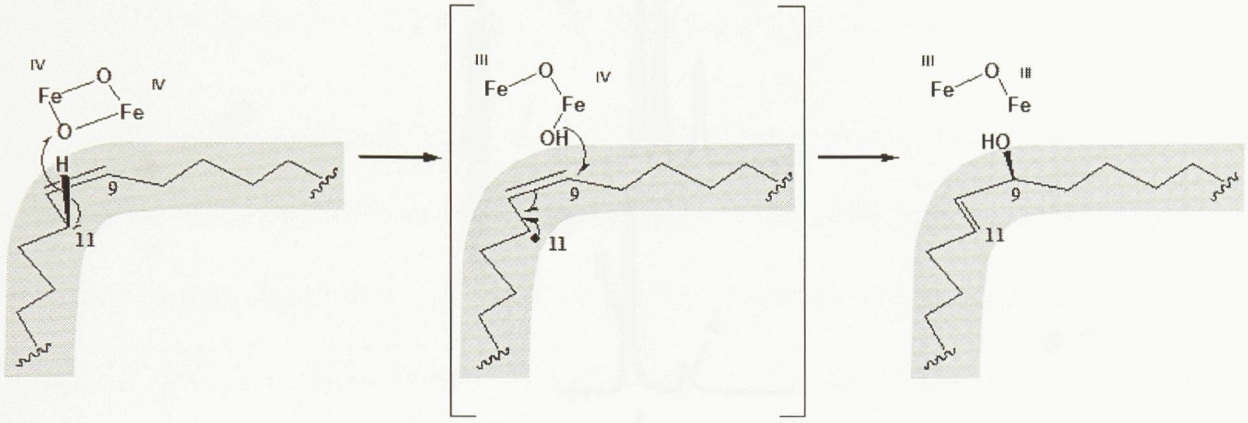

Figure 2.60 Proposed mechanism for the formation of 9OH10*E* by the mutant enzyme. Gray curve represents hydrophobic binding pocket.

2.2.5.3 Determination of the stereochemistry of the allylic alcohol and diene products obtained from the incubation of elaidate with the mutant desaturase

When the mutant enzyme was incubated with 9*E*-octadecenoate, two major products were obtained in a roughly equal ratio, an allylic alcohol (major/minor mixture) and a 9,11-dienoic acid. Both allylic alcohols produced shared the same mass spectrum as the products of the oleate incubation experiment (Section 2.2.5.1), indicating that they are also 9-OH-10-ene allylic alcohols. In co-elution experiments (data not shown) using the allylic alcohol standards, it was determined that the major allylic alcohol being produced was **9OH10*Z***, and the minor product was **9OH10*E***.

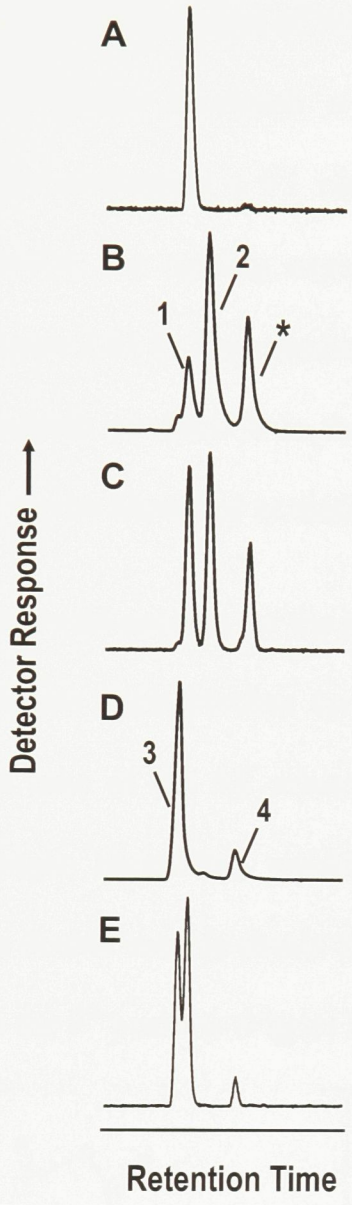

Figure 2.61 GC chromatogram of A) enzymic diene product; B) synthetic 9*E*11*Z* (1), 9*Z*11*Z* (2) (* unreduced intermediate); C) enzymic diene product spiked with synthetic mixture of 9*E*11*Z* and 9*Z*11*Z*; D) synthetic 9*Z*11*E* (3) and 9*E*11*E* (4); E) enzymic product spiked with synthetic 9*Z*11*E* and 9*E*11*E*.

Identification of the dienoic product obtained when the mutant enzyme was incubated with 9*E*-octadecanoic acid was also performed using GC co-elution experiments and shown in Figure 2.61. A portion of the GC chromatogram featuring the unidentified dienoic product is shown in panel A. In panel **B**, the chromatogram of the synthetic standard containing a 58:11:31 mixture of methyl 9*Z*,11*Z*-octadecadienoate (2): methyl 9*E*,11*Z*-octadecadienoate (1): methyl 9Z-11-octadecenynoate (*) is shown. Spiking this mixture with enzymatic

product (Figure 2.61 C) results in the enhancement of the **9*E*11*Z*** peak. To be thorough in showing that none of the other dienes co-eluted with the enzymatic product, the chromatogram of the diene standard containing a 9:1 ratio of **9*Z*11*E*:9*E*11*E*** is shown in Figure 2.61 D (3 and 4 respectively); the spiking experiment of this standard with the enzymatic product is featured in Figure 2.61 E. The retention times of these dienoic standards clearly differ from the mutant enzyme product. It is therefore concluded that the diene product obtained from the enzyme can be identified as methyl 9*E*,11*Z*-octadecadienoate.

A proposed mechanism that would account for the products obtained when the mutant enzyme is incubated with 9E substrate again invokes the steric effects of the boomerang-shaped active site. Similar to the case of the 9*E* substrate experiments described above (Section 2.2.5.2), the initial hydrogen abstraction would take place at the 11th position, followed by a rearrangement of the double bond to obtain the observed *Z* stereochemistry and a delivery of the hydroxyl group to the 9th position (Figure 2.62).

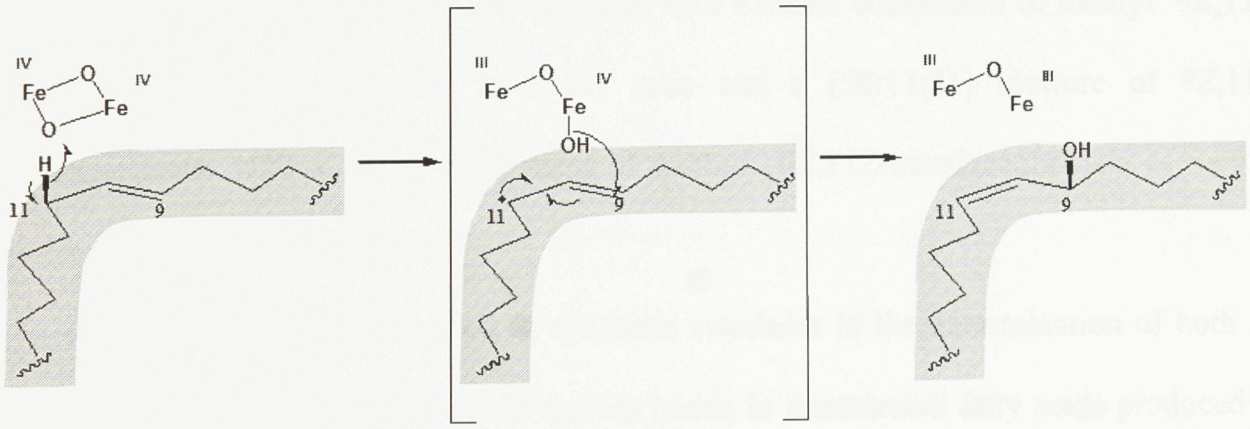

Figure 2.62 Proposed mechanism for the formation of 9OH10*Z* from elaidate by the mutant enzyme. Gray curve represents hydrophobic binding pocket.

The dienoic product can be attributed to an incomplete insertion of the substrate into the binding pocket resulting in the 11th and 12th carbons being adjacent to the diiron species in the active site. In this case, the reaction that occurs is analogous to that observed in the

wild type enzyme, with the abstraction of two hydrogen atoms, the 11th followed by the 12th, to introduce a *Z* double bond (Figure 2.63).

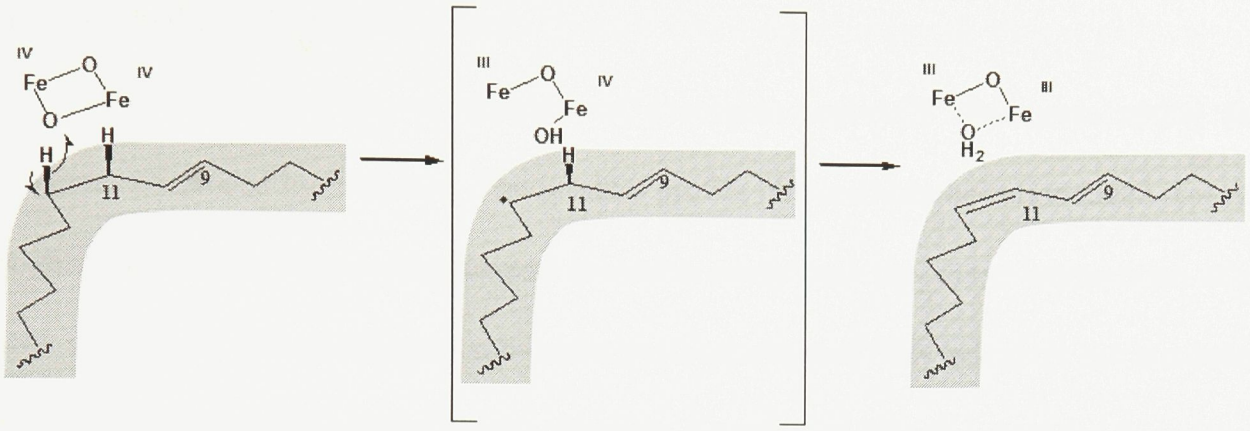

Figure 2.63 Proposed mechanism for the formation of 9*E*11*Z* from elaidate by the mutant enzyme. Gray curve represents hydrophobic binding pocket.

2.2.6 Conclusions and future directions

In this work, (10*Z*)- and (10*E*)-9-hydroxy-10-octadecenoate and (9*Z*)- and (9*E*)-11-hydrozy-9-octadecenoate were synthesized using known methods. The dienoic fatty acid methyl esters, methyl 9*Z*,11*E*-octadecadienoate with a minor component of methyl 9*E*,11*E*-octadecadienoate were prepared in a 9:1 ratio and a (58:11:31) mixture of 9*Z*,11*Z*-octadecadienoate with a minor component of methyl 9*E*,11*Z*-octadecadienoate as well as unreduced enyne staring material.

These compounds were used as synthetic standards in the determination of both the identity and the stereochemistry of the double bonds in unsaturated fatty acids produced by the triple mutant, T117R/G188L/D280K of the castor Δ^9 acyl-ACP desaturase using GC/MS co-elution experiments. When the ACP derivative of (9*Z*)-octadecenoate is presented to the mutant enzyme, methyl (10*E*)-9-hydroxy-10-octadecenoate is the major product and a minor amount of the corresponding *Z* allylic alcohol is also produced. When the ACP derivative of

(9*E*)-octadecenoate is introduced to the mutant enzyme, an equal amount of (10*Z*)-9-hydroxy-10-octadecenoate and (9*E*,11*Z*)-octadecadienoate is produced with a minor amount of (10*E*)-9-hydroxy-10-octadecenoate.

This is the first known example of a soluble acyl-ACP desaturase acting as a mutagenesis-induced hydroxylase. The product profile obtained can be rationalized based on the geometry of the boomerang-shaped substrate cavity and the steric interactions of the diiron centre with the unsaturated substrates. 9,10-unsaturated fatty acids are not a substrate for the wild-type enzyme and thus this catalytic diversity is entirely novel for this class of enzymes.

To validate the proposed reaction model and gain a better understanding of the structure-function relationship of this enzyme, further stereochemical investigations are required including the enantioselectivity of hydrogen abstraction and hydroxyl delivery. The cryptoregiochemistry of diene formation from elaidate is also of great interest.

2.3 Summary

Improved understanding of the mechanism of oxidation of desaturases and the active site architecture can be exploited in the development of novel desaturase enzymes and in the rational design of enzyme inhibitors. Investigations of these reactions are performed through substrate experiments and through site-directed mutagenesis experiments of structurally defined desaturases. The three properties of this oxidation reaction that are being studied in an effort to better understand the structure-function relationships are the crypto-regiochemistry, the enantioselectivity and the chemoselectivity.

In the original work presented herein, the use of fluorine-tagged thia fatty acid analogues as stereochemical probes for desaturase-mediated oxidation was investigated. A general method has been developed to produce chiral fluorine-tagged dialkyl sulfoxides for use as standards. The effect of several chiral solvating agents on the ^{1}H-decoupled ^{19}F NMR signal of the fluorine reporter group has been qualitatively determined. It has been shown that this method requires confirmation of stereochemical assignments via synthetic standards is required when using ^{19}F NMR spectroscopy and is an attractive option for use at the analytical level.

Some of this work is currently being submitted to *Bioorganic & Medicinal Chemistry Letters*:

> Tremblay, A.E; Lao, K.Y.Y; Hodgson, D.J; Dawson, B; Buist, P.H. Synthesis of chiral fluorine-tagged reference standards for the ^{19}F NMR-based stereochemical analysis of sulfoxides at trace analytical levels. **2009**.

Contributions have also been made to the site-directed mutagenesis experiment of the Shanklin group at Brookhaven National Laboratory, which has demonstrated the catalytic diversity of soluble plant desaturases. The synthesis of allylic alcohol and dienoic fatty acid standards has led to the identification of novel products obtained from a triple mutant of the castor Δ^9 desaturase. The identification of these products has provided some insight into the mechanism of the oxidation occurring and the active site architecture which will be able to direct future studies in this area.

This work has been presented in the following publication:

> Whittle, E; Tremblay, A.E; Buist, P.H; Shanklin, J. Revealing the catalytic potential of an acyl-ACP desaturase: tandem selective oxidation of saturated fatty acids. *Proceedings of the National Academy of Science U S A*. **2008**, *105*, 14738-43.

All of the work presented in this thesis constitutes a logical extension of my previous work in this field, described in the following publications.

Tremblay, A.E; Buist, P.H; Whittle, E; Shanklin, J. Stereochemistry of Δ^4 dehydrogenation catalyzed by an ivy (*Hedera helix*) Δ^9 desaturase homolog. *Organic & Biomolecular Chemistry* **2007**, *5*, 1270 -1275.

Tremblay, A.E; Buist, P.H; Hodgson, D.J; Dawson, B; Whittle, E; Shanklin, J. In vitro enzymatic oxidation of a fluorine-tagged sulfido substrate analogue: a ^{19}F NMR investigation. *Magnetic Resonance in Chemistry* **2006**, *44*, 629-632.

Stuart, L.J; Buck, J.P; Tremblay, A.E; Buist, P.H. Configurational analysis of Cyclopropyl Fatty Acids from *Escherichia coli*. *Organic Letters* **2006**, *8*, 79-81.

Chapter 3: Experimental

3.1 Materials and methods

^{1}H NMR (300 MHz), ^{13}C NMR (75 MHz), and unless otherwise noted ^{1}H-decoupled ^{19}F (282 MHz) NMR spectra were obtained on a Bruker Avance 300 spectrometer with the exception of the ^{1}H-decoupled ^{19}F (376 MHz) NMR of enzymic 15-fluoro-11-sulfoxyocatecanoate which was performed by Dr. Derek Hodgson on a Bruker AM 400 spectrometer at Health Canada (Centre for Biologics Research, Biologics and Genetic Therapies Directorate). All compounds were dissolved in $CDCl_3$, that was dried by passing the solvent through a short column packed with neutral alumina (Activated aluminum oxide, Brockmann I standard grade, 150 mesh, 58 A). Chemical shifts for ^{1}H and ^{13}C NMR spectra are reported in ppm (δ) relative to TMS (0.00 ppm) and normalized to a chemical shift value of 7.2650 ppm (^{1}H) and 77.0275 ppm ($_{13}C$) for residual $CHCl_3$ (^{1}H) and $CDCl^3$ (^{13}C). ^{19}F chemical shifts were measured relative to external $CFCl_3$. Abbreviations used to assign multiplicity of peaks are as follows: *s* = singlet, *d* = doublet, *t* = triplet, *m* = multiplet and *b* = broad. *J*-values are reported in Hertz (Hz).

GC/MS data of synthetic standards were obtained courtesy of the University of Ottawa's mass spectrometry facility (Dr. Clem Kazakoff) using a Kratos Concept ^{1}H mass spectrometer at 70 eV interfaced with a J & W 30 m x 0.21 mm, DB-5 capillary column. The temperature program started at 120 °C and increased at 10 °C/min until 320 °C and held for 2 minutes. Mass spectra of sulfinate esters, sulfoxides and the CSA acid were obtained using an EI direct probe.

GC/MS of enzymic products and co-elution experiments were obtained courtesy of John Shanklin and Ed Whittle at Brookhaven National Laboratories using a Hewlett-Packard

HP5890 gas chromatograph-mass spectrometer fitted with 60-m x 250-μm SP-2340 capillary columns (Supelco). The oven temperature was raised from 100 °C to 160 °C at a rate of 25 °C/ min and from 160 °C to 240 °C at a rate of 10 °C/min with a flow rate of 1.1 ml min/1. Mass spectrometry was performed with a Hewlett–Packard HP5973 mass selective detector.

Purification by flash chromatography was done using Merck silica gel (60 A), grade 9385 (230-400 mesh) with an air pressure of ca. 5 psi. Thin layer chromatography was done on a glass backed plate coated with Merck silica gel (60 A). Visualization was achieved by a compbination of UV, I_2 vapour and water spray as appropriate.

All reagents obtained commercially were acquired from Sigma-Aldrich and used without purification unless indicated. Pyridine was dried over NaOH pellets, Tetrahydrofuran (THF) and diethyl ether (Et_2O) were freshly distilled from Na-benzophenone ketyl. Toluene was freshly distilled from NaH. All air- and moisture-sensitive reactions were performed under N_2. Organic extracts were typically dried by gravity filtration through anhydrous Na_2SO_4, and solvents were evaporated in vacuo on a Büchi RE 111 Rotavapor.

3.2 Synthesis of fluorine-tagged chiral sulfoxide standards

3.2.1 (10*R*)- and (10*S*)-18-fluoro-10-sulfoxy-1-octadecanol

3.2.1.1 1-Bromo-8-fluorooctane

To (diethylamino)sulfur trifluoride (DAST) (2.57 ml, 3.16 g, 19.6 mmol) at room temperature under N_2, was added 8-bromo-1-octanol (1.68 ml, 2.05 g, 9.8 mmol) dropwise. Heated to 50 °C for 4 hours with stirring, at which point a brown solution was obtained. This solution was poured into ice water (150 ml) and extracted with CH_2Cl_2 (3 x 50 ml). The combined extracts were washed with sat. $NaHCO_3$ (3 x 30 ml) and H_2O (50 ml), then dried (Na_2SO_4) and filtered through Florisil. The solvent was removed by roto-evaporated to obtain the title compound (1.97 g, 9.3 mmol, 95%) as an amber liquid. TLC (EtOAc/hexane 15:85): R_f 0.63. B.p. 120° (22.5 mm Hg). IR (film): 2933, 2857, 1464, 1247, 1047, 1002, 724, 645 cm^{-1} ^{1}H-NMR (300 MHz , $CDCl_3$): 4.43 (*dt*, $^2J_{HF}$ = 47.3, $^3J_{HH}$ = 6.2, 2H, H**8**), 3.41 (*t*, *J* = 6.8, 2H, H**1**), 1.86 (p_{obs}, *J* = 7.1, 2H, H**2**), 1.69 (*dm*, $^3J_{HF}$ = 24.9, 2H, H**7**), 1.34-1.50 (*m*, 8H , H**3**-**6**). ^{13}C-NMR (75 MHz , $CDCl_3$): 84.12 (*d*, *J* = 163.1, C**8**), 33.90 (C**2**), 32.75 (C**1**), 30.35 (*d*, *J* = 19.2, C**7**), 29.03, 28.63, 28.05 (C**3**), 25.08 (*d*, *J* = 5.4, C**6**). ^{19}F NMR (282.4 MHz, $CDCl_3$): -218.30.

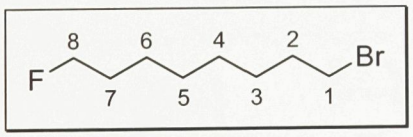

3.2.1.2 Thioacetic acid S-(8-fluoro-octyl) ester

To a solution of potassium thioacetate (1.08 g, 9.5 mmol) in anh. DMF (25 ml) was added 1-bromo-8-fluorooctane (1.97 g, 9.3 mmol) dissolved in DMF (15 ml) under N_2 at room temperature. After stirring at room temperature overnight, the reaction mixture was diluted with CH_2Cl_2 (100 ml), washed with dH_2O (5 x 60 ml), sat. NaCl (75 ml), dried (Na_2SO_4) and roto-evaporated. The resulting oil was then partitioned between hexanes (2 x 20 ml) and dH_2O (20 ml), the combined organic layers were dried (Na_2SO_4) and evaporated to give the title compound (1.87 g, 9.1 mmol, 97 %) as an amber oil. TLC (EtOAc/hexane 15:85): R_f 0.54. IR (film): 2932, 2857, 1693 (C=O), 1464, 1430, 1354, 1135, 1047, 1003, 956, 725, 627 cm^{-1}. ^{1}H-NMR (300 MHz , $CDCl_3$): 4.41 (*dt*, $^2J_{HF}$ = 47.3, $^3J_{HH}$ = 6.2, 2H, H**8**), 2.85 (*t*, *J* = 7.3, 2H, H**1**), 2.31 (*s*, 3H, H**10**), 1.5-1.8 (*m*, 4H, H**2**,**7**), 1.23–1.45 (*m,* 8H, H**3-6**). ^{13}C-NMR (75 MHz , $CDCl_3$): 195.94 (C**9**), 84.09 (*d*, *J* = 163.2, C**8**), 30.58 (C**10**), 30.33 (*d*, *J* = 19.3, C**7**), 29.43, 29.06, 29.02, 28.93, 28.63, 25.05 (*d*, *J* = 5.4, C**6**). ^{19}F NMR (282.4 MHz, $CDCl_3$): -218.27.

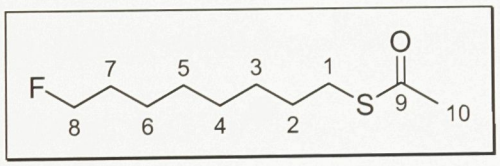

3.2.1.3 8-Fluoro-octanesulfinyl chloride

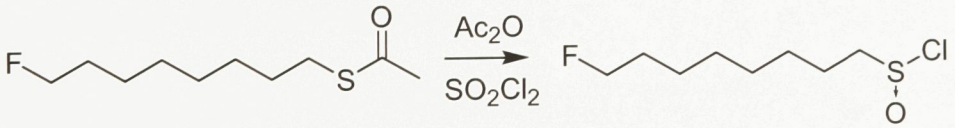

Thioacetic acid S-(8-fluoro-octyl) ester (1.84 g, 8.9 mmol) and acetic anhydride (0.84 ml, 0.91 g, 8.9 mmol) were combined in a 3-neck RBF equipped with magnetic stirbar and N_2 inlet. The reaction vessel was cooled to -10 °C and sulfuryl chloride (1.44 ml, 2.40 g, 17.8

mmol) was added dropwise over a half hour. Stirring was continued for another half hour at -10 °C. The solution was roto-evaporated to give the title compound (1.88 g, crude) as an amber oil: 4.44 (*dt*, $^2J_{HF}$ = 47.3, $^3J_{HH}$ = 6.1, 2H; H**8**), 3.39 (*m*, 2H; H**1**), 1.93 (*m*, 2H; H**2**), 1.6-1.8 (*m*, 2H; H**7**), 1.3–1.6 (*m,* 8 H; H**3-6**). ^{13}C-NMR (75 MHz , $CDCl_3$): 84.08 (*d*, *J* = 163.3; C**8**), 64.43 (C**1**), 30.32 (*d*, *J* = 19.3, C**7**), 29.05, 28.86, 28.25 (C**3**), 25.08 (*d*, *J* = 5.2, C**6**), 22.22 (C**2**). ^{19}F NMR (282.4 MHz, $CDCl_3$): -218.40.

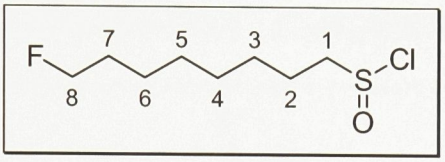

3.2.1.4 1,2:5,6-Di-O-isopropylidene-α-D-glucofuranosyl (+)-(*R*)-8-fluorooctanesulfinate

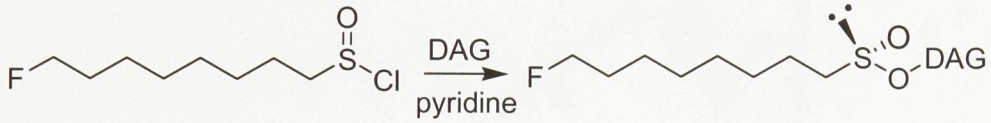

To diacetone-D-glucose (0.77 g, 2.9 mmol) in dry THF (12 ml) under N_2 gas at -78°C was added pyridine (0.29 ml, 3.5 mmol) followed by crude sulfinyl chloride (3.52 mmol). Mixture was stirred for 3 hours (-78 °C). Reaction was quenched dropwise with water (5 ml) then dissolved in DCM (50 ml). The resulting mixture was washed with 5% HCl (50 ml), 2% $NaHCO_3$ (50 ml), and sat. NaCl (50 ml), then dried over Na_2SO_4 and concentrated by rotaevaporation. The title compound was obtained by flash chromatography using 40% Et_2O/hexanes to obtain a thick, pale oil (0.79 g, 1.8 mmol, 62%, *dr R/S*: 91/9). $[\alpha]_D^{21}$ = +1.39° (*c* 1.1, acetone). TLC (EtOAc/hexane 1:1): R_f 0.70. IR (film): 2987, 2935, 2859, 1457, 1374, 1256, 1217, 1165, 1136, 1076, 1023, 955, 887, 837, 754, 730, 687 cm^{-1}. ^{1}H-NMR (300 MHz , $CDCl_3$): 5.91 (*d*, *J* = 3.5, 1H, H**1**), 4.78 (*d*, *J* = 3.5, 1H, H**2**), 4.71 (*d*, *J* = 1.2, 1H, H**3**), 4.43 (*dt*, $^2J_{HF}$ = 47.3, $^3J_{HH}$ = 6.1, 2H; H**8′**), 3.96-4.17 (*m*, 4H; H**4-6**), 2.81 (*2dt*, *J* = 7.8, 13.4, 2H; H**1′**), 1.70 (*m*, 2H), 1.28-1.47 (*m*, 10H), 1.50 (*s*, 3H; H**B**), 1.41 (*s*, 3H;

H**B**), 1.32 (*s*, 3H; H**B**), 1.30 (*s*, 3H; H**B**). ^{13}C-NMR (75 MHz , $CDCl_3$): 112.40 (C**A**), 109.42 (C**A**), 105.35 (C**1**), 84.07 (*d*, *J* = 163.1; C**8′**), 83.84 (C**2**), 83.05 (C**4**), 80.93 (C**3**), 72.14 (C**5**), 67.70 (C**6**), 57.86 (C**1′**), 30.33 (*d*, *J* = 19.3; C**7′**), 29.09, 28.93, 28.66, 26.86 (C**B**), 26.74 (C**B**), 26.19 (C**B**), 25.29 (C**B**), 25.10 (*d*, *J* = 5.3, C**6′**), 21.03 (C**2′**). ^{19}F NMR (282.4 MHz, $CDCl_3$): -218.36 EI-MS: *m/z* 423 (27 $[M - 15]^+$), 365 (3), 249 (7), 185 (19), 170 (14, $[FC_8H_{16}SO]^+$), 127 (28, $[C_6H_7O_3]^+$), 101 (100, $[C_5H_9O_2]^+$), 85 (13), 59 (20), 43 (39, $[C_2H_3O]^+$); HR-EI-MS *m/z* 423.1851 ($[M-CH_3]^+$, $C_{19}H_{32}O_7FS$ requires 423.1853).

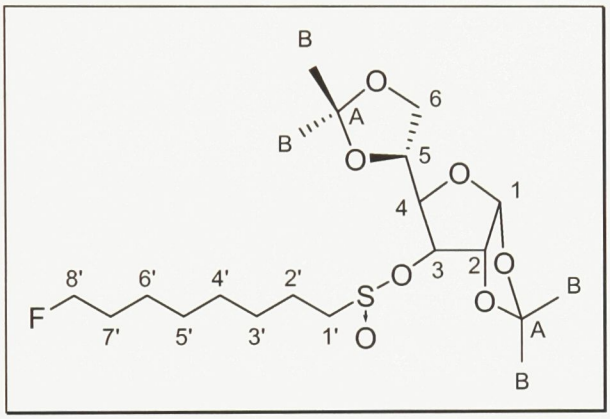

3.2.1.5 1,2:5,6-Di-O-isopropylidene-α-D-glucofuranosyl (-)-(*S*)-8-fluorooctanesulfinate

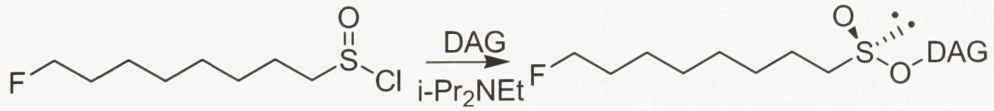

Obtained as 1,2:5,6-Di-O-isopropylidene-α-d-glucofuranosyl (+)-(*R*)-8-fluorooctanesulfinate, except for the solvent (toluene) and the base (*i*-Pr_2NEt). (30% yield, *dr R/S*: 17/83). $[\alpha]_D^{21}$ = -36.2° (*c* 1.2, acetone). TLC (EtOAc/hexane 1:1): R_f 0.67. IR (film): 2988, 2934, 2859, 1714, 1457, 1373, 1256, 1220, 1165, 1135, 1075, 1022, 830. ^{1}H-NMR (300 MHz , $CDCl_3$): 5.91 (*d*, *J* = 3.6, 1H; H**1**), 4.74 (*d*, *J* = 2.3, 1H; H**3**), 4.60 (*d*, *J* = 3.7, 1H, H**2**), 4.43 (*dt*, $^2J_{HF}$ = 47.3, $^3J_{HH}$ = 6.1, 2H; H**8′**), 3.98-4.32 (*m*, 4H; H**4-6**), 2.78 (*m*, 2H; H**1′**), 1.60-1.79 (*m*, 2H), 1.30-1.48 (*m*, 10H), 1.51 (*s*, 3H; H**B**), 1.43 (*s*, 3H; H**B**), 1.34 (*s*, 3H; H**B**), 1.31 (*s*, 3H; H**B**). ^{13}C-NMR (75 MHz , $CDCl_3$): 112.46 (C**A**), 109.24 (C**A**), 104.97 (C**1**),

84.08 (*d*, J = 163.1; C**8′**), 83.61 (C**2**), 80.38 (C**4**), 79.21 (C**3**), 72.40 (C**5**), 66.71 (C**6**), 57.37 (C**1′**), 30.32 (*d*, J = 19.5; C**7′**), 29.06, 28.92, 28.64, 26.74 (C**B**), 26.71 (C**B**), 26.27 (C**B**), 25.19 (C**B**), 25.10 (*d*, J = 5.3, C**6′**), 21.26 (C**2′**). ^{19}F NMR (282.4 MHz, $CDCl_3$): -218.37 EI-MS: *m/z* 423 (31 [M - 15]$^+$), 367 (4). 365 (3), 249 (3), 185 (17), 127 (30, $[C_6H_7O_3]^+$), 101 (100, $[C_5H_9O_2]^+$), 85 (12), 59 (19), 43 (44, $[C_2H_3O]^+$); HR-EI-MS *m/z* 423.1858 ([M-CH_3]$^+$, $C_{19}H_{32}O_7FS$ requires 423.1853).

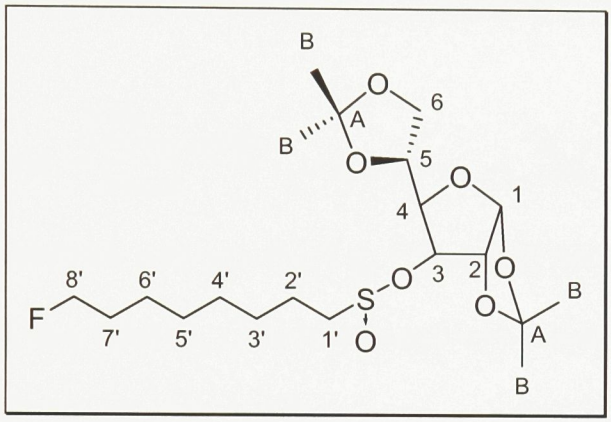

3.2.1.6 (9-Bromo-nonyloxy)-*tert*-butyl-dimethyl-silane

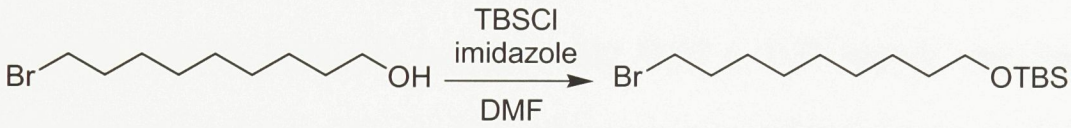

9-bromo-1-nonanol (2.33 g, 10.4 mmol), *tert*-butyldimethylsilyl chloride (1.85 g, 12.3 mmol) and imidazole (1.85 g, 27.1 mmol) were combined in an RBF. DMF (2.6 ml) was added and the mixture was stirred at room temperature under N_2 gas overnight. The resulting cloudy yellow mixture was diluted with ether (10 ml) and washed sat. NaCl (10 ml). The organic phase was evaporated *in vacuo* the resulting oil was partitioned between hexanes (3 x 10 ml) and dH_2O (10 ml). The combined organic phases were washed with sat. NaCl (10 ml), dried (Na_2SO_4) and concentrated *in vacuo* to yield the title compound (2.97 g, 8.8 mmol, 85%) as a pale oil. TLC (EtOAc/hexane 15:85): R_f 0.67. ^{1}H-NMR (300 MHz , $CDCl_3$): 3.60 (*t*, J = 6.6, 2 H; H**1**), 3.42 (*t*, J = 6.8, 2 H; H**9**), 1.86 (*m*, 2 H; H**8**), 1.47-1.59 (*m*, 2 H; H**2**),

1.32 (*m,* 10H; H**3-7**), 0.89 (*s*, 9 H; H**11**), 0.05 (*s*, 6 H; H**10**). ^{13}C-NMR (75 MHz , $CDCl_3$): 63.29 (C**1**), 34.03 (C**9**), 32.86 (C**2**), 29.42 (C**8**), 29.33, 29.72, 28.17 (C**7**), 31.60 (C**11**), 25.77 (C**3**), 18.90 (C**12**), -5.24 (C**10**).

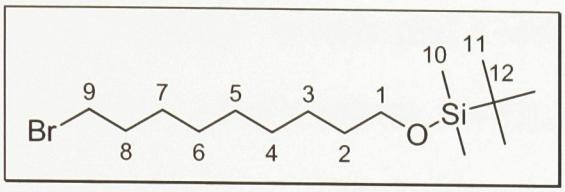

3.2.1.7 *tert*-Butyl-[10-(8-fluoro-octane-1-(*S*)-sulfinyl)-decyloxy]-dimethyl-silane

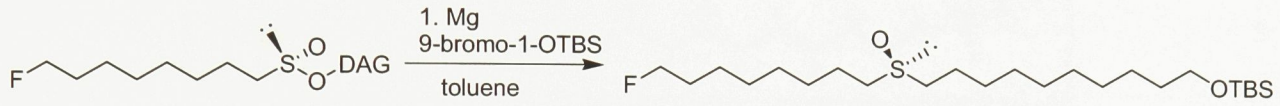

Freshly worn magnesium turnings (0.14 g, 5.9 mmol) were covered with dry THF (1.5 ml) under N_2 gas. To this mixture, (9-bromo-nonyloxy)-*tert*-butyl-dimethyl-silane (1.49 g, 4.4 mmol) in dry THF (7 ml). The resulting mixture refluxed for 7 hours. Cooled the mixture to RT.

In another vessel, (*R*)-DAG sulfinate ester (0.33 g, 0.77 mmol) was dissolved in toluene (16 ml) and cooled to 0°C. To this solution was transferred a portion of the newly formed Grignard reagent solution (4.5 ml, 2.6 mmol). This solution was stirred for 30 min. at 0°C then allowed to come to RT. and the reaction was continued for 24 hours. The solution was quenched with sat. NH_4Cl (10 ml) and then extracted with DCM (2 x 10 ml). Combined organic phases were dried over Na_2SO_4 and concentrated by rotoevaporation. The title compound was obtained by flash chromatography using 60% EtOAc/hexanes to obtain a white solid (0.27 g, 0.61 mmol, 80%). TLC (EtOAc/hexane 75:25): R_f 0.30. IR (KBr): 3434, 2927, 2854, 1636, 1471, 1388, 1361, 1256, 1103, 1017, 934, 837, 776, 726, 663 cm^{-1}. ^{1}H-NMR (300 MHz , $CDCl_3$): 4.42 (*dt*, $^2J_{HF}$ = 47.3, $^3J_{HH}$ = 6.1, 2H; H**17**), 3.58 (*t*, *J* = 6.6, 2H; H**1**), 2.64 (*m*, 4H; H**9-10**), 1.68-1.84 (*m*, 4H; H**8**, H**11**), 1.58-1.84 (*m*, 2H, H**16**), 1.22-1.54

(*m*, 20H), 0.88 (*s*, 9H; H**20**), 0.03 (*s*, 6H; H**19**). ^{13}C-NMR (75 MHz , $CDCl_3$): 84.09 (*d*, *J* = 163.2; C**17**), 63.26 (C**1**), 52.47, 52.38 (C**9**,**10**), 32.82 (C**2**), 30.32 (*d*, *J* = 19.2, C**16**), 29.33, 29.30, 29.15, 29.08, 28.94, 28.87, 28.76, 25.97 (3C; C**20**), 25.74, 25.07 (*d*, *J* = 5.3, C**15**), 22.60, 22.58, 18.36 (C**18**), -5.27 (2C; C**19**). ^{19}F NMR (282.4 MHz, $CDCl_3$): -218.36. EI-MS: *m/z* 419 (2 $[M - OH]^+$), 379 (100, $[M - t\text{-Bu}]^+$), 359 (3), 199 (3), 101 (7), 89 (3), 75 (24), 69 (16), 55 (16), 41 (10).

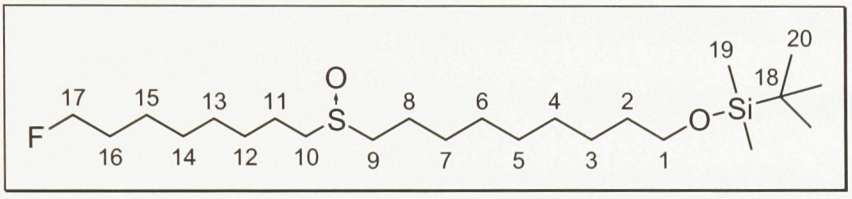

3.2.1.8 *tert*-Butyl-[10-(8-fluoro-octane-1-(*R*)-sulfinyl)-decyloxy]-dimethyl-silane

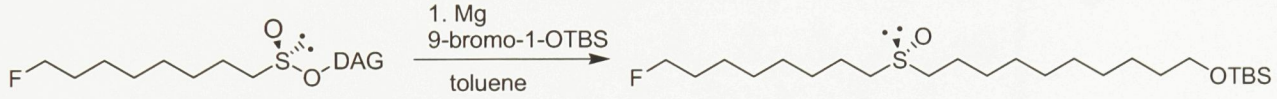

Obtained as for tert-Butyl-[10-(8-fluoro-octane-1-(*S*)-sulfinyl)-decyloxy]-dimethyl-silane, using (S)-DAG sulfinate ester (69% yield). Structural data identical for that of tert-Butyl-[10-(8-fluoro-octane-1-(*S*)-sulfinyl)-decyloxy]-dimethyl-silane.

3.2.1.9 10-(8-Fluoro-octane-1-(*S*)-sulfinyl)-decan-1-ol

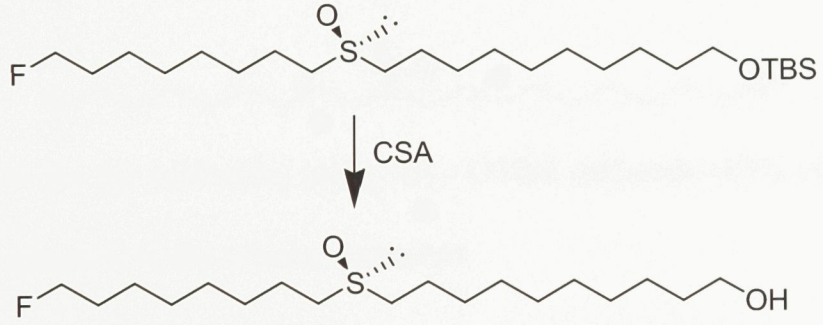

A solution of (S)-OTBS-sulfoxide (18 mg, 0.041 mmol) in MeOH (1.4 ml) was cooled to 0 °C with stirring. (1*S*)-(+)-10-Camphorsulfonic acid (2 mg, 9 µmol) was added and the resulting solution was stirred for 45 minutes. The reaction was quenched with sat.

$NaHCO_3$ (3.5 ml) and extracted with DCM (3 x 2 ml). The extracts were dried (Na_2SO_4) and dried under a gentle flow of N_2 to obtain the title compound as a white solid (11 mg, 0.033 mmol, 81%). %). TLC (EtOAc/hexane 75:25): R_f 0.03. IR (KBr): 3437, 2923, 2850, 1636, 1468, 1417, 1063, 1018, 932, 879, 727 cm^{-1}. ^{1}H-NMR (300 MHz , $CDCl_3$): 4.43 (*dt*, $^2J_{HF}$ = 47.3, $^3J_{HH}$ = 6.1, 2H; H**17**), 3.63 (*t*, *J* = 6.5, 2H; H**1**), 2.65 (*m*, 4H; H**9**-**10**), 1.28-1.84 (*m*, 26H). ^{13}C-NMR (75 MHz , $CDCl_3$): 84.14 (*d*, *J* = 163.0; C**17**), 62.95 (C**1**), 52.44, 52.39 (C**9**,**10**), 32.73 (C**2**), 30.33 (*d*, *J* = 19.3, C**16**), 29.25, 29.25, 29.09, 29.09, 28.95, 28.82, 28.76, 25.67, 25.08 (*d*, *J* = 5.2, C**15**), 22.59, 22.59. ^{19}F NMR (282.4 MHz, $CDCl_3$): -218.34. EI-MS: *m/z* 305 (72 [M - OH]$^+$), 157 (27), 143 (20, [$C_9H_{18}OH$]), 83 (33), 69 (100), 55 (78), 41 (36). HR-EI-MS *m/z* 305.2319 ([M-OH]$^+$, $C_{17}H_{34}OFS$ requires 305.2314).

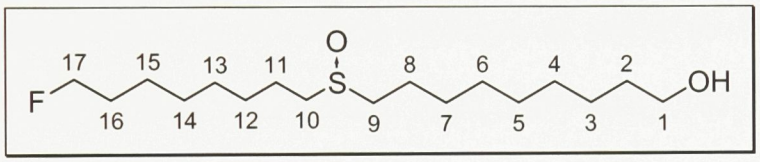

3.2.1.10 10-(8-Fluoro-octane-1-(*R*)-sulfinyl)-decan-1-ol

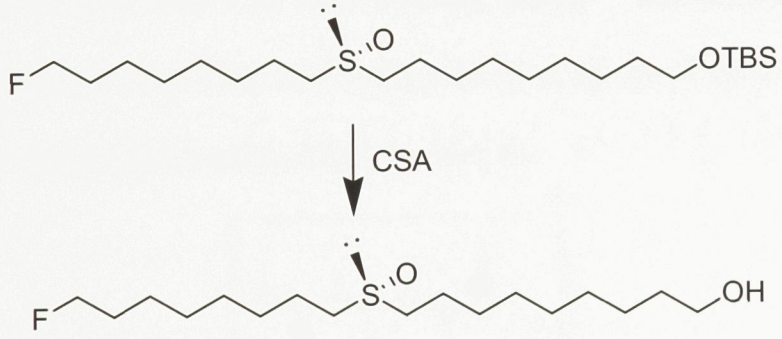

Obtained as for (*S*) sulfoxide, using (*R*)—OTBS sulfoxide (83% yield). The data for this compound is identical to the other enantiomer.

3.2.2 (11*R*)- and (11*S*)-15-fluoro-11-sulfoxy-pentadecane

3.2.2.1 Thioacetic acid S-(4-fluoro-butyl) ester

To a solution of potassium thioacetate (1.09 g, 9.5 mmol) in anh. DMF (25 ml) was added 1-bromo-4-fluorobutane (1.49 g, 9.6 mmol) dissolved in DMF (15 ml) under N_2 at room temperature. After stirring at room temperature overnight, the reaction mixture was diluted with CH_2Cl_2 (75 ml), washed with dH_2O (5 x 50 ml), sat. NaCl (50 ml), dried (Na_2SO_4) and roto-evaporated. The resulting oil was then partitioned between hexanes (2 x 20 ml) and dH_2O (20 ml), the combined organic layers were dried (Na_2SO_4) and evaporated to give the title compound (1.27 g, 8.4 mmol, 88 %) as an amber oil. TLC (EtOAc/hexane 15:85): R_f 0.73. IR (film): 2966, 1693 (C=O), 1430, 1355, 1135, 1047, 957, 914, 734, 627 cm^{-1}. ^{1}H-NMR (300 MHz , $CDCl_3$): 4.44 (*dt*, $^2J_{HF}$ = 47.2, $^3J_{HH}$ = 5.5, 2H,H **4**), 2.90 (*t*, *J* = 7.1, 2H, H**1**), 2.31 (*s*, 3H, H**6**), 1.65-1.83 (*m*, 4H, H**3-2**). ^{13}C-NMR (75 MHz, $CDCl_3$): 195.70 (C**5**), 83.39 (*d*, *J* = 164, C**4**), 30.57 (C**1**), 28.55 (C**6**), 29.38 (*d*, *J* = 19.7, C**2**), 25.49 (*d*, *J* = 4.8, C**2**). ^{19}F NMR (282.4 MHz, $CDCl_3$): -218.99.

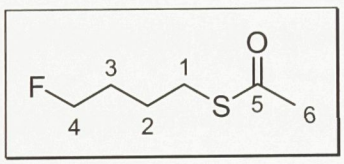

3.2.2.2 4-Fluoro-butanesulfinyl chloride

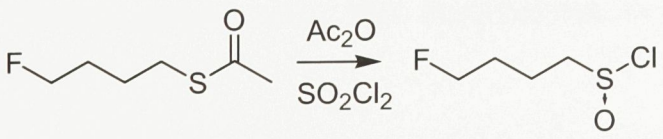

Thioacetic acid S-(4-fluoro-butyl) ester (1.11 g, 7.3 mmol) and acetic anhydride (0.71 ml, 0.77 g, 7.5 mmol) were combined in a 3-neck RBF equipped with magnetic stirbar and

N_2 inlet. The reaction vessel was cooled to -10 °C and sulfuryl chloride (1.21 ml, 2.01 g, 14.9 mmol) was added dropwise over 30 minutes. Stirring was continued for another half hour at -10 °C. The solution was roto-evaporated to give the title compound (1.20 g, crude) as an amber oil: ^{1}H-NMR (300 MHz , $CDCl_3$): 4.51 (*dt*, $^2J_{HF}$ = 47.1, $^3J_{HH}$ = 5.6, 2H; H**4**), 3.46 (*t*, 2H; H**1**), 2.04-2.17 (*m*, 2H), 1.91 (*m,* 2H). ^{13}C-NMR (75 MHz , $CDCl_3$): 83.14 (*d*, *J* = 165.0; C**4**), 63.47 (C**1**), 28.29 (*d*, *J* = 19.9, C**3**), 18.62 (*d*, *J* = 4.5, C**2**). ^{19}F NMR (282.4 MHz, $CDCl_3$): -219.42.

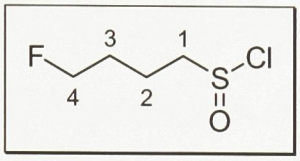

3.2.2.3 1,2:5,6-Di-O-isopropylidene-α-D-glucofuranosyl (+)-(*R*)-4-fluorobutanesulfinate and 1,2:5,6-Di-O-isopropylidene-α- D -glucofuranosyl (+)-(*S*)-4-fluorobutanesulfinate

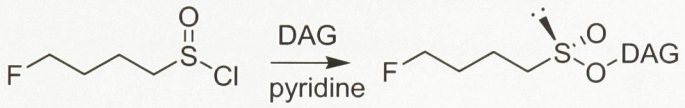

To diacetone-D-glucose (0.82 g, 3.0 mmol) in dry THF (13 ml) under N_2 gas at -78°C was added pyridine (0.30 ml, 3.7 mmol) followed by crude 4-fluoro-butanesulfinyl chloride (3.65 mmol). Mixture was stirred for 1.5 hours (-78 °C), then at room temperature for 1.5 hours. Reaction was quenched dropwise with water (5 ml) then diluted with DCM (50 ml). The resulting mixture was washed with 5% HCl (50 ml), 2% $NaHCO_3$ (50 ml), and sat. NaCl (50 ml), then dried over Na_2SO_4 and concentrated by rotaevaporation. The enantiomers were isolated by flash chromatography using 50% Et_2O/hexanes to obtain very thick, pale oils.

1,2:5,6-Di-*O*-isopropylidene-α-D-glucofuranosyl (+)-(*R*)-4-fluorobutane-sulfinate (0.76 g, 2.0 mmol, 66%) $dr_{R/S}$>99/1. $[\alpha]_D^{21}$ = +3.91° (*c* 1.1, acetone). TLC (EtOAc/hexane 1:1): R_f

0.49. IR (film): 2988, 1714, 1456, 1374, 1256, 1219, 1166, 1075, 1022, 956, 887, 838, 754, 687 cm^{-1}. ^{1}H-NMR (300 MHz , $CDCl_3$): 5.89 (*d*, *J* = 3.5, 1H, H**1**), 4.76 (*d*, *J* = 3.5, 1H, H**2**), 4.71 (*br s*, 1H, H**3**), 4.46 (*dt*, $^2J_{HF}$ = 47.2, $^3J_{HH}$ = 5.6, 2H; H**4′**), 3.95-4.17 (*m*, 4H; H**4-6**), 2.86 (*2dt*, *J* = 7.5, 13.5, 2H; H**1′**), 1.74-1.94 (*m*, 4H; H**2′**,**3′**), 1.48 (*s*, 3H; H**B**), 1.40 (*s*, 3H; H**B**), 1.30(*s*, 3H; H**B**), 1.28 (*s*, 3H; H**B**). ^{13}C-NMR (75 MHz , $CDCl_3$): 112.37 (C**A**), 109.43 (C**A**), 105.31 (C**1**), 83.79 (C**2**), 83.14 (C**4**), 83.12 (*d*, *J* = 165.0; C**4′**), 80.88 (C**3**), 72.10 (C**5**), 67.66 (C**6**), 57.15 (C**1′**), 29.39 (*d*, *J* = 19.8, C**3′**), 26.83 (C**B**), 26.70 (C**B**), 26.15 (C**B**), 25.15 (C**B**), 17.38 (*d*, *J* = 4.8, C**2′**). ^{19}F NMR (282.4 MHz, $CDCl_3$): -219.53. EI-MS: *m/z* 367 (10 $[M - 15]^+$), 309 (2), 249 (4), 245, (30), 187 (11), 185 (6), 159 (3), 127 (24, $[C_6H_7O_3]^+$), 123 (12, $[FC_4H_8SO]^+$), 113 (8, $[C_4H_7SO]^+$), 101 (100, $[C_5H_9O_2]^+$), 85 (17), 59 (40), 43 (16, $[C_2H_3O]^+$); HR-EI-MS *m/z* 367.1240 ($[M-CH_3]^+$, $C_{15}H_{24}O_7FS$ requires 367.1227).

that 99/1 while the (*S*)-O-DAG sulfinate ester had $dr_{R/S}$ = 2/98.

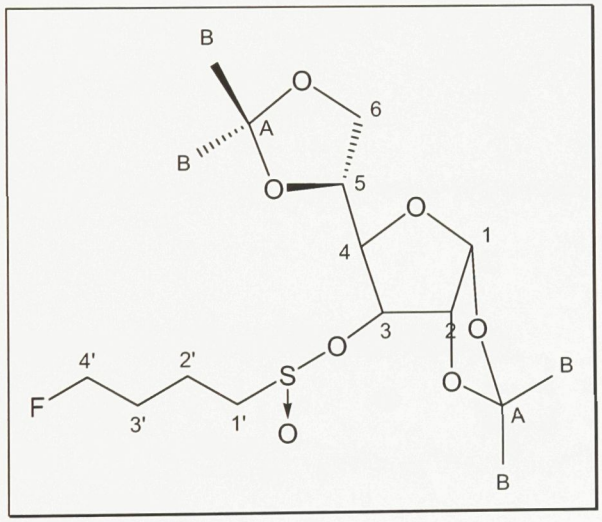

1,2:5,6-Di-*O*-isopropylidene-α-D-glucofuranosyl (-)-(*S*)-4-fluorobutane-sulfinate (0.20 g, 0.52 mmol, 17%) $dr_{R/S}$>2/98. $[\alpha]_D^{21}$ = -36.47° (*c* 1.1, acetone). TLC (EtOAc/hexane 1:1): R_f 0.44. IR (film): 2987, 1714, 1456, 1374, 1255, 1217, 1165, 1135, 1075, 1021, 837, 754 cm^{-1}; ^{1}H-NMR (300 MHz , $CDCl_3$): 5.91 (*d*, *J* = 3.7, 1H, H**1**), 4.75 (*d*, *J* = 2.5, 1H, H**3**), 4.61 (*d*, *J* = 3.7, 1H, H**2**), 4.49 (*dt*, $^2J_{HF}$ = 47.4, $^3J_{HH}$ = 5.6, 2H; H**4′**), 3.95-4.35 (*m*, 4H; H**4-6**), 2.86 (*m*,

2H; H**1′**), 1.74-1.94 (*m*, 4H; H**2′**,**3′**), 1.51 (*s*, 3H; H**B**), 1.43 (*s*, 3H; H**B**), 1.34 (*s*, 3H; H**B**), 1.32 (*s*, 3H; H**B**). ^{13}C-NMR (75 MHz , $CDCl_3$): 112.47 (H**A**), 109.29 (H**A**), 104.96 (H**1**), 83.57 (H**2**), 83.19 (*d*, $^1J_{CF}$ = 164.9; H**4′**), 80.35 (H**4**), 79.28 (H**3**), 72.30 (H**5**), 67.78 (H**6**), 56.67 (H**1′**), 29.42 (*d*, $^2J_{CF}$ = 19.9, H**3′**), 26.76 (H**B**), 26.69 (H**B**), 26.25 (H**B**), 25.16 (H**B**), 17.66 (*d*, $^3J_{CF}$ = 4.6, H**2′**). ^{19}F NMR (282.4 MHz, $CDCl_3$): -219.51. EI-MS: *m/z* 367 (17 [M - 15]$^+$), 309 (5), 249 (8), 245, (8), 190 (9), 185 (9), 127 (29, $[C_6H_7O_3]^+$), 123 (20, $[FC_4H_8SO]^+$), 113 (11, $[C_4H_7SO]^+$), 101 (100, $[C_5H_9O_2]^+$), 85 (14), 59 (25), 43 (47, $[C_2H_3O]^+$); HR-EI-MS *m/z* 367.1218 ($[M\text{-}CH_3]^+$, $C_{15}H_{24}O_7FS$ requires 367.1227).

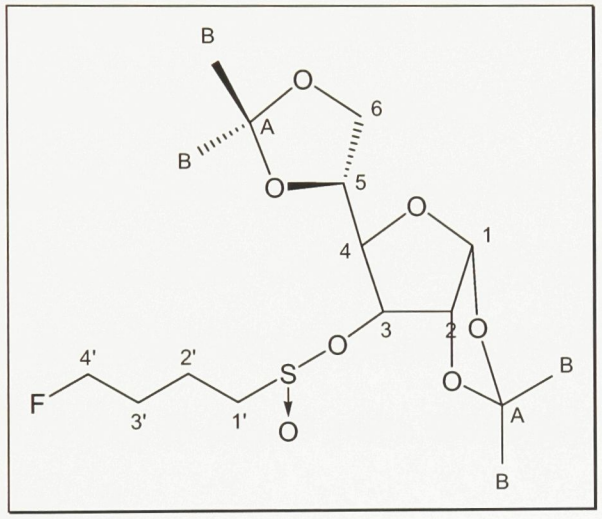

3.2.2.4 1-(4-Fluoro-butane-1-(*S*)-sulfinyl)-decane

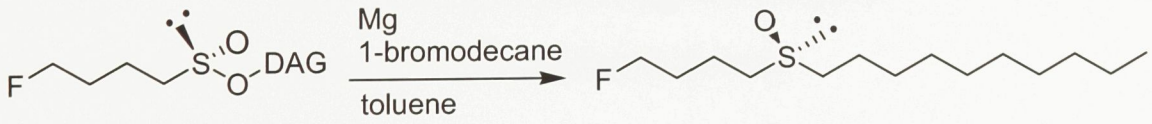

Freshly worn magnesium turnings (0.18 g, 7.4 mmol) were covered with dry THF (2 ml) under N_2 gas. To this mixture, 1-bromodecane (1.11 g, 5.0 mmol) in dry THF (9 ml). The resulting mixture was refluxed for 5.5 hours then cooled to RT.

In another vessel, (*R*)-DAG sulfinate ester (0.30 g, 0.79 mmol) was dissolved in toluene (16 ml) and cooled to 0°C. To this solution was transferred a portion of the newly

formed Grignard reagent solution (5.3 ml, 2.4 mmol). This solution was stirred for 30 min. at 0°C then allowed to come to RT. and the reaction was continued for 24 hours. The solution was quenched with sat. NH_4Cl (10 ml) and then extracted with DCM (3 x 10 ml). Combined organic phases were dried over Na_2SO_4 and concentrated by rotoevaporation. The title compound was obtained by flash chromatography using 80% EtOAc/hexanes to obtain a white solid (72 mg, 0.27 mmol, 35%). 99 % *ee*, $[\alpha]_D^{25}$ +1.7 (c 1.1, $CHCl_3$); Mp 59-60°C TLC (EtOAc/hexane 75:25): R_f 0.10. IR (KBr): 2919, 2849, 1470, 1412, 1047, 1012, 923, 725 cm^{-1}; ^{1}H-NMR (300 MHz , $CDCl_3$): 4.49 (*dt*, $^2J_{HF}$ = 47.1, $^3J_{HH}$ = 5.6, 2 H; H**14**), 2.57-2.77 (*m*, 4H; H**10-11**), 1.93 (*m*, 2H), 1.70-2.02 (*m*, 2H, H**13**), 1.70-1.88 (*m*, 2H), 1.44 (*m*, 2H; H**13**), 1.20-1.52 (*m*, 12H; H**10**), 0.87 (*t*, *J* = 6.7, 3H; H**1**). ^{13}C-NMR (75 MHz, $CDCl_3$): 83.37 (*d*, *J* = 164.7; C**14**), 52.57, 51.81 (C**10**,**11**), 31.85, 29.51 (*d*, *J* = 19.9, C**13**), 29.47, 29.35, 29.25, 29.19, 28.86, 22.65, 22.59, 19.06 (*d*, *J* = 4.7, C**12**), 14.08 (C**1**). ^{19}F NMR (282.4 MHz, $CDCl_3$): -219.23. EI-MS: *m/z* 247 (79, $[M - 17]^+$), 189 (9), 173 (16), 161 (6), 124 (15), 123 (9), 85 (19), 71 (24), 55 (96), 43 (100). HR-EI-MS *m/z* 247.1895 ($[M\text{-}OH]^+$, $C_{14}H_{28}FS$ requires 247.1895).

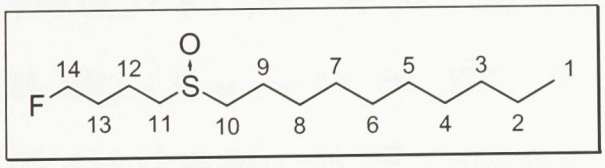

3.2.2.5 1-(4-Fluoro-butane-1-(*R*)-sulfinyl)-decane

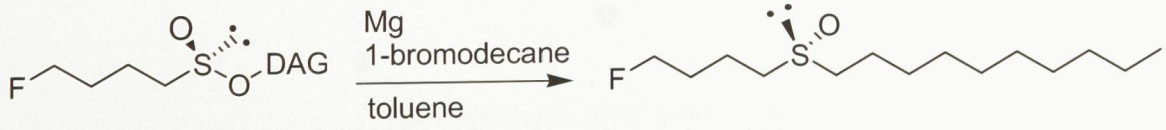

Obtained as for 1-(4-Fluoro-butane-1-(*S*)-sulfinyl)-decane, using (S)-DAG sulfinate ester. All spectra data are identical to those obtained for 1-(4-Fluoro-butane-1-(*S*)-sulfinyl)-decane except 90 % *ee*, $[\alpha]_D^{25}$ -1.4 (c 1.1, $CHCl_3$).

3.3 Synthesis of chiral shift agents, (*R*)- and (*S*)-(9-anthryl)-methoxyacetic acid

3.3.1 Ethyl 2-(9-anthryl)-2-oxoacetate

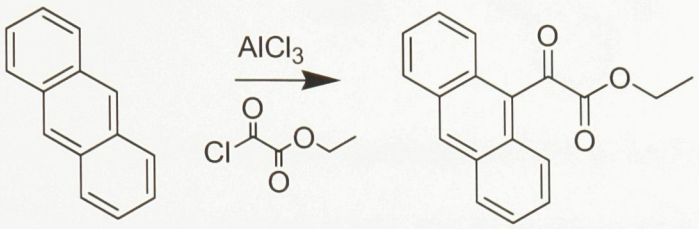

To a suspension of aluminum chloride (6.06 g, 45.5 mmol) in DCM (50 ml) at 0°C under an inert atmosphere was added anthracene (4.18 g, 23.5 mmol) and ethyl chlorooxoacetate (2.5 ml, 3.06 g, 22.4 mmol) in DCM (250 ml) dropwise over 2 hours with stirring. The reaction mixture was allowed to warm to room temperature and stirring was continued for 14 hours. The mixture was cooled to 0 °C and 1M HCl (50 ml) was added dropwise. The organic phase was removed and the aqueous phase was extracted with DCM (4 x 100 ml). The organic phases were combined and the solvent removed by roto-evaporated. The title compound was isolated via flash chromatography (DCM) as a yellow solid (6.09 g, 21.9 mmol, 98%). TLC (DCM): R_f 0.68. M.p. 81-83°C. ^{1}H-NMR (300 MHz , $CDCl_3$): 8.58 (*s*, 1H, **10**), 8.04 (*d*, *J* = 8.3, 2H), 7.96 (*dd*, *J* = 8.7, 0.9, 2H), 7.53 (*m*, 4H, H**2-3, H5-6**), 4.38 (*q*, *J* = 7.1, 2H, H**1′**), 1.31 (*t*, *J* = 7.1, 3H , H**2′**). ^{13}C-NMR (75 MHz , $CDCl_3$): 192.16 (C**4′**), 162.96 (C**3′**), 131.17 (C**10**), 130.75, 129.68 (C**9**), 129.29, 128.97, 128.97, 127.65, 127.65, 125.61, 125.61, 123.95, 123.95, 62.83 (C**1′**), 13.84 (C**2′**). UV λ_{max} ($CHCl_3$): 255 nm.

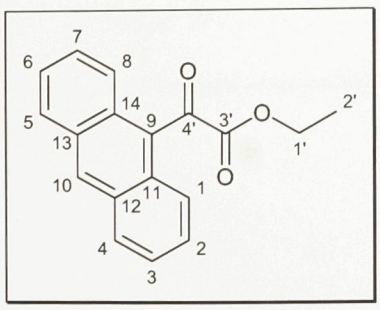

3.3.2 Ethyl 2-(9-anthryl)-2-hydroxyacetate

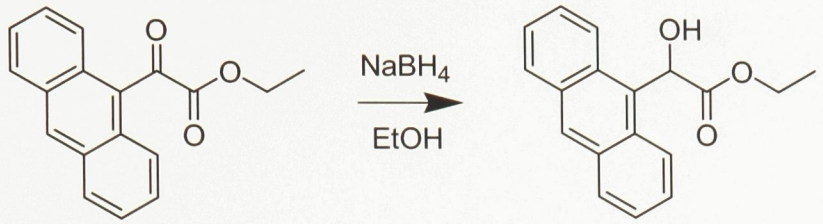

To a solution of ethyl 2-(9-anthryl)-2-oxoacetate (6.04 g, 21.7 mmol) in abs. Ethanol (200 ml) cooled to 0°C was added sodium borohydride (1.02 g, 27.0 mmol). The resulting mixture was stirred for 1 hour then quenched with 0.5M HCl (50 ml). The solution was extracted with DCM (4 x 100 ml), washed with water (2 x 100 ml) and brine (100 ml), then dried (Na_2SO_4). The solvent removed *in vacuo* to obtain the title compound as a brown solid (5.67 g, 20.2 mmol, 93%). TLC (2.5% MeOH in DCM): R_f 0.30. M.p. 123-125°C. ^{1}H-NMR (300 MHz , $CDCl_3$): 8.50 (*s*, 1H, H**10**); 8.34 (*d*, J = 8.7, 2H, H**1,8**), 8.03 (*dd*, J = 8.3, 1.4, 2H, H**4,5**), 7.51 (*m*, 4H, H**2-3**, H**6-7**), 6.59 (*s*, 1H, H**4′**), 4.20 (*dq*, J^2 = 10.8, J^3 = 7.2, 1H, H**1′**), 4.14 (*dq*, J^2 = 10.8, J^3 = 7.2, 1H, H**1′**), 1.04 (*t*, J= 7.1, 3H, H**2′**). ^{13}C-NMR (75 MHz, $CDCl_3$): 175.28 (C**3′**), 131.58, 130.41, 129.32, 129.32, 129.27 (C**10**), 128.47, 126.62, 126.62, 125.87, 124.94, 124.94, 123.78, 123.78, 68.15 (C**4′**), 62.34 (C**1′**), 13.91 (C**2′**). UV λ_{max} ($CHCl_3$): 259 nm.

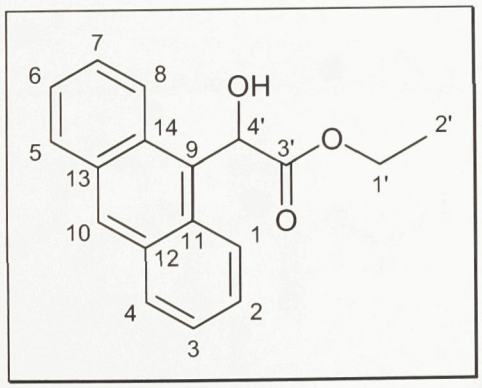

3.3.3 Ethyl 2-(9-anthryl)-2-methoxyacetate

To a solution of ethyl 2-(9-anthryl)-2-hydroxyacetate (5.65 g, 20.2 mmol) and methyl iodide (6 ml, 13.7 g, 96.4 mmol) in DCM (50 ml) was added silver(I) oxide (5.69 g, 24.6 mmol). The resulting suspension was stirred for 14 hours at room temperature. H_2O (50 ml) was added to the reaction mixture and the resulting solution was extracted with DCM (3 x 50 ml). The organic extracts were combined, vacuum filtered and the solvent removed by roto-evaporation. The title compound was isolated by flash chromatography (DCM to 10% MeOH in DCM gradient) as a yellow solid (2.23 g, 7.58 mmol, 38%). TLC (DCM): R_f 0.33. M.p. 79-80°C. ^{1}H-NMR (300 MHz , $CDCl_3$): 8.58 (*d*, J = 8.9, 2H, H**1,8**), 8.49 (*s*, 1H, H**10**), 8.03 (*d*, J = 8.2, 2H, H**4,5**), 7.52 (*m*, 4H, H**2-3**, H**6-7**), 6.29 (*s*, 1H, H**4′**), 4.20 (*dq*, J^2 = 10.8, J^3 = 7.1, 1H, H**1′a**), 4.06 (*dq*, J^2 = 10.8, J^3 = 7.1, 1H, H**1′b**), 3.42 (*s*, 3H, H**5′**), 1.04 (*t*, J= 7.1, 3H, H**2′**). ^{13}C-NMR (75 MHz , $CDCl_3$): 171.35 (C**3′**), 131.45, 130.58, 129.19, 129.12, 129.12, 127.37, 126.45, 126.45, 124.97, 124.97, 124.42, 77.16 (C**4′**), 61.32 (C**1′**), 57.41 (C**5′**), 13.97 (C**2′**). UV λ_{max} ($CHCl_3$): 259 nm.

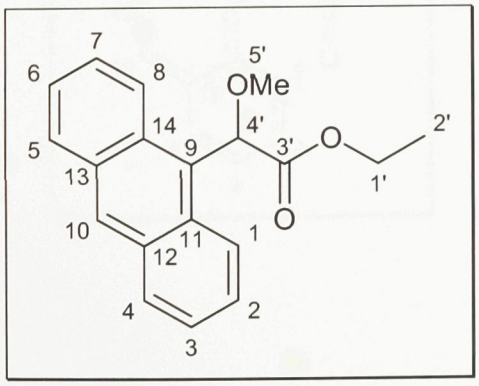

3.3.4 (9-anthryl)-methoxy-acetic acid

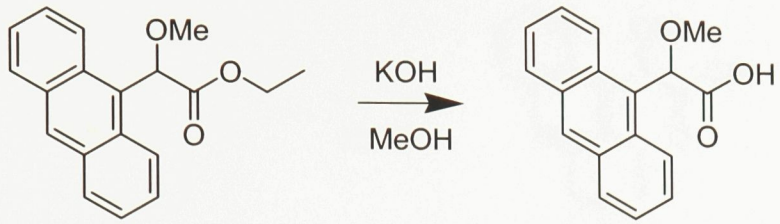

Ethyl 2-(9-anthryl)-2-methoxyacetate (2.18 g, 7.40 mmol) was dissolved in 10% KOH/MeOH (80 ml) and the resulting solution was stirred at room temperature (6 hours). The solution was acidified with 1M HCl and filtered to collect product. The filtrate was redissolved in ethyl acetate and washed with water. The solvent was removed by roto-evaporation to yield the title compound was a yellow solid (1.81 g, 6.80 mmol, 92%). TLC (10% MeOH/DCM): R_f 0.21. M.p. 192-195°C. ^{1}H-NMR (300 MHz , $CDCl_3$): 8.51 (*s*, 1H, H**10**), 8.45 (*d*, *J* = 8.7, 2H, H**1,8**), 8.03 (*d*, *J* = 8.1, 2H, H**4,5**), 7.51 (*m*, 4H,H **2-3**, H**6-7**), 6.32 (*s*, 1H, H**2′**), 3.38 (*s*, 3H, H**3′**). ^{13}C-NMR (75 MHz, $CDCl_3$): 174.70 (C**1′**), 134.16, 131.47, 130.75, 129.77, 129.33, 127.26, 126.85, 126.00, 125.08, 123.98, 124.42, 76.53 (C**2′**), 57.41 (C**3′**). UV λ_{max} (MeOH): 255 nm. EI-MS: *m/z* 266 (16, $[M]^+$), 221 (100, $[M\text{-}COOH]^+$), 208 (31), 178 (35), 152 (23).

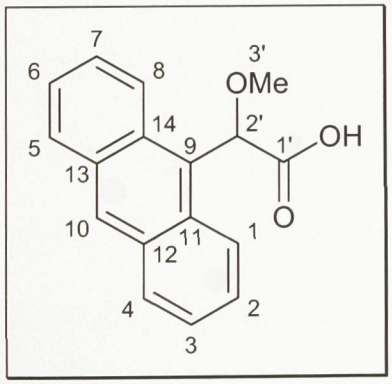

3.3.5 Resolution of (*R*)- and (*S*)-(9-anthryl)-methoxy-acetic acid

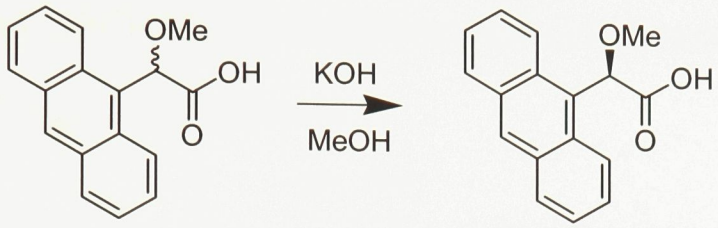

To a hot solution of (9-anthryl)-methoxy-acetic acid (1.22 g, 4.6 mmol) in MeOH (60 ml) was added (*R*)-(+)-methylbenzylamine (0.58 ml, 0.55 g, 4.6 mmol). The resulting mixture was slowly cooled to 0 °C. The resulting white, needle-shaped crystals were collected and the filtrate was reserved. This process was repeated several times for a combined precipitate of 0.87 g. A portion (0.46 g) of the solid was dissolved in H_2O (30 ml) and acidified with 1M HCl. The resulting solution was extracted with DCM (2 x 30 ml) and roto-evaporated to recover the (*R*)-enantiomer of the title compound as a yellow solid (0.23 g, 0.87 mmol). $[\alpha]_D^{21} = -194°$ (*c* 0.001, EtOH).

The reserved filtrate was dried by roto-evaporation. The resulting solid product was acidified and extracted as above to recover a (*S*)-enantiomer enriched sample of the title compound (0.68 g, 2.6 mmol). $[\alpha]_D^{21} = +143°$ (*c* 0.001, EtOH).

3.4 Synthesis of allylic alcohol standards

3.4.1 (10*Z*)- and (10*E*)- Methyl 9-hydroxy-10-octadecenoate

3.4.1.1 Methyl 9-hydroxynonanoate

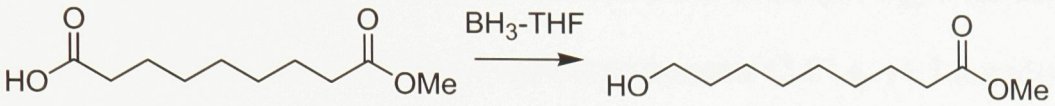

To *mono*-methyl azelate (2.55 g, 12.6 mmol) in dry THF (6 ml) in a RBF at -10 °C under N_2 was slowly added borane tetrahydrofuran complex solution (12.6 ml, 1.0 M in THF, 12.6 mmol). Mixture was stirred for 10 minutes then allowed to come to room temperature and stirred for another 4 hours. Solution cooled to 0 °C then quenched with 3 mg K_2CO_3 in H_2O (25 ml), diluted with Et_2O (50 ml). The ethereal layer was reserved and the aqueous phase was extracted with Et_2O (2 x 50 ml). The combined organic phases were washed with sat. NaCl (40 ml) and, (Na_2SO_4) and evaporated to give crude methyl 9-hydroxynonanoate (1.36 g) as a pale oil. Purified by flash chromatography (30 % EtOAc/hexanes) to give the title compound as a colorless oil (0.62 g, 26 % yield) at room temperature. R_f 0.19 (30% EtOAc/hexanes). IR (film): 3225, 2931, 2857, 1740, 1458, 1439, 1197, 1056, 732. ^{1}H NMR (300 MHz, $CDCl_3$) δ 3.63 (s, 3H, H**10**), 3.59 (t, J = 6.6 Hz, 2H; H**9**), 2.27 (t, J = 7.5 Hz, 2H; H**2**), 1.74 (br. s, 1H; H**11**), 1.48-1.65 (m, 4H; H**3**,**8**), 1.30-1.35 (m, 8H; H**4-7**). ^{13}C NMR (75.5 MHz, $CDCl_3$) δ 174.48 (C**1**), 63.01 (C**9**), 51.58 (C**10**), 34.19 (C**2**), 32.85 (C**8**), 31.03, 29.32, 29.17, 25.79, 25.02 (C**3**). MS (rel. intensity) *m*/z 245 (57, $[M-15]^+$), 213 (95, $[M-47]^+$), 107 (25), 103 (58), 89 (64), 75 (58), 74 (22), 73 (90), 69 (84), 59 (19), 55 (100).

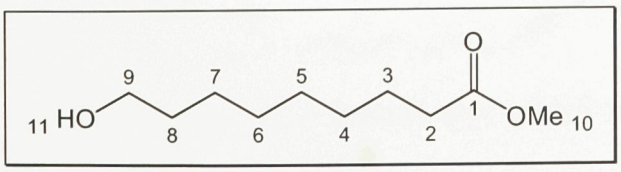

3.4.1.2 Methyl 9-oxononanoate

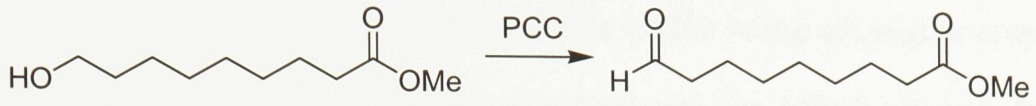

Pyridinium chlorochromate (4.79 g, 22.2 mmol) and Celite (4.79 g) were combined in dry THF (20 ml) to form a slurry. Methyl 9-hydroxynonanoate (2.77 g, 14.7 mmol) dissolved in THF (10 ml) was added with stirring. Mixture stirred at room temperature until TLC analysis showed no presence of starting material (ca. 3.5 hours). Diluted with ether (60 ml) and filtered through Florisil. Washed Florisil with ether (2 x 40 ml) and collected filtrate and washings. Removed solvent *in vacuo* to yield title compound as a pale oil (2.13 g, 11.4 mmol, 78% yield) at room temperature. R_f 0.45 (30% EtOAc/hexanes); IR (film): 2933, 2857, 1738, 1437, 1363, 1173, 757. ^{1}H NMR (300 MHz, $CDCl_3$) δ 9.73 (t, J = 1.8 Hz, 1H; H**11**), 3.63 (s, 3H; H**10**), 2.39 (dt, J = 1.8 Hz, J' = 7.3 Hz, 2H; H**8**), 2.27 (t, J = 7.5 Hz, 2H; H**2**), 1.52-1.65 (m, 4H; H**3**,**7**), 1.29 (m, 6H; H**4**-**6**). ^{13}C NMR (75.5 MHz, $CDCl_3$) δ 202.91 (C**9**), 174.32 (C**1**), 51.57 (C**10**), 43.95 (C**8**), 34.11 (C**2**), 29.08, 29.04, 28.99, 24.93 (C**3**), 22.70 (C**7**); MS (rel. intensity) *m*/z 155 (18, $[M-31]^+$), 143 (27, $[M-43]^+$), 111 (26), 87 (66), 74 (100, $[CH_3O(C{=}O)CH_2]^+$), 69 (28), 59 (32, $[COOCH_3]^+$), 57 (17), 55 (56), 44 (13), 43 (47).

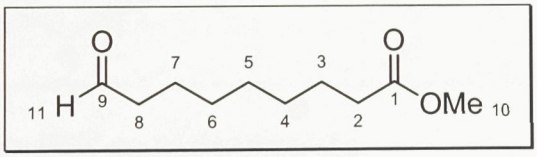

3.4.1.3 Methyl 9-hydroxy-10-octadecynoate

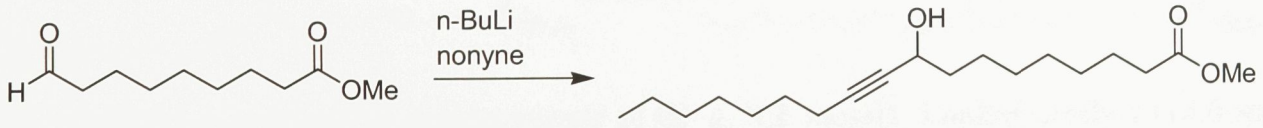

n-BuLi (5 ml, 2.5 M in hexanes, 12.5 mmol) was added with stirring to 1-nonyne (1.40 g, 11.3 mmol) in THF (20 ml) at -78° C under N_2. Solution was stirred for 20 minutes at -78° C. Methyl 9-oxononanoate (2.10 g, 11.2 mmol) was dissolved in THF under N_2 and

cooled to -78° C. The n-BuLi solution was transferred by syringe to the aldehyde solution. This solution was stirred and -78° C for 30 minutes before being allowed to come to room temperature (ca. 30 minutes). Reaction was quenched with sat. NH_4Cl (30 ml). The organic phase was removed and the aqueous phase extracted with ether (2 x 40 ml). The organic phases were combined and washed with sat. NaCl (40 ml) and dried (Na_2SO_4). The solvent was removed *in vacuo* to afford the title compound (3.11 g, 10.0 mmol, 89 % yield) as a colorless oil at room temperature. R_f 0.40 (25% EtOAc/hexanes). IR (film): 3468, 2931, 2857, 2247, 1739, 1462, 1173, 914, 734. ^{1}H NMR (300 MHz, $CDCl_3$) δ 4.33 (m, 1H; H**9**), 3.66 (s, 3H; H**19**), 2.30 (t, J = 7.5 Hz, 2H; H**2**), 2.19 (dt, J = 1.9 Hz, J' = 6.9 Hz, 2H; H**12**), 1.19-1.88 (m, 22H; H**3-8**, H**13-17**), 0.88 (t, J = 6.6 Hz, 3H; H**18**). ^{13}C NMR (75.5 MHz, $CDCl_3$) δ 174.31 (C**1**), 85.49 (C**10**), 81.33 (C**11**), 62.66 (C**9**), 51.44 (C**19**), 38.12 (C**8**), 34.05 (C**2**), 31.72 (C**16**), 29.14, 29.06, 29.02, 28.77, 28.77, 28.66, 25.11, 24.88 (C**3**), 22.59 (C**17**), 18.65 (C**12**), 14.06 (C**18**). MS (rel. intensity) *m*/z 367 (3, $[M-15]^+$), 335 (1, $[M-47]^+$), 283 (4), 225 (100, $[CH_3(CH_2)_6C\equiv CCHOSi(CH_3)_3]^+$), 181 (3), 159 (4), 129 (2), 93 (6), 73 (53), 55 (6).

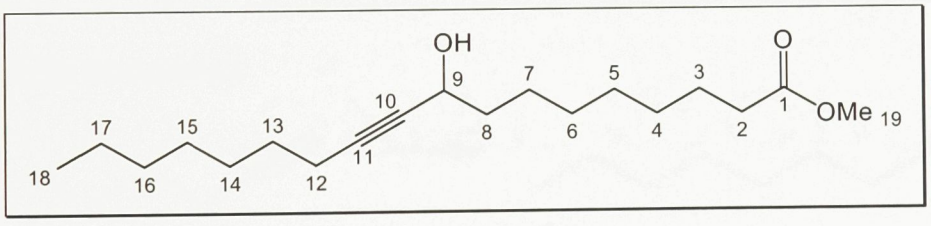

3.4.1.4 Methyl 9-hydroxy-10*Z*-octadecenoate

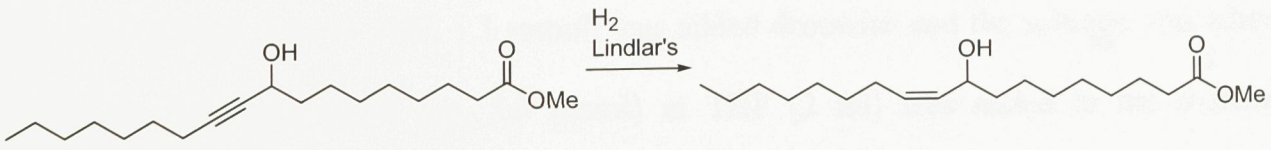

Methyl 9-hydroxy-10-octadecynoate (1.01 g, 3.2 mmol), Lindlar catalyst (18.6 mg) and quinoline (1 µl) were combined in EtOAc/Hex (33%, 5 ml) in a RBF attached to a hydrogenation system. The system was evacuated, flushed with H_2 and purged (3 times). The

system was then filled with H_2 and the reaction was left to proceed (3 days) with stirring. The resulting mixture was filtered through a silica gel/Celite plug and the filtrate was collected. The solvent was removed *in vacuo* to yield the title compound as a pale oil (0.94 g, 3.0 mmol, 93 % yield). R_f 0.33 (25% EtOAc/hexanes). IR (film): 3455, 2928, 2856, 1741, 1463, 1172, 1022. ^{1}H NMR (300 MHz, $CDCl_3$) δ 5.49 (dt, J = 10.7 Hz, J' = 7.3 Hz, 1H; H**11**), 5.36 (dd, J = 10.7 Hz, J' = 8.8 Hz, 1H; H**10**), 4.41 (dt, J = 8.8 Hz, J' = 6.5 Hz, 1H; H**9**), 3.66 (s, 3H; H**19**), 2.30 (t, J = 7.5 Hz, 3H; H**2**), 2.07 (m, 2H; H**12**), 1.23-1.73 (m, 22H; H**3-8**, H**13-17**), 0.88 (t, J = 6.8 Hz, 3H; H**18**). ^{13}C NMR (75.5 MHz, $CDCl_3$) δ 174.32 (C**1**), 132.55 (C**11**), 132.39 (C**10**), 67.68 (C**9**), 51.45 (C**19**), 37.47 (C**8**), 34.08 (C**2**), 31.82 (C**16**), 29.72, 29.39, 29.25, 29.20, 29.16, 29.06, 27.71 (C**12**), 25.32 (C**7**), 24.92 (C**3**), 22.65 (C**17**), 14.10 (C**18**). MS (rel. intensity) *m*/z 369 (1, $[M-15]^+$), 337 (2, $[M-47]^+$), 285 (3), 227 (100, $[CH_3(CH_2)_6(CH)_2CHOSi(CH_3)_3]^+$), 129 (19), 95 (6), 73 (14), 55 (4).

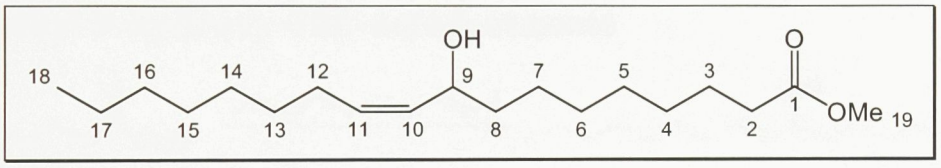

3.4.1.5 1,1*E*-iodononene

$ZrCp_2Cl_2$ (1.28 g, 4.4 mmol) was dissolved in dry THF (15 ml) under N_2. At 0° C, DIBAL-H (4.4 ml, 1 M in THF, 1.1 mmol) was added dropwise and the solution was stirred 30 minutes. 1-nonyne (0.50 mg, 4.0 mmol) in THF (2 ml) was added to the solution. Reaction mixture was warmed to room temperature and stirred for one hour before being cooled to -78° C. I_2 (1.33 g, 5.2 mmol) in THF (6 ml) was added dropwise and the mixture was stirred for an additional 30 minutes. The reaction was quenched with 1N HCl (15 ml)

and extracted with Et_2O. Extracts were washed with 10% $Na_2S_2O_3$ (3 x 20 ml), 10% $NaHCO_3$ (2 x 20 ml) and sat. NaCl (20 ml), then dried (Na_2SO_4) Solvent removed by rotoevaporation to yield title compound as an oil (766 mg, 3.0 mmol, 76% yield R_f 0.90 (2.5% EtOAc/hexanes). IR (film): 2961, 2926, 2856, 2362, 1258, 1087, 1012, 791, 662. ^1H NMR (300 MHz, $CDCl_3$) δ 6.51 (dt, J = 14.3 Hz, J' = 7.2 Hz, 1H; H**2**), 5.97 (dt, J = 14.3 Hz, J' = 1.4 Hz, 1H; H**1**), 2.06 (dq, J = 1.2 Hz, J' = 7.1 Hz, 2H; H**3**), 1.22-1.44 (m, 10H; H**4-8**), 0.88 (t, J = 6.7 Hz, 3H; H**9**). ^{13}C NMR (75.5 MHz, $CDCl_3$) δ 146.83 (C**2**), 74.25 (C**1**), 36.06 (C**3**), 31.76 (C**7**), 29.04, 28.90, 28.37, 22.64 (C**8**), 14.09 (C**9**); MS (rel. intensity) *m*/z 253 (4), 252 (36), 167 (23), 154 (26), 83 (50), 70 (17), 69 (97), 57 (24), 56 (26), 55 (71), 43 (100).

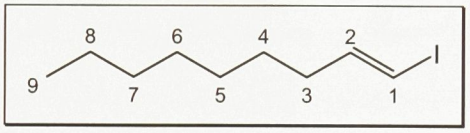

3.4.1.6 Methyl 9-hydroxy-10*E*-octadecenoate

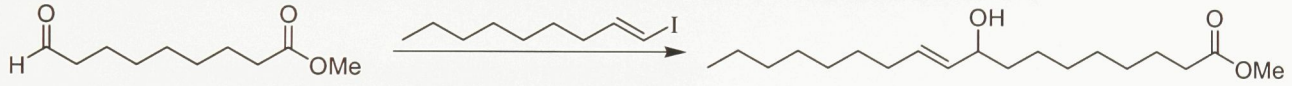

n-BuLi (0.6 ml, 2.5M in hexanes, 1.5 mmol) was added to a solution of 1,1E-iodononene (350 mg, 1.4 mmol) in hexanes (5 ml) under N_2 and the resulting mixture was stirred for 20 minutes at room temperature. The reaction mixture was cooled to 0° C and methyl 9-oxononanoate (264 mg, 1.4 mmol) in hexanes (0.8 ml) was added. Stirred 10 minutes at 0° C and then warmed to room temperature and stirred an additional 10 minutes. Quenched reaction with sat. NH_4Cl (5 ml) and removed the organic layer. Extracted from aqueous phase with ether (3 x 10 ml). Combined organic phases and washed with sat. NaCl (10 ml), dried (Na_2SO_4) and removed solvent via rotoevaporation. Purified by flash chromatography (20% EtOAc/hex) to yield the title compound as a yellow oil (30 mg, 0.1

mmol, 7% yield). R_f 0.35 (25% EtOAc/hexanes). IR (film): 3493, 2928, 2855, 1740, 1437, 1173, 970. ^{1}H NMR (300 MHz, $CDCl_3$) δ 5.61 (*dt*, *J* = 15.4, 6.6, 1H; H**11**), 5.43 (*dd*, *J* = 7.1, 15.3, 1H; H**10**), 4.03 (*dt*, *J* = 10.3, 6.6, 1H; H**9**), 3.65 (s, 3H; H**19**), 2.29 (t, *J* = 7.7 Hz, 2H; H**2**), 1.37-1.96 (m, 2H; H**12**), 1.21-1.67 (m, 22H; H**3-8**, H**13-17**), 0.87 (t, *J* = 6.6 Hz, 3H; H**18**). ^{13}C NMR (75.5 MHz, $CDCl_3$) δ 174.30 (C**1**), 132.98 (C**11**), 132.21 (C**10**), 73.16 (C**9**), 51.44 (C**19**), 37.26 (C**8**), 34.06 (C**2**), 32.17 (C**12**), 31.82 (C**16**), 29.32, 29.17, 29.17, 29.13, 29.10, 29.04, 25.39 (C**7**), 24.89 (C**3**), 22.64 (C**17**), 14.09 (C**18**); MS (rel. intensity) *m*/z 369 (1, $[M-15]^+$), 337 (3, $[M-47]^+$), 227 (100, $[CH_3(CH_2)_6(CH)_2CHOSi(CH_3)_3]^+$), 129 (21), 73 (17).

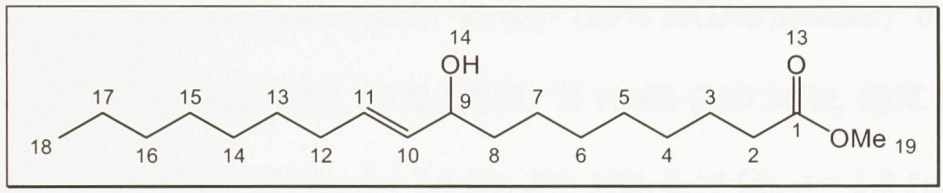

3.4.2 (9*Z*)- and (9*E*)- Methyl 11-hydroxy-9-octadecenoate

3.4.2.1 11-hydroxy-9-octadecynoic acid

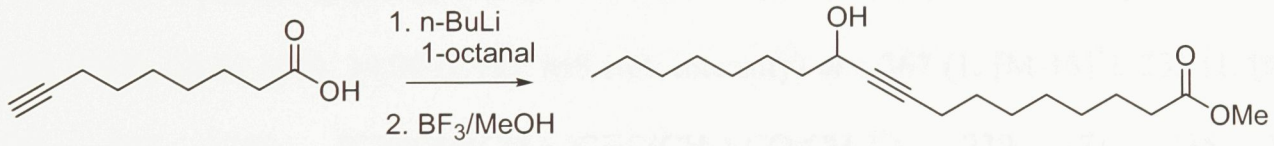

To 8-decynoic acid (prepared by acetylenic displacement of 8-bromooctanoic acid) (495 mg, 2.9 mmol) in THF (6 ml) at -78° C under N_2 was added n-BuLi (2.4 ml, 2.5 M in hexanes, 6 mmol) and the resulting mixture was stirred (20 min). This mixture was transferred to a solution of octanal (429 mg, 3.3 mmol) in THF (6 ml) at -78° C with stirring. The resulting solution was stirred 30 minutes and then warmed to room temperature and stirred an additional 30 minutes. The reaction was quenched with sat. NH_4Cl (9 ml). The organic phase was removed and the aqueous phase extracted with ether (2 x 10 ml). The

organic phases were combined and washed with sat. NaCl (40 ml) and dried (Na_2SO_4). The solvent was removed *in vacuo* to yield the crude acid of the title compound (988 mg). Boron trifluoride diethyl etherate (2 ml, 16.2 mmol) in MeOH (20 ml) was added to the crude flask under N_2 and the resulting solution was refluxed for 1h, and then allowed to cool to room temperature. The solution was rotoevaporated until only 2 ml of an amber oil remained. This oil was diluted with DCM (10 ml) and H_2O and the organic phase was removed. The aqueous phase was extracted with DCM (2 x 10 ml) and the combined extracts were washed with sat. NaCl (15 ml) and dried (Na_2SO_4) then concentrated in vacuo. The resulting oil was purified by flash chromatography (20% EtOAc/hex) to recover the title compound as a pale oil (94.2 mg, 0.3 mmol, 10% overall yield). R_f 0.37 (25% EtOAc/hexanes). IR (film): 3453, 2931, 2857, 1741, 1461, 1437, 1363, 1173, 1017. ^{1}H NMR (300 MHz, $CDCl_3$) δ 4.34 (m, 1H; H**11**), 3.66 (s, 3H; H**19**), 2.30 (t, J = 7.5 Hz, 2H; H**2**), 2.19 (dt, J = 6.9 Hz, J' = 1.8 Hz, 2H; H**8**), 1.22-1.88 (m, 22H; H**3-7**, H**12-17**), 0.88 (t, J = 6.6 Hz, 3H; H**18**). ^{13}C NMR (75.5 MHz, $CDCl_3$) δ 174.33 (C**1**), 85.30 (C**10**), 81.48 (C**9**), 62.74 (C**11**), 51.48 (C**19**), 38.21 (C**12**), 34.03 (C**2**), 31.78 (C**16**), 29.25, 29.23, 28.95, 28.66, 28.52, 28.52, 25.22, 24.83 (C**3**), 22.65 (C**17**), 18.62 (C**8**), 14.09 (C**18**); MS (rel. intensity) m/z 367 (1, $[M\text{-}15]^+$), 335 (1, $[M\text{-}47]^+$), 283 (100, $[CH(OSi(CH_3)_3)C\Xi C(CH_2)_7CO_2CH_3]^+$), 239 (7), 225 (5, $[CH_3(CH_2)_6CH(OSi(CH_3)_3)CH\Xi CH]^+$), 73 (36).

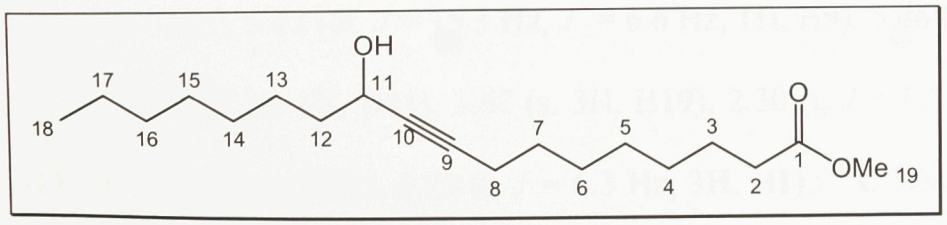

3.4.2.2 (9*Z*)- and (9*E*)- Methyl 11-hydroxy-9-octadecenoate

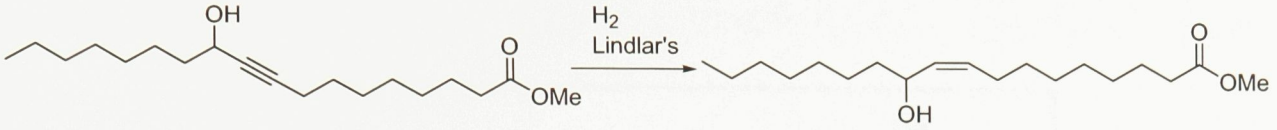

Methyl 11-hydroxy-9-octadecynoate (30 mg, 0.1 mmol), Lindlar catalyst (22.1 mg) and quinoline (1 µl) were combined in EtOAc/Hex (33%, 5 ml) in a RBF attached to a hydrogenation system. The system was evacuated, flushed with H_2 and purged (3 times). The system was then filled with H_2 and the reaction was left to proceed (3 days) with stirring. The resulting mixture was filtered through a silica gel/Celite plug and the filtrate was collected. The solvent was removed *in vacuo* to yield a mixture of the title compound and methyl 11-hydroxy-9*E*-octadecenoate (44:56), as a pale oil (28 mg, 0.1 mmol, 93 % yield). R_f 0.40 (25% EtOAc/hexane). ^{1}H NMR (300 MHz, $CDCl_3$) δ 5.46 (m, 1H), 5.37 (m, 1H), 4.42 (dt, J = 8.4 Hz, 6.6 Hz 1H, H**11**), 3.67 (s, 3H, H**19**), 2.30 (t, J = 7.5 Hz, 2H, H**2**), 2.03 (m, 2H, H**12**), 1.23-1.68 (m, 22H), 0.88 (t, J = 6.3 Hz, 3H, H**18**). ^{13}C NMR (100 MHz, $CDCl_3$) δ 174.31 (C**1**), 132.73 (C**9**), 132.16 (C**10**), 67.72 (C**11**), 51.45 (C**19**), 37.55 (C**12**), 34.06 (C**2**), 31.82 (C**16**), 29.62, 29.57, 29.28, 29.08, 29.05, 29.05, 29.05, 27.66 (C**8**), 25.40 (C**13**), 24.90 (C**3**), 22.66 (C**17**), 14.09 (C**18**). EI MS m/z 369 (1), 337 (3), 285 (100), 227 (15), 129 (13), 73 (24).

Methyl 11-hydroxy-9*E*-octadecenoate

R_f 0.32 (25% EtOAc/hexane). 5.62 (dt, J = 15.3 Hz, J' = 6.6 Hz, 1H, H**9**), 5.46 (m, 1H, H**10**), 4.03 (dt, J = 6.9 Hz, J' = 6.6 Hz 1H, H**11**), 3.67 (s, 3H, H**19**), 2.30 (t, J = 7.5 Hz, 2H, H**2**), 2.03 (m, 2H, H**12**), 1.23-1.68 (m, 22H), 0.88 (t, J = 6.3 Hz, 3H, H**1**). ^{13}C NMR (100 MHz, $CDCl_3$) δ 174.31 (C**1**), 133.16 (C**9**), 132.01 (C**10**), 73.21 (C**11**), 51.45 (C**19**), 37.36 (C**12**), 34.06 (C**2**), 32.13 (C**8**), 31.82 (C**16**), 29.62, 29.52, 29.48, 28.90, 28.07, 27.92, 25.50 (C**13**),

24.90 (C**3**), 22.66 (C**17**), 14.08 (**C18**). EI MS identical to methyl 11-hydroxy-(9*Z*)-octadecenoate

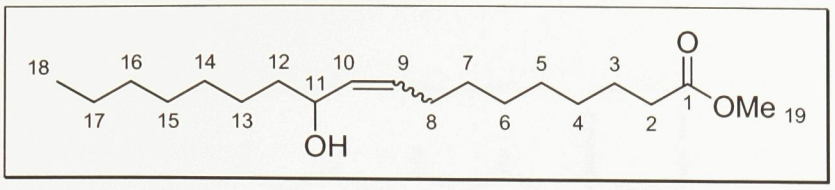

3.5 Synthesis of dienoic acid standards

3.5.1 (9*Z*,11*E*)-, (9*E*,11*E*)-, (9*Z*,11*Z*)- and (9*E*,11*Z*)- Methyl 9,11-octadecadienoate

3.5.1.1 9-Bromononanoic acid

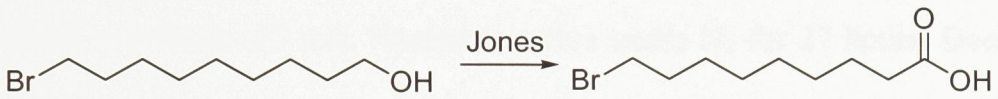

To a cooled (0° C) solution of 9-bromo-1-nonanol (4.46 g, 20.0 mmol) in acetone (515 ml) a solution of Jones reagent [CrO_3 (7.00 g, 70.0 mmol), 3M H_2SO_4 (26.5 ml) in H_2O (4.5 ml)] was slowly added with stirring. The reaction was stirred at 0° C for 3 hours, then allowed to come to room temperature and left stirring overnight. Bubbled SO_2 through the mixture with stirring until a dark green color was obtained. Added Et_2O (175 ml), H_2O (85 ml) and sat. NaCl (45 ml). Removed organic phase and extracted aqueous solution with Et_2O (2 x 175 ml). Washed ethereal phases in two portions, each with H_2O (2 x 250 ml), and sat. NaCl (2 x 125 ml), then dried (Na_2SO_4). Removed solvent *in vacuo*. Wet solid partitioned between DCM (15 ml) and H_2O. Organic phase was retained and aqueous phase extracted with DCM (2 x 15 ml). Extracts were washed with sat. NaCl (15 ml), dried (Na_2SO_4) and solvent removed *in vacuo* to recover the title compound as white needle crystals (4.41 g, 18.6 mmol, 93% yield). M.P. 32-33° C. IR (KBr): 2932, 2851, 1698, 1465, 1435, 1410, 1301, 1244, 1206, 935, 647. ^{1}H NMR (300 MHz, $CDCl_3$) δ 3.41 (t, J = 6.8 Hz, 2H; H**9**), 2.36 (t, J =

7.5 Hz, 2H; H**2**), 1.86 (quintet, J = 7.1 Hz, 2H; H**8**), 1.64 (m, 2H; H**3**), 1.27-1.49 (m, 8H; H**4-7**). ^{13}C NMR (75.5 MHz, $CDCl_3$) δ 180.37 (C**1**), 34.03 (C**2**), 33.95 (C**9**), 32.73 (C**8**), 29.01, 28.88, 28.51, 28.05, 24.56 (C**3**).

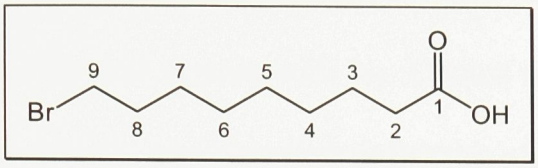

3.5.1.2 (8-Carboxyoctyl)triphenylphosphonium bromide

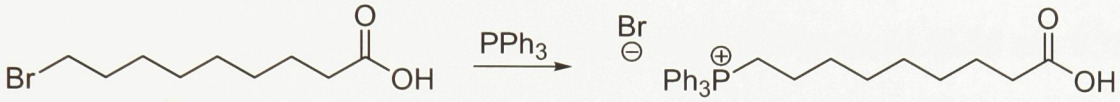

Added triphenyl phosphine (3.94 g, 15 mmol) to 9-bromononanoic acid (3.58 g, 15 mmol) dissolved in toluene (25 ml). Heated to reflux under N_2 for 27 hours. Decanted upper layer and dissolved lower golden layer in DCM (150 ml) and rotoevaporated to yield the title compound as a thick yellowish resin-like product (5.38 g, 10.8 mmol, 72% yield). IR (film): 2931, 2856, 1729, 1438, 1113, 921, 724, 690. ^{1}H NMR (300 MHz, $CDCl_3$) δ 7.67-7.85 (m, 15H; H**11-13**), 3.64 (m, 2H; H**9**), 2.33 (t, J = 7.3 Hz, 2H; H**2**), 1.59 (m, 6H), 1.23 (m, 6H). ^{13}C NMR (75.5 MHz, $CDCl_3$) δ 177.08 (C**1**), 135.06 (d, J = 2.9 Hz, 3C; C**13**), 133.59 (d, J = 9.9 Hz, 6C; C**12**), 130.52 (d, J = 12.4 Hz, 6C; C**11**), 118.31 (d, J = 85.3 Hz, 3C; C**10**), 34.43 (C**2**), 29.98 (d, J = 16.0 Hz, 3C; C**8**), 28.38, 28.38, 28.32, 24.51 (C**3**), 22.61 (d, J = 49.7 Hz; C**9**), 22.39 (d, J = 4 Hz; **7**).

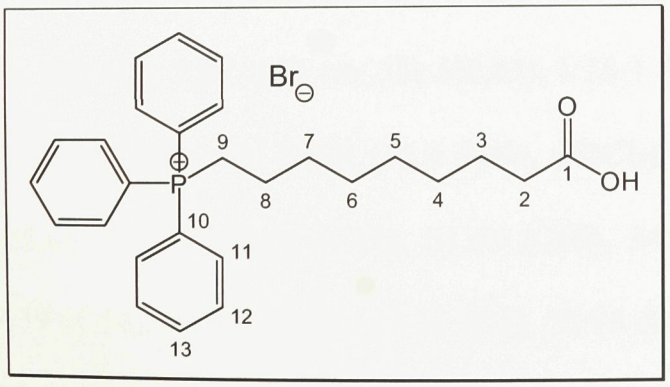

3.5.1.3 Methyl (9*Z*,11*E*)- and (9*E*,11*E*)-Octadecadienoate

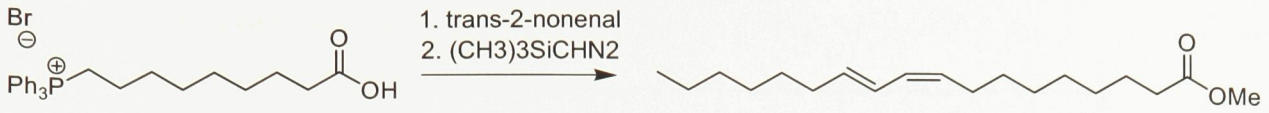

Dried (8-Carboxyoctyl)triphenylphosphonium bromide (1.99 g, 4.0 mmol) overnight under vacuum at 90° C then flooded system with N_2. Cooled to -78 °C before adding dry THF (30 ml) followed by potassium bis(trimethylsilyl)amide solution (0.5M in toluene, 20 ml) dropwise with stirring. Stirred an additional 2 hours, allowing solution to come to room temperature. Re-cooled the solution to -78 °C and added *E*-2-nonenal (0.86 ml, 0.73 g, 5.2 mmol) dropwise. Stirred mixture overnight, during which time room temperature was achieved. Added 1M HCl (50 ml) and extracted the mixture with ethyl acetate (3 x 50 ml). Combine organic phases were dried (Na_2SO_4) and rotoevaporated to yield a crude brown product (1.97 g). A sample of the crude product (0.33 g) was dissolved in 3:2 toluene/methanol (10 ml) and treated with (trimethylsilyl)diazomethane (2M in hexanes, 0.6 ml, 1.2 mmol) followed by a few drops AcOH to ensure complete conversion. The solvent was removed *in vacuo* and the product purified by flash chromatography to obtain a mixture of the methyl 9Z,11E octadecadienoate and methyl 9*E*,11*E*-octadecadienoate (9:1 ratio) (121 mg, 0.4 mmol, yield 65%). R_f 0.45 (5% EtOAc/hexanes). IR (film): 2927, 2855, 1743, 1459, 1436, 1197, 1171, 984, 947. UV_{max} 232 nm. ^1H NMR (300 MHz, $CDCl_3$) δ 6.30 (m, 1H; H**11**), 5.95 (t, J = 10.8 Hz, 1H; H**10**), 5.67 (m, 1H; H**12**), 5.30 (m, 1H; H**9**), 3.68 (s, 3H; H**19**), 2.31 (t, J = 7.5 Hz, 2H; H**2**), 2.01-2.21 (m, 4H; H**8**,**13**), 1.26-1.70 (m, 18H; H**2-7**, H**14-17**), 0.90 (t, J = 6.7 Hz, 3H; H**18**). ^{13}C NMR (75.5 MHz, $CDCl_3$) δ 174.31 (C**1**), 134.78 (C**12**), 129.92 (C**9**), 128.68 (C**10**), 125.56 (C**11**), 51.44 (C**19**), 34.10 (C**2**), 32.91 (C**13**), 31.75 (C**16**), 29.65, 29.39 (C**14**), 29.13, 29.10, 29.05 (C**4**), 28.93 (C**15**), 27.65 (C**8**), 24.94 (C**3**), 22.63 (C**17**), 14.11 (C**18**). MS (rel. intensity) *m*/z 295 (5, $[M+1]^+$), 294 (23, $[M]^+$), 263

(7, $[M-31]^+$), 251 (1, $[M-43]^+$), 220 (3), 178 (3), 150 (10), 136 (10), 123 (12), 109 (27), 95 (55), 81 (73), 67 (100), 55 (36).

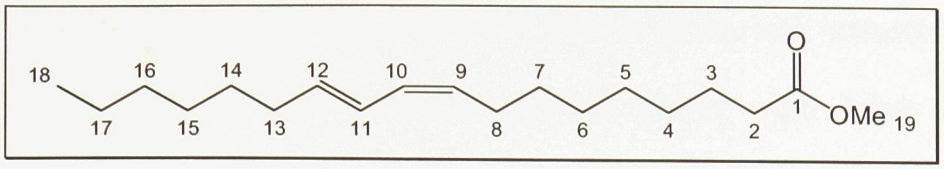

Methyl 9*E*,11*E*-Octadecadienoate

The analytical data for this is similar to that of methyl 9*Z*,11*E*-octadecadienoate except for: ^{1}H NMR (300 MHz, $CDCl_3$) δ 5.78-6.05 (m, 2H; H**10**,**11**), 5.56 (m, 2H; H**9**,**12**), 3.68 (s, 3H, H**19**), 2.31 (t, J = 7.5 Hz, 2H; H**2**), 2.01-2.21 (m, 4H; H**8**,**13**), 1.26-1.70 (m, 18H; H**3-7**, H**14-17**), 0.90 (t, J = 6.7 Hz, 3H; H**18**). ^{13}C NMR (75.5 MHz, $CDCl_3$) δ 174.31 (C**1**), 132.52 (C**12**), 132.25 (C**9**), 130.41 (C**11**), 130.28 (C**10**), 51.44 (C**19**), 34.10 (C**2**), 32.63 (C**13**), 32.56 (C**8**), 31.75 (C**16**), 29.65, 29.39 (C**14**), 29.13, 29.10, 29.05 (C**4**), 28.93 (C**15**), 24.94 (C**3**), 22.63 (C**17**), 14.11 (C**18**). MS (rel. intensity) m/z 295 (5, $[M+1]^+$), 294 (24, $[M]^+$), 263 (8, $[M-31]^+$), 220 (3), 178 (3), 150 (10), 136 (10), 123 (11), 109 (27), 95 (51), 81 (70), 67 (100), 55 (33).

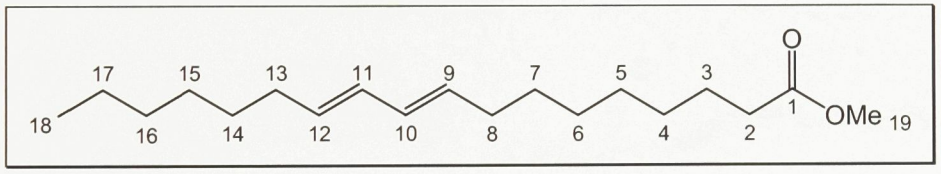

3.5.1.4 2-Nonynal

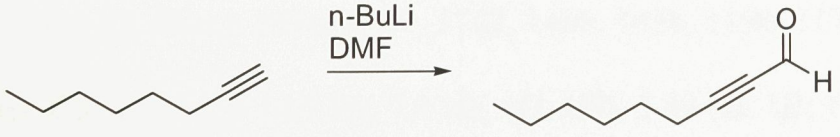

Dissolved 1-octyne (1.12 g, 10 mmol) in anhydrous ether (10 ml) under N_2 with stirring and cooled to -78 °C. Added n-BuLi (2.5M in hexanes, 4 ml, 10 mmol) dropwise and stirred solution 30 minutes. Slowly added anhydrous DMF (1.2 ml, 15 mmol). The reaction

mixture was allowed to come to room temperature and stirred for an additional 30 minutes. Added ice water (15 ml) and acidified using conc. HCl to pH 3, followed by neutralization with powdered $NaHCO_3$ to pH 7. Separated the organic phase and extracted the aqueous phase with EtOAc (4 x 10 ml). Combined organic phases were dried (Na_2SO_4) and rotoevaporated to yield the title compound as a yellow oil (1.08 g, 7.9 mmol, 79% yield). R_f 0.42 (2.5% EtOAc/hexanes). IR (film): 2932, 2860, 2281, 2201, 1672, 1467, 1387, 1138, 824, 791, 726. ^{1}H NMR (300 MHz, $CDCl_3$) δ 9.17 (s, 1H; H**1**), 2.40 (t, J = 7.1 Hz, 2H; H**4**), 1.59 (m, 2.0 Hz, 2H; H**5**), 1.22-1.45 (m, 6H, H**6-8**), 0.88 (t, J = 6.8 Hz, 3H; H**9**). ^{13}C NMR (75.5 MHz, $CDCl_3$) δ 177.21 (C**1**), 99.34 (C**3**), 81.63 (C**2**), 31.13 (C**7**), 28.44, 27.45, 22.40 (C**8**), 19.06 (C**4**), 13.94 (C**9**); MS (rel. intensity) m/z 137 (2, $[M-1]^+$), 123 (7), 109 (28), 95 (24), 81 (45), 68 (48), 67 (48), 55 (36), 43 (100), 41 (74).

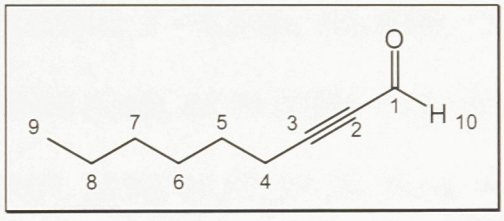

3.5.1.5 Methyl 9*Z*,11-octadecenynoate

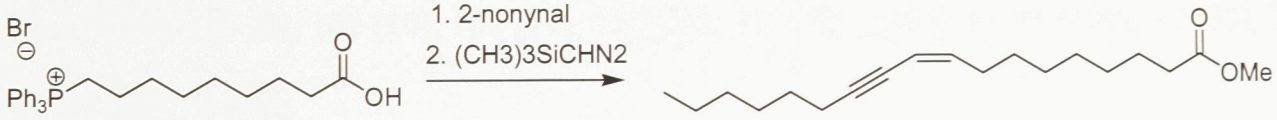

As for methyl 9*Z*,11*E*-octadecadienoate, using 2-nonynal (yield 90%). Product a mixture of methyl 9*Z*,11-octadecenynoate and methyl 9*E*,11-octadecenynoate (3:1). R_f 0.32 (2.5% EtOAc/hexanes). IR (film): 2930, 2857, 1742, 1460, 1436, 1196, 1171, 738. ^{1}H NMR (300 MHz, $CDCl_3$) δ 5.56 (dt, J = 10.7 Hz, 7.4 Hz, 1H; H**9**), 5.44 (m, 1H; H**10**), 3.67 (s, 3H; H**19**), 2.31 (m, 4H; H**2**,**8**), 1.55-1.70(m, 20H; H**3-7**, H**13-17**), 0.90 (t, J = 6.8 Hz, 3H; H**18**). ^{13}C NMR (75.5 MHz, $CDCl_3$) δ 174.29 (C**1**), 142.44 (C**9**), 109.40 (C**10**), 94.50 (C**12**), 77.35

(C**11**), 51.43 (C**19**), 34.10 (C**2**), 31.37 (C**16**), 29.96, 29.09, 29.08, 28.99, 28.86, 28.82, 28.56, 24.94 (C**3**), 22.59 (C**17**), 19.53 (C**13**), 14.05 (C**18**). MS (rel. intensity) *m*/z 293 (1, $[M+1]^+$), 292 (3, $[M]^+$), 261 (17, $[M-31]^+$), 236 (4), 222 (31), 175 (5), 161 (8), 149 (11), 135 (17), 121 (28), 119 (12), 107 (57), 93 (100), 87 (34), 79 (98), 67 (62), 55 (49).

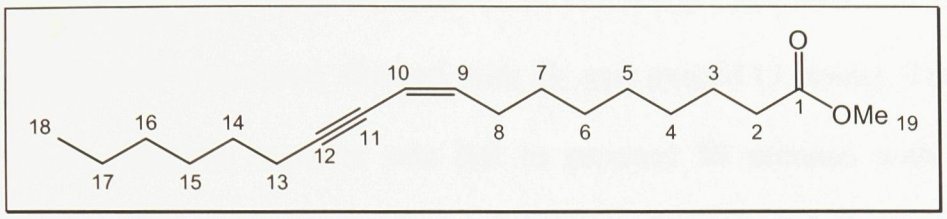

Methyl 9*E*,11-octadecenynoate

The analytical data for this compound is similar to that of methyl 9*Z*,11-octadecenynoate except for: ^{1}H NMR (300 MHz, $CDCl_3$) δ 6.04 (dt, J = 15.8 Hz, 7.0 Hz, 1H; H**9**), 5.45 (m, 1H; H**10**), 3.67 (s, 3H; H**19**), 2.31 (m, 4H; H**2**,**8**), 2.07 (m, 2H; H**13**), 1.55-1.70 (m, 18H; H**3-7**, H**14-17**), 0.90 (t, J = 6.8 Hz, 3H; H**18**). ^{13}C NMR (75.5 MHz, $CDCl_3$) δ 174.29 (C**1**), 143.18 (C**9**), 109.89 (C**10**), 88.76 (C**12**), 79.13 (C**11**), 51.43 (C**19**), 34.08 (C**2**), 32.91, 31.60 (C**16**), 29.08, 29.07, 28.86, 28.82, 28.76, 28.61, 24.91 (C**3**), 22.55 (C**17**), 19.36 (C**13**), 14.12 (C**18**). MS (rel. intensity) *m*/z 292 (1, $[M]^+$), 261 (9, $[M-31]^+$), 236 (4), 222 (50), 175 (4), 161 (6), 149 (10), 135 (19), 121 (28), 119 (12), 107 (55), 93 (100), 87 (30), 79 (93), 67 (60), 55 (46).

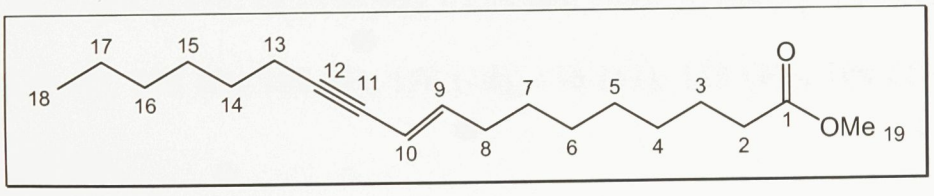

3.5.1.6 Methyl 9*Z*,11*Z*-octadecadienoate

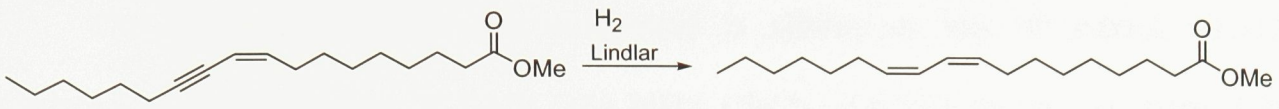

Methyl 9*Z*,11-octadecenynoate (53 mg, 0.18 mmol), Lindlar catalyst (6 mg) and quinoline (25 µl) were combined in hexanes (6 ml) in a RBF attached to a hydrogenation system. The system was evacuated, flushed with H_2 and purged (3 times). The system was then filled with H_2 and the reaction was left to proceed 30 minutes with stirring. The resulting mixture was filtered through a silica gel/Celite plug and the filtrate was collected. The solvent was removed *in vacuo*. The resulting oil was purified by flash chromatography (2.5% EtOAc/hex) to yield a mixture of the title compound, methyl 9*E*,11*Z*-octadecadienoate and unreacted starting material (58:11:31). Product was a colorless oil (42 mg, 0.14 mmol, 45 % yield). R_f 0.44 (5% EtOAc/hexane). IR (film): 2927, 2855, 1742, 1459, 1436, 1170. UV_{max} 235 nm. ^{1}H NMR (300 MHz, $CDCl_3$) δ 6.25 (d, J = 9.2 Hz, 2H, H**10-11**), 5.45 (m, 2H; H**9**,**12**), 3.68 (s, 3H; H**19**), 2.31 (t, J = 7.6 Hz, 2H; H**2**), 2.17 (m, 4H; H**8**,**13**), 1.24-1.69 (m, 18H; H**3-7**, H**14-17**), 0.89 (t, J = 6.7 Hz, 3H; H**18**). ^{13}C NMR (100 MHz, $CDCl_3$) δ 174.32 (C**1**), 132.19 (C**12**), 131.91 (C**9**), 123.66 (C**10**), 123.52 (C**11**), 51.45 (C**19**), 34.10 (C**2**), 31.80 (C**16**), 29.98 (C**4**), 29.63 (C**14**), 29.10-29.63 (C**5-7**), 29.06 (C**15**), 27.50 (C**13**), 27.43 (C**8**), 24.94 (C**3**), 22.64 (C**17**), 14.11 (C**18**). EI MS m/z 295 (4, $[M+1]^+$), 294 (22, $[M]^+$), 263 (8, $[M-31]^+$), 220 (4), 178 (3), 164 (4), 150 (10), 136 (11), 123 (13), 109 (29), 95 (56), 81 (76), 67 (100), 55 (38).

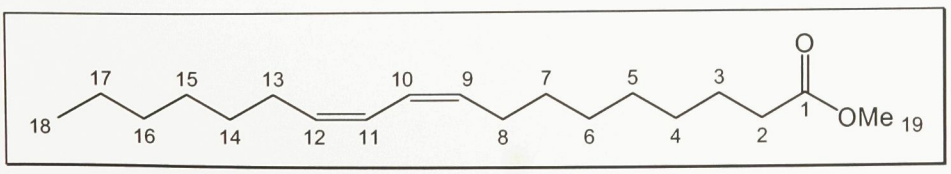

Methyl 9*E*,11*Z*-octadecadienoate

The analytical data for this compound is similar to that of methyl 9*Z*,11*Z*-octadecadienoate except for: ^{1}H NMR (300 MHz, $CDCl_3$) δ 6.19-6.36 (m, 1H; H**10**), 5.95, (m, 1H; H**9**), 5.65 (m, 1H; H**11**), 5.36 (m, 1H; H**12**), 3.68 (s, 3H; H**19**), 2.31 (t, J = 7.6 Hz, 2H; H**2**), 1.93-2.16 (m, 4H; H**8**,**13**), 1.24-1.69 (m, 18H; H**3-7**, H**14-17**), 0.89 (t, J = 6.7 Hz, 3H; H**18**). ^{13}C NMR (100 MHz, $CDCl_3$) δ 174.32 (C**1**), 134.51 (C**9**), 130.19 (C**12**), 128.55 (C**11**), 125.70 (C**10**), 51.45 (C**19**), 34.10 (C**2**), 32.85 (C**8**), 31.75 (C**16**), 29.72 (C**14**), 29.20-29.48 (C**4-7**), 28.97 (C**15**), 27.72 (C**13**), 24.94 (C**3**), 22.64 (C**17**), 14.11 (C**18**). EI MS m/z 294 (28, $[M]^+$), 263 (8, $[M-31]^+$), 150 (6), 136 (8), 123 (13), 109 (28), 95 (55), 81 (78), 67 (100), 55 (36).

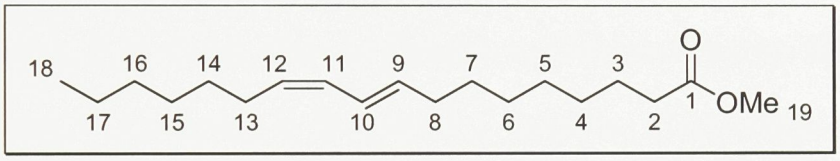

References

[1] M. I. Gurr, J. L. Harwood, *Lipid Biochemistry: An Introduction*, 4 ed., Chapman and Hall, London, **1991**.

[2] A. A. Millar, M. A. Smith, L. Kunst, *Trends in Plant Science* **2000**, *5*, 95.

[3] P. H. Buist, *Natural Product Reports* **2004**, *21*, 249.

[4] D. K. B. A. K. Bloch, *The Journal of Biological Chemistry* **1960**, *235*, 337.

[5] Y. Lindqvist, W. Huang, G. Schneider, J. Shanklin, *EMBO Journal* **1996**, *15*, 4081.

[6] J. E. Guy, E. Whittle, D. Kumaran, Y. Lindqvist, J. Shanklin, *The Journal of Biological Chemistry* **2007**, *282*, 19863.

[7] J. Shanklin, E. B. Cahoon, *Annu. Rev. Plant Physiol. Plant Mol. Biol* **1998**, *49*, 611.

[8] J. Shanklin, E. Whittle, B. G. Fox, *Biochemistry* **1994**, *33*, 12787.

[9] K. M. Mayer, S. R. McCorkle, J. Shanklin, *BMC Bioinformatics* **2005**, *2*, 284.

[10] B. Behrouzian, P. H. Buist, *Current Opinion in Chemical Biology* **2002**, *6*, 577.

[11] E. B. Cahoon, Y. Lindqvist, G. Schneider, J. Shanklin, *Proceedings of the National Academy of Sciences of the United States of America* **1997**, *94*, 4872.

[12] P. H. Buist, B. Behrouzian, *Journal of the American Chemical Society* **1996**, *118*, 6295.

[13] B. Behrouzian, P. H. Buist, J. Shanklin, *Chemical Communications* **2001**, 401.

[14] P. H. Buist, D. M. Marecak, *Journal of the American Chemical Society* **1992**, *114*, 5073.

[15] B. Behrouzian, P. H. Buist, J. Shanklin, *Chemical Communications* **2001**, 401.

[16] A. E. Tremblay, E. Whittle, P. H. Buist, J. Shanklin, *Organic & Biomolecular Chemistry* **2007**, *5*, 1270.

[17] W. H. Pirkle, S. D. Beare, R. L. Muntz, *Tetrahedron Letters* **1974**, *26*, 2295.

[18] J. M. Seco, S. Latypov, E. Quinoa, R. Riguera, *Tetrahedron Letters* **1994**, *35*, 2921.

[19] B. Behrouzian, C. K. Saville, B. Dawson, P. H. Buist, J. Shanklin, *Journal of the American Chemical Society* **2002**, *124*, 3277.

[20] J. Zhou, W. L. Kelly, B. O. Bachmann, M. Gunsior, C. A. Townsend, E. I. Solomon, *Journal of the American Chemical Society* **2001**, *123*, 7388.

[21] D. J. Hodgson, K. Y. Y. Lao, B. Dawson, P. H. Buist, *Helvetica Chimica Acta* **2003**, *86*, 3688.

[22] K. Y. Y. Lao, D. J. Hodgson, B. Dawson, P. H. Buist, *Bioorganic & Medicinal Chemistry Letters* **2005**, *15*, 2799.

[23] P. H. Buist, D. M. Marecak, H. L. Holland, F. M. Brown, *Tetrahedron: Asymmetry* **1995**, *6*, 7.

[24] P. H. Buist, *Unpublished results*.

[25] M. J. Cryle, J. J. De Voss, *Angewandte Chemie International Edition* **2006**, *45*, 8221.

[26] I. Fernández, N. Khiar, J. M. Llera, F. Alcudia, *Journal of Organic Chemistry* **1992**, *57*, 6789.

[27] I. Fernandez, N. Khiar, *Chemical Reviews* **2003**, *103*, 3651.

[28] M. Axelrod, P. Bickart, J. Jacobus, M. M. Green, K. Mislow, *Journal of the American Chemical Society* **1968**, *90*, 4835.

[29] K. K. Andersen, *Tetrahedron Letters* **1962**, *3*, 93.

[30] A. E. Tremblay, B.Sc. Thesis Report, Carleton University (Ottawa), **2007**.

[31] D. Balcells, G. Ujaque, I. Fernàndez, N. Khiar, *Advanced Synthesis & Catalysis* **2007**, *349*, 2103.

[32] D. Balcells, F. Maseras, N. Khiar, *Organic Letters* **2004**, *6*, 2197.

[33] I. Fernández, N. Khiar, *Chemical Reviews* **2003**, *103*, 3651.

[34] K. Mislow, T. Simmons, J. T. Melillo, J. Andrew L. Ternay, *Journal of the American Chemical Society* **1964**, *86*.

[35] W. J. Middleton, *Journal of Organic Chemistry* **1974**, *40*, 574.

[36] T.-C. Zheng, M. Burkart, D. E. Richardson, *Tetrahedron Letters* **1993**, *40*, 603.

[37] J.-H. Youn, R. Hermann, *Synthesis* **1987**, 72.

[38] S. Thea, G. Cevasco, *Tetrahedron Letters* **1987**, *28*, 5193.

[39] F. Daligault, A. Arboré, C. Nugier-Chauvin, H. Patin, *Tetrahedron: Asymmetry* **2004**, *15*, 917.

[40] F. Palacios, A. M. O. d. Retana, J. M. Alonso, *Journal of Organic Chemistry* **2006**, *71*, 6141.

[41] J. H. Bowie, D. H. Williams, S.-O. Lawesson, J. Ø. Madsen, C. Nolde, G. Schroll, *Tetrahedron* **1966**, *22*, 3515.

[42] B.-L. Li, Z.-G. Zhang, L.-L. Du, W. Wang, *Chirality* **2008**, *20*, 35.

[43] V. C. Pham, A. Jossang, T. Sevenet, V. H. Nguyen, B. Bodo, *Tetrahedron* **2007**, *63*, 11244.

[44] J. M. Seco, E. Quio, R. Riguera, *Chemical Reviews* **2004**, *104*, 17.

[45] G. R. Sullivan, J. A. Dale, H. S. Mosher, *Journal of Organic Chemistry* **1973**, *38*, 2143.

[46] E. V. Ivanova, H. M. Muchall, P. H. Buist, Abstract 729: Computational evaluation of the role of Pirkle-type complexes of chiral sulfoxides in the determination of their absolute configuration. Canadian Society for Chemistry Conference, **May 2008** Edmonton, Canada.

[47] E. Whittle, J. Shanklin, *The Journal of Biological Chemistry* **2001**, *276*, 21500.

[48] J. A. Broadwater, E. Whittle, J. Shanklin, *The Journal of Biological Chemistry* **2002**, *277*, 15613.

[49] B. W. Baker, R. P. Linstead, B. C. L. Weedon, *Journal of the Chemical Society* **1955**, 2218.

[50] Z. Huang, E. Negishi, *Organic Letters* **2006**, *8*, 3675.

[51] P. Wipf, H. Jahn, *Tetrahedron* **1996**, *52*, 12853.

[52] B. W. Gung, H. Dickinson, *Organic Letters* **2002**, *4*, 2517.

[53] E. N. Frankel, R. F. Garwood, B. P. S. Khambay, G. P. Moss, B. C. L. Weedon, *Journal of the Chemical Society, Perkin Transactions 1* **1984**, 2233.

[54] D. Amans, V. Bellosta, J. Cossy, *Organic Letters* **2007**, *9*, 4761.

[55] D. L. Pavia, G. M. Lampman, G. S. Kriz, *Introduction to spectroscopy*, 3rd ed., Brooks/Cole Thompson, Fort Worth, **2001**.

[56] W. N. Smith, O. F. Beumel, *Synthesis* **1974**, 441.

[57] L. D. Metcalfe, A. A. Schmidt, *Analytical Chemistry* **1961**, *33*, 363.

[58] E. Vedejs, C. F. Marth, *Journal of the American Chemical Society* **1988**, *110*, 3948.

[59] J. Clayden, N. Greeves, S. Warren, P. Wothers, *Organic Chemistry*, Oxford University Press, Oxford, **2001**.

[60] P. E. Duffy, S. M. Quinn, H. M. Roche, P. Evans, *Tetrahedron* **2006**, *62*, 4838.

[61] A. Presser, A. Hüfner, *Monatshefte für Chemie* **2004**, *135*, 1015.

[62] H. Kuroda, E. Hanaki, H. Izawa, M. Kano, H. Itahashi, *Tetrahedron* **2004**, *60*, 1913.

[63] M. G. Organ, H. Ghasemi, *Journal of Organic Chemistry* **2004**, *69*, 695.

[64] M. S. F. L. K. Jie, M. K. Pasha, M. S. Alam, *Lipids* **1997**, *32*, 1041.